Review on Axion Search Experiments

Junu Jeong

Center for Axion and Precision Physics Research, Institute for Basic Science

CAPP
Center for Axion and Precision Physics Research

KAIST

Axions, Weyl and Beyond

31 August 2023, Busan

[VISIT BUSAN]

Outline

- Why Axion?
- Axion Searches
- Summary

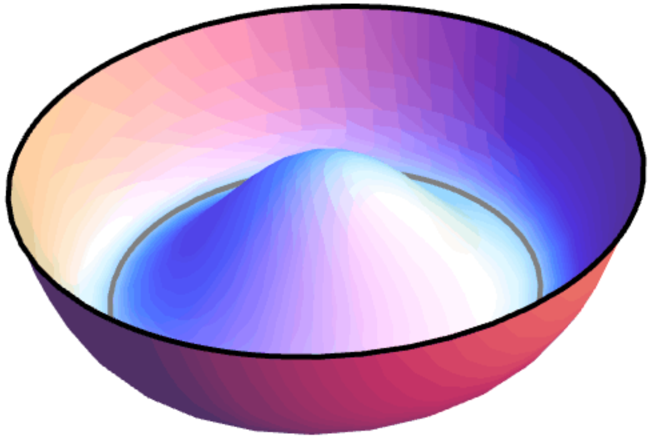

Why Axion?

Theoretically Well Motivated

Electric dipole moment?

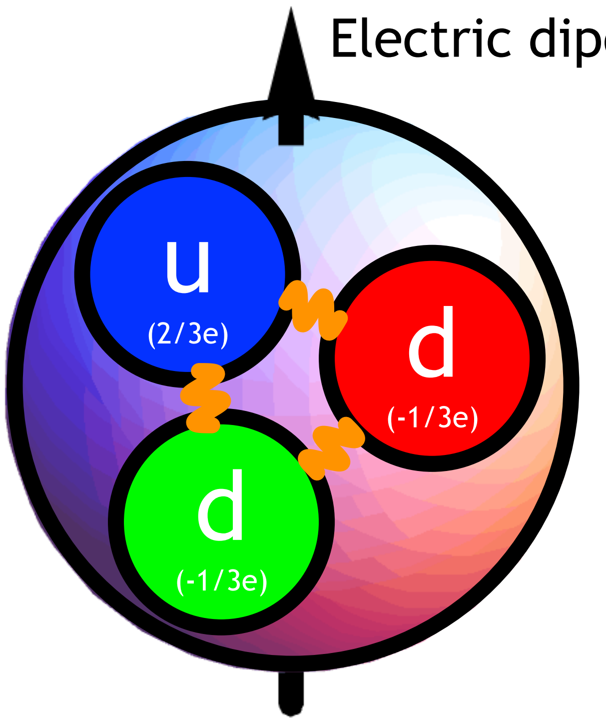

Why no EDM for neutron & proton?
⇒ SSB of global U(1) symmetry
⇒ pesudo-Nambu-Goldstone Boson, **Axion**
Similar to Higgs (Gauge Sym. ⇒ Global Sym.)

Why Axion?

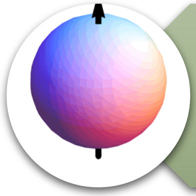

Theoretically Well Motivated

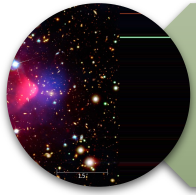

Dark Matter Candidate

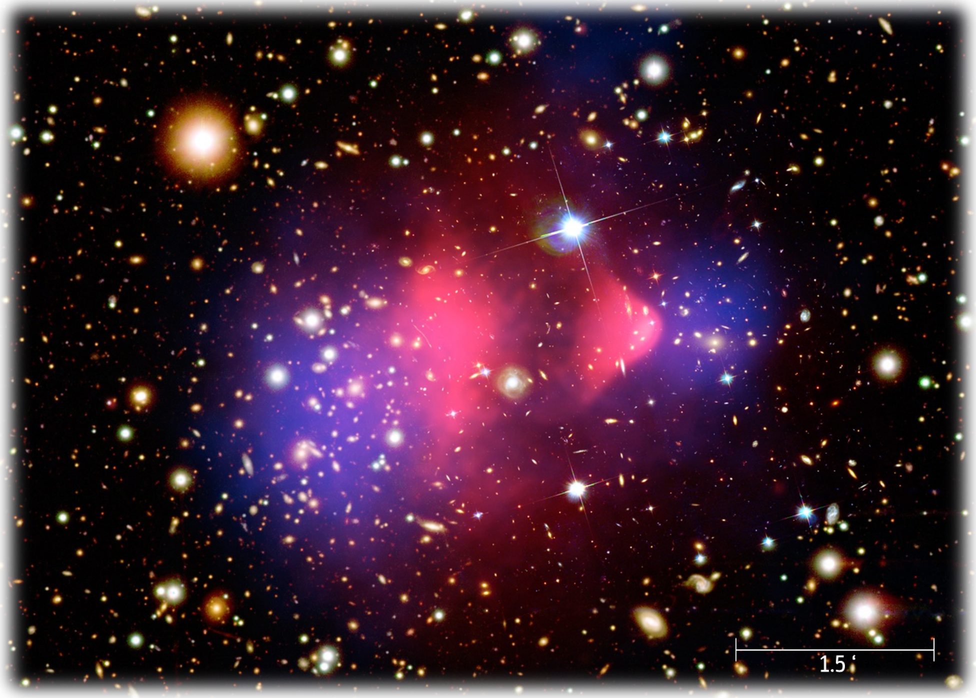

Invisible axion (mass less than meV)

- Feebly interacts with standard particles
- Non-relativistic in sufficient quantities

Why Axion?

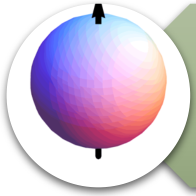

Theoretically Well Motivated

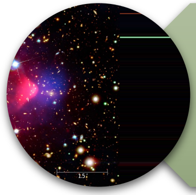

Dark Matter Candidate

Tabletop Experiment

Less expensive but sensitive

- Much smaller compared to colliders
- **Idea is most important**

Why Axion?

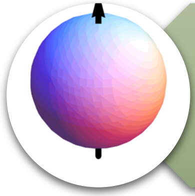
Theoretically Well Motivated

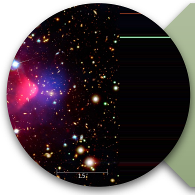
Dark Matter Candidate


Tabletop Experiment

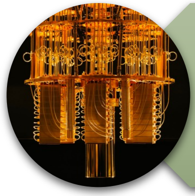
Quantum Technology

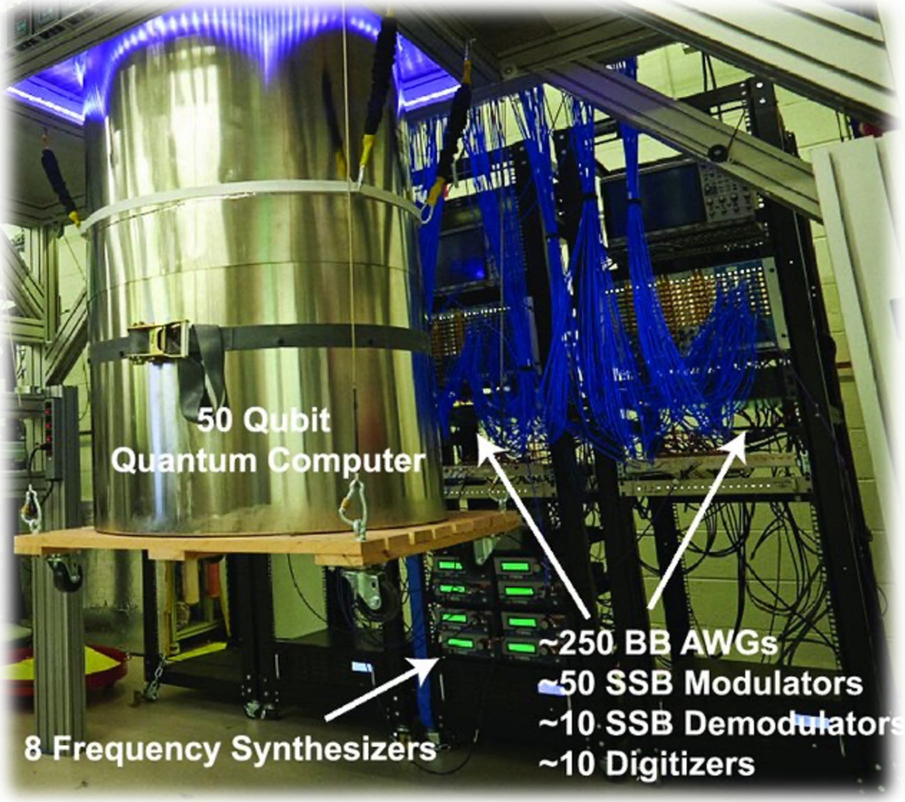

In line with quantum computer technology

- Microwave engineering in cryogenics
- Quantum-limited noise amplifiers
- Single photon detector

Why Axion?

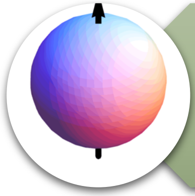

Theoretically Well Motivated

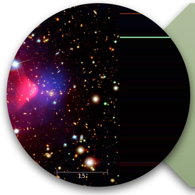

Dark Matter Candidate

Tabletop Experiment

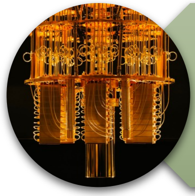

Quantum Technology

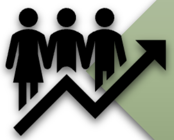

Growing Community

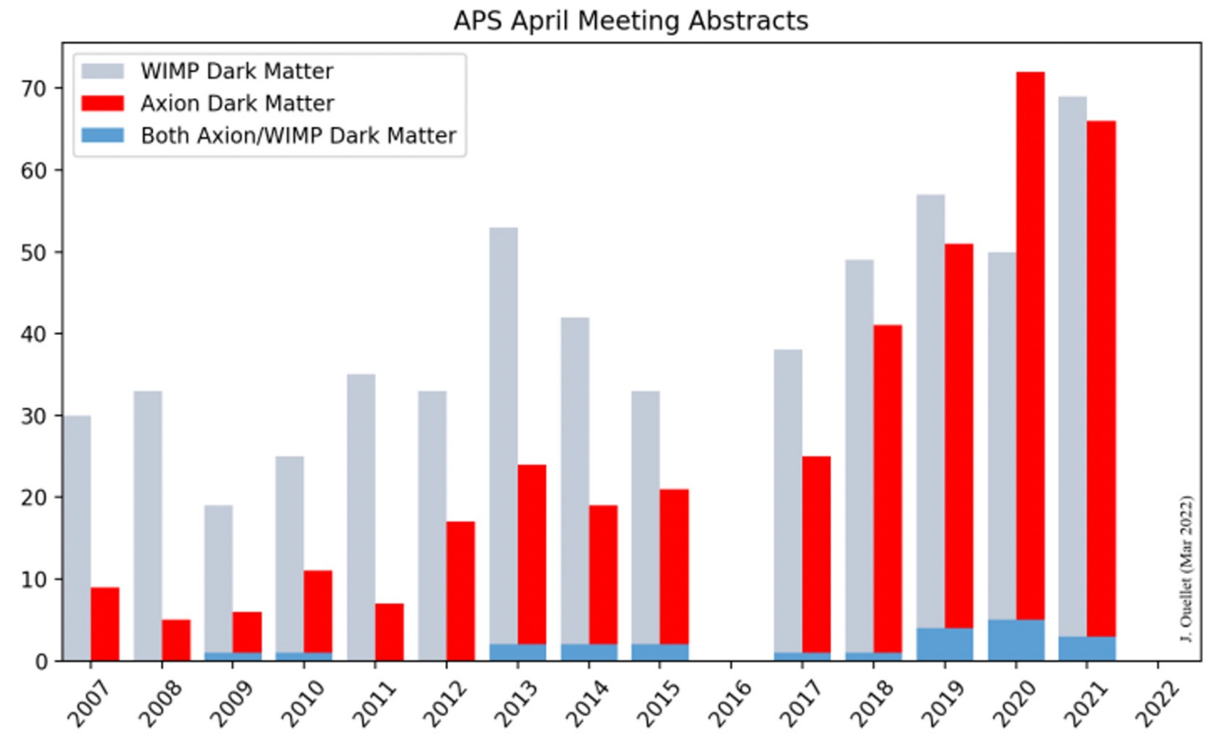

As a result,
axion community is growing so fast!

Axion Searches

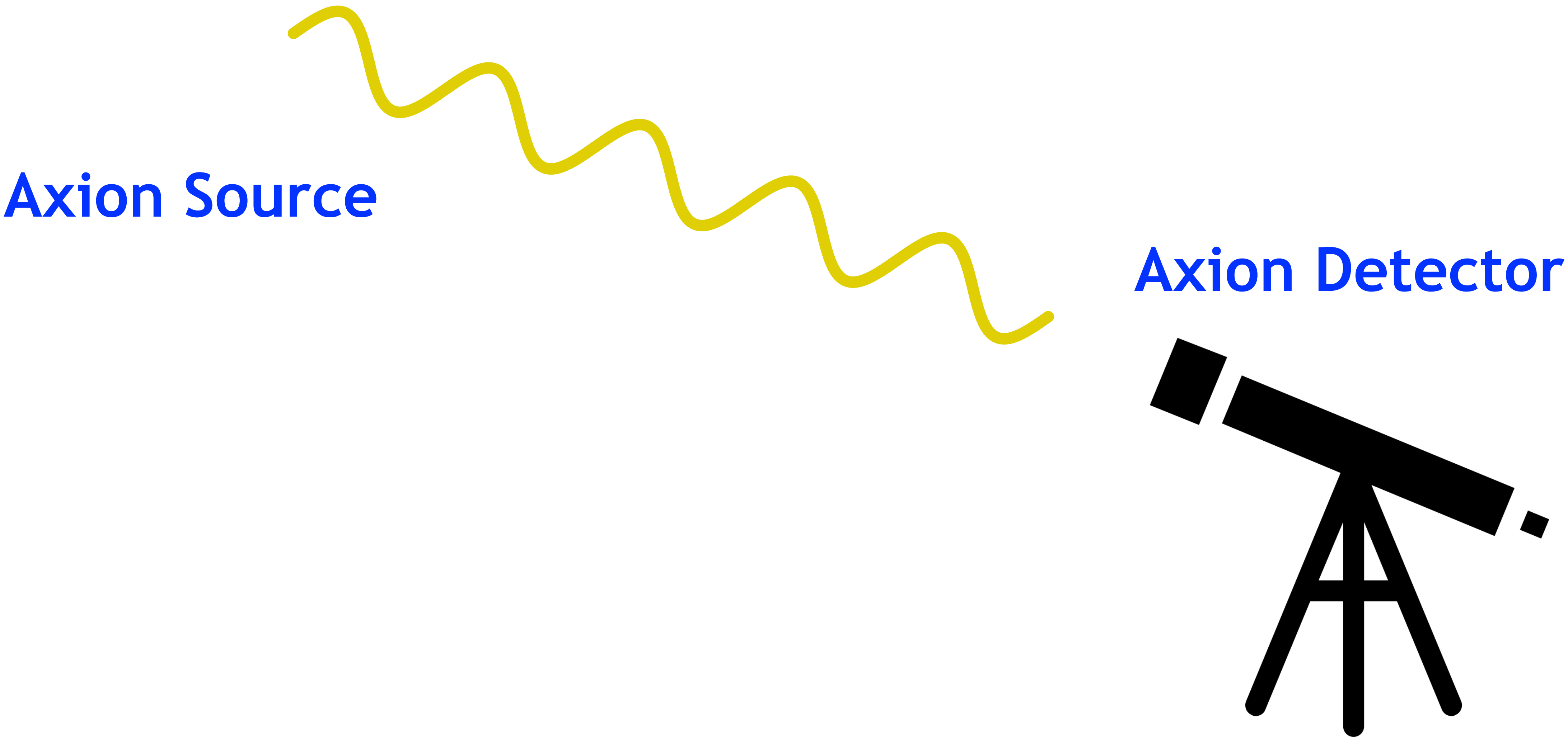

Axion Searches

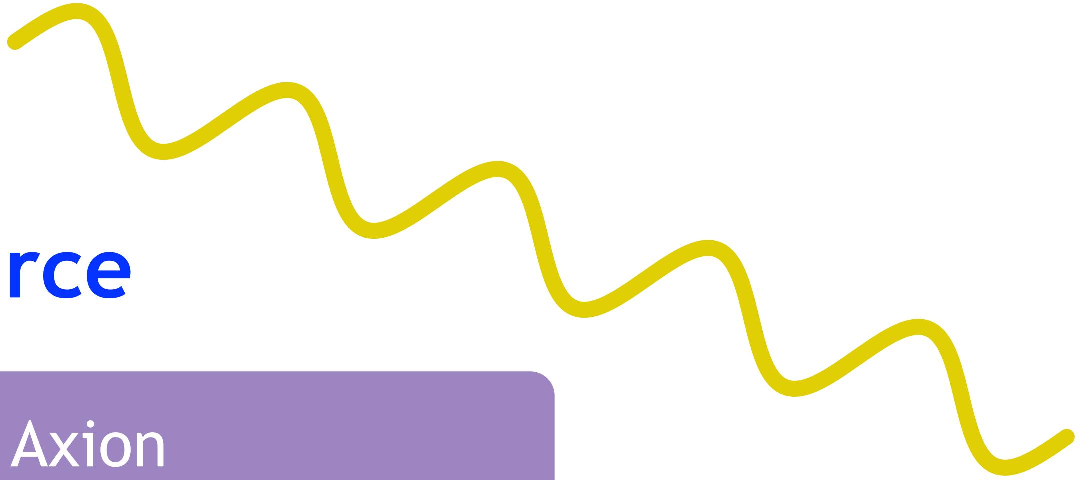

Axion Source

- Dark Matter Axion
- Solar Axion
- Lab-Produced Axion
- Others

Axion Detector

Axion Searches

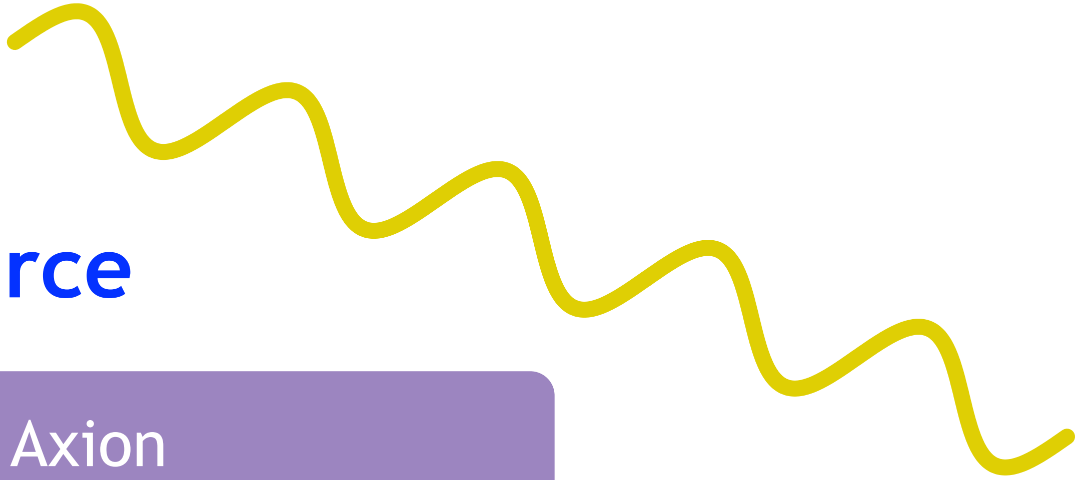

Axion Source

- Dark Matter Axion
- Solar Axion
- Lab-Produced Axion
- Others

- Axion-Photon Coupling
- Axion-Fermion Coupling

Axion Detector

Axion-Photon Coupling

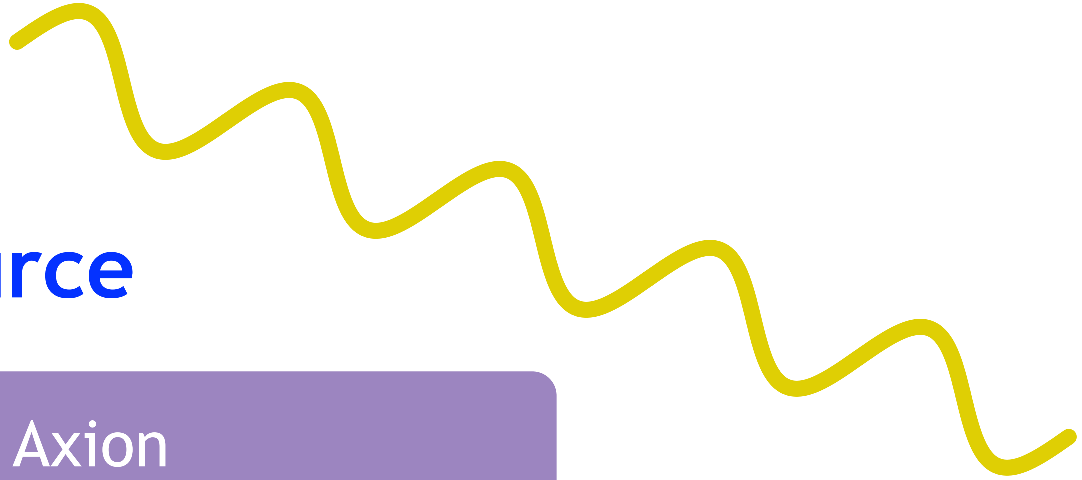

Axion-Photon Coupling

Axion-Fermion Coupling

Axion Source

Dark Matter Axion

Solar Axion

Lab-Produced Axion

Others

Axion Detector

Axion-Photon Coupling

Axion-Gluon coupling

$$\mathcal{L}_\theta = \frac{g^2 a/f_a}{32\pi^2} G^a_{\mu\nu}\tilde{G}^{a\mu\nu}$$

Axion-Photon Coupling

Axion-Gluon coupling

$$\mathcal{L}_\theta = \frac{g^2 a/f_a}{32\pi^2} G^a_{\mu\nu}\tilde{G}^{a\mu\nu}$$

low energy

Axion-Photon coupling

$$\mathcal{L}_{a\gamma} = -\frac{g_{a\gamma\gamma}}{4} a F_{\mu\nu}\tilde{F}^{\mu\nu} = g_{a\gamma\gamma} a \mathbf{E}\cdot\mathbf{B}$$

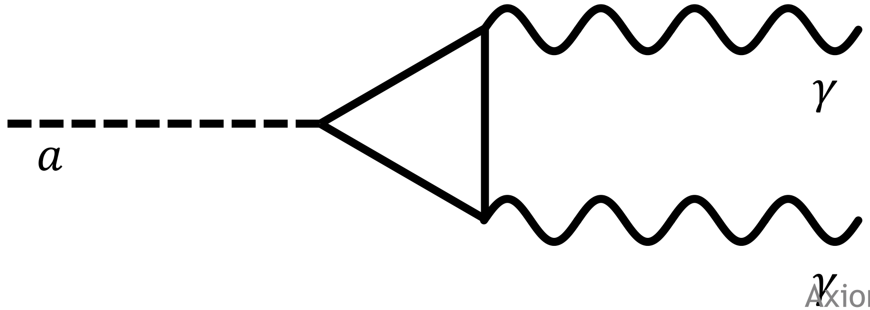

Axion-Photon Coupling

Axion-Gluon coupling

$$\mathcal{L}_\theta = \frac{g^2 a/f_a}{32\pi^2} G^a_{\mu\nu}\tilde{G}^{a\mu\nu}$$

low energy

Axion-Photon coupling

$$\mathcal{L}_{a\gamma} = -\frac{g_{a\gamma\gamma}}{4} a F_{\mu\nu}\tilde{F}^{\mu\nu} = g_{a\gamma\gamma} a \mathbf{E}\cdot\mathbf{B}$$

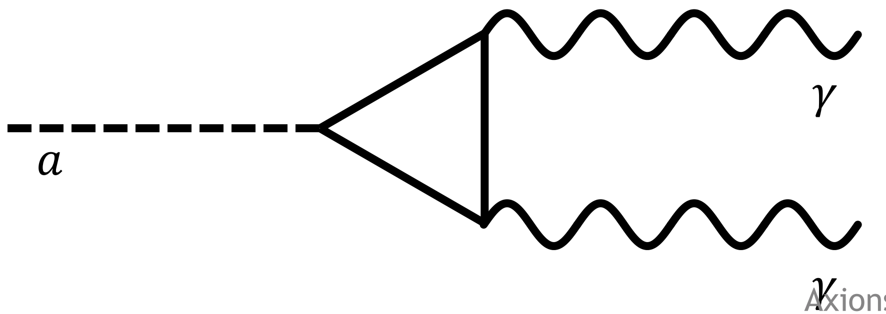

least action principle

Classical Equation of Motion

$$\nabla\cdot\mathbf{E} = \rho_e - g_{a\gamma\gamma}\nabla a\cdot\mathbf{B}$$

$$\nabla\cdot\mathbf{B} = 0$$

$$\nabla\times\mathbf{E} = -\partial_t\mathbf{B}$$

$$\nabla\times\mathbf{B} = \partial_t\mathbf{E} + \mathbf{J}_e + g_{a\gamma\gamma}(\nabla a\times\mathbf{E} + \partial_t a\mathbf{B})$$

Recent Limits on the Axion-Photon Coupling

Haloscope
Dark Matter Axion

Helioscope
Solar Axion

Lab-Produced
Lab-Produced Axion

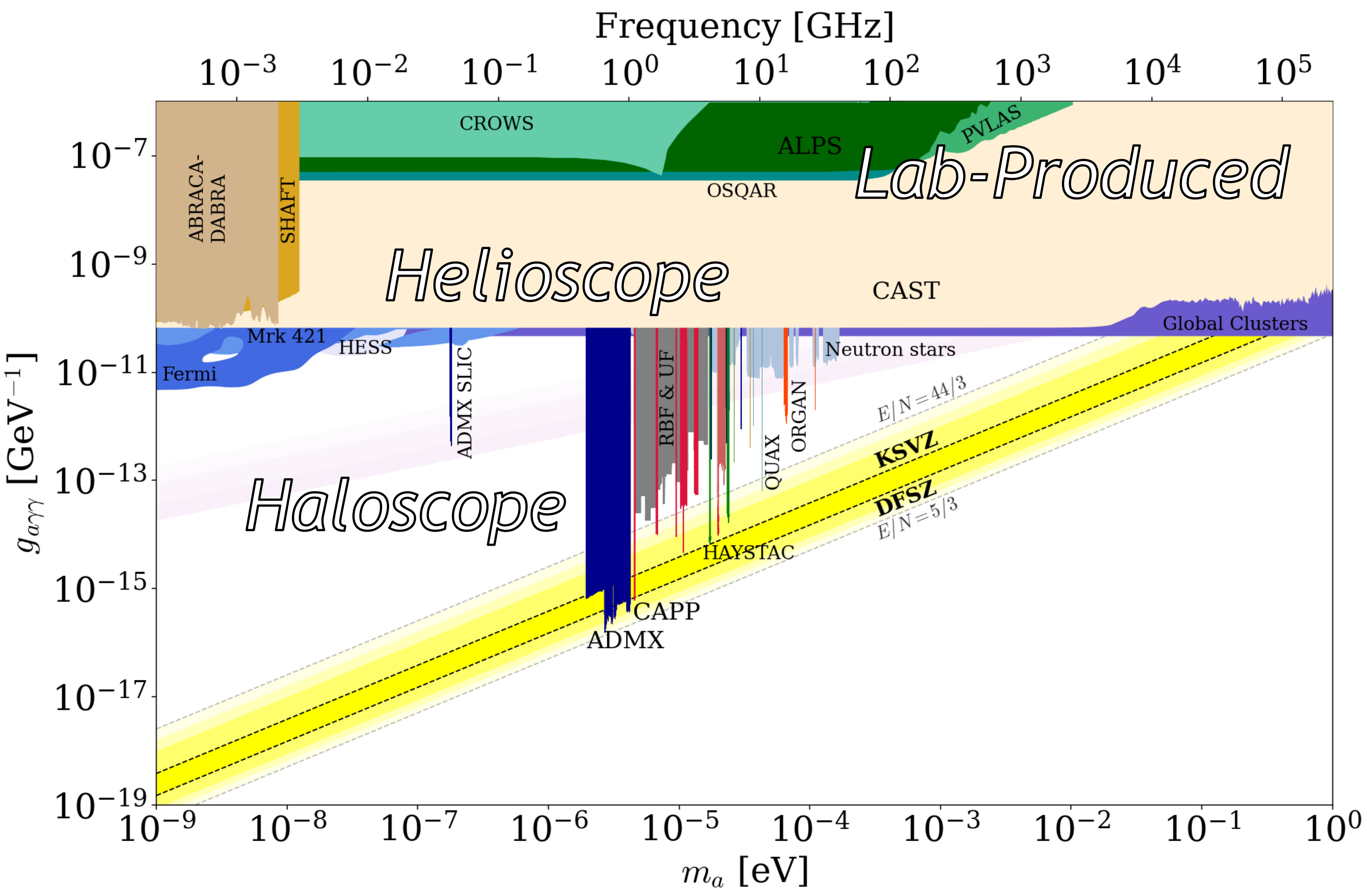

Axion Haloscope

Axion-Photon Coupling

Axion-Fermion Coupling

Axion Source

Dark Matter Axion

Solar Axion

Lab-Produced Axion

Others

Axion Detector

Dark Matter Axion

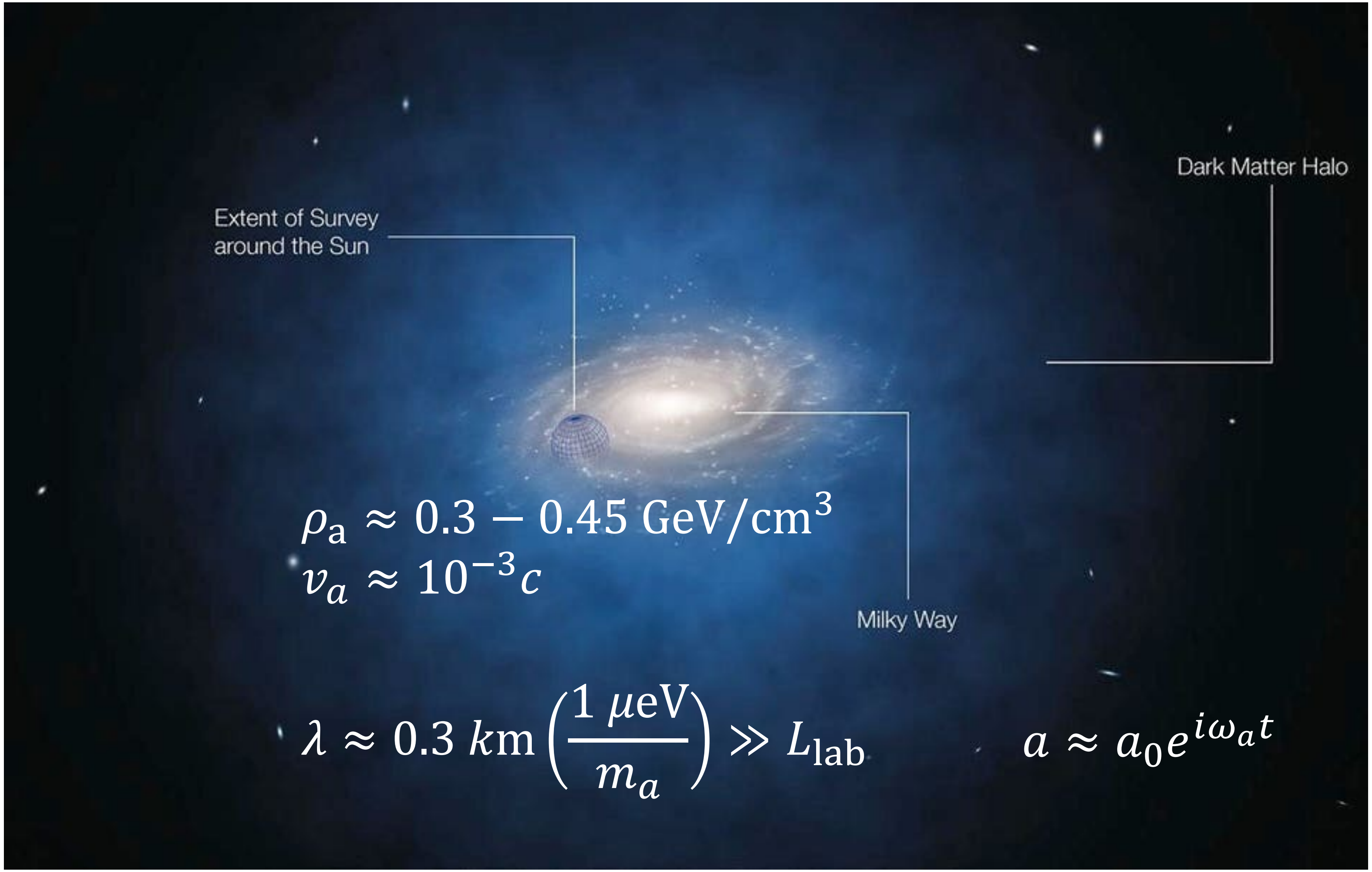

$$\rho_{\mathrm{a}} \approx 0.3 - 0.45\ \mathrm{GeV/cm^3}$$
$$v_a \approx 10^{-3} c$$

$$\lambda \approx 0.3\ km \left(\frac{1\ \mu\mathrm{eV}}{m_a}\right) \gg L_{\mathrm{lab}}$$

$$a \approx a_0 e^{i\omega_a t}$$

Cavity Haloscope

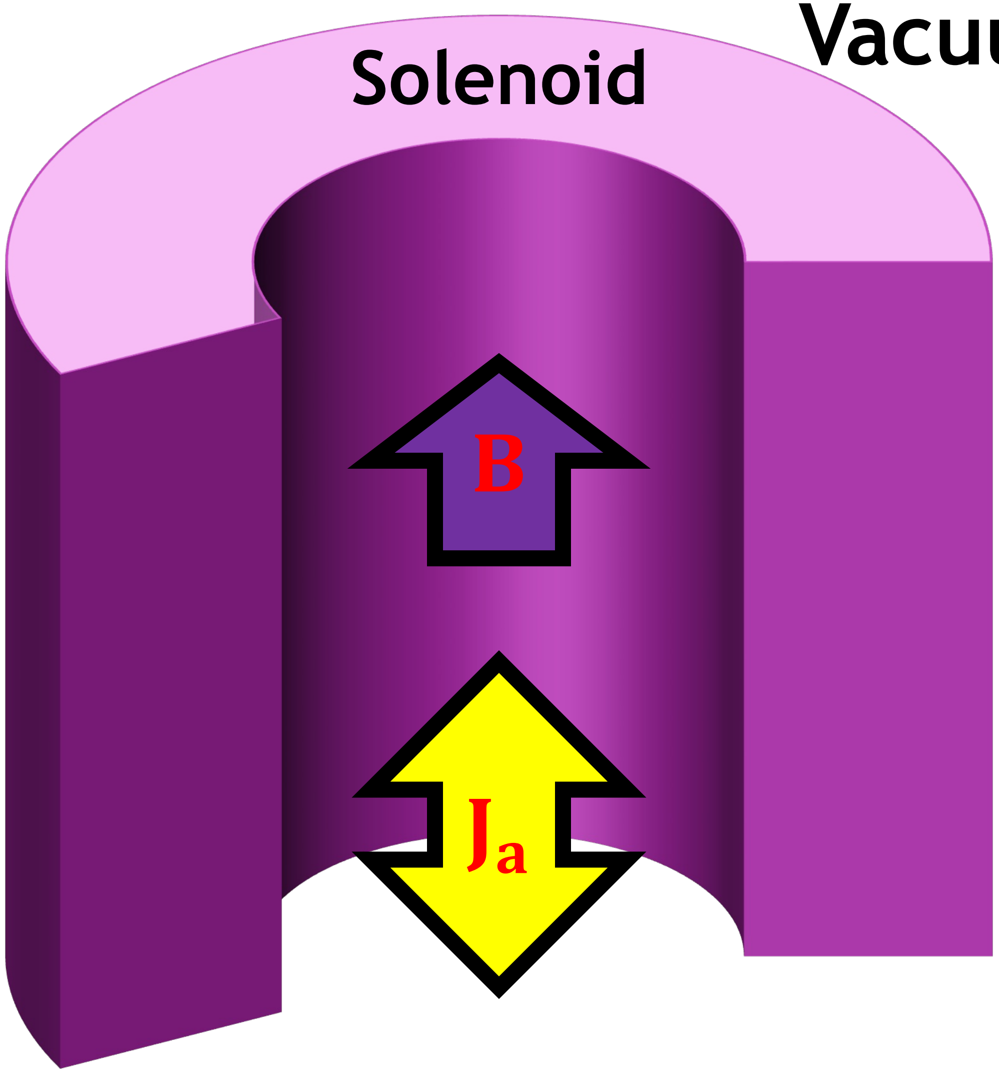

Vacuum current density

$$g_{a\gamma\gamma}(\nabla a \times \mathbf{E} + \partial_t a \mathbf{B})$$

Cavity Haloscope

[P. Sikivie]

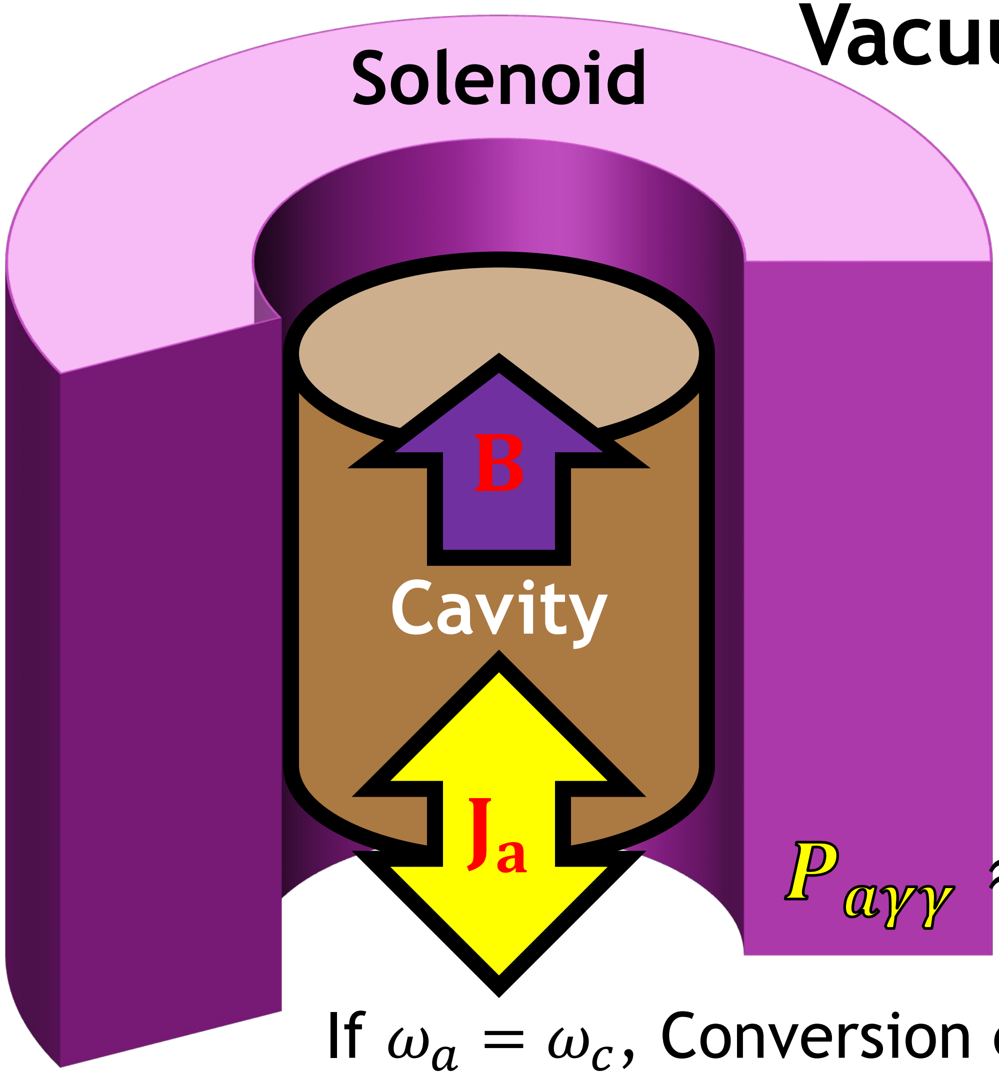

Vacuum current density

$g_{a\gamma\gamma}(\nabla a \times \mathbf{E} + \partial_t a \mathbf{B})$

Conversion

$$P_{a\gamma\gamma} \approx \frac{g_{a\gamma\gamma}^2 \rho_a}{m_a} \langle B^2 \rangle V_c Q_c C$$

If $\omega_a = \omega_c$, Conversion enhanced

Cavity Haloscope

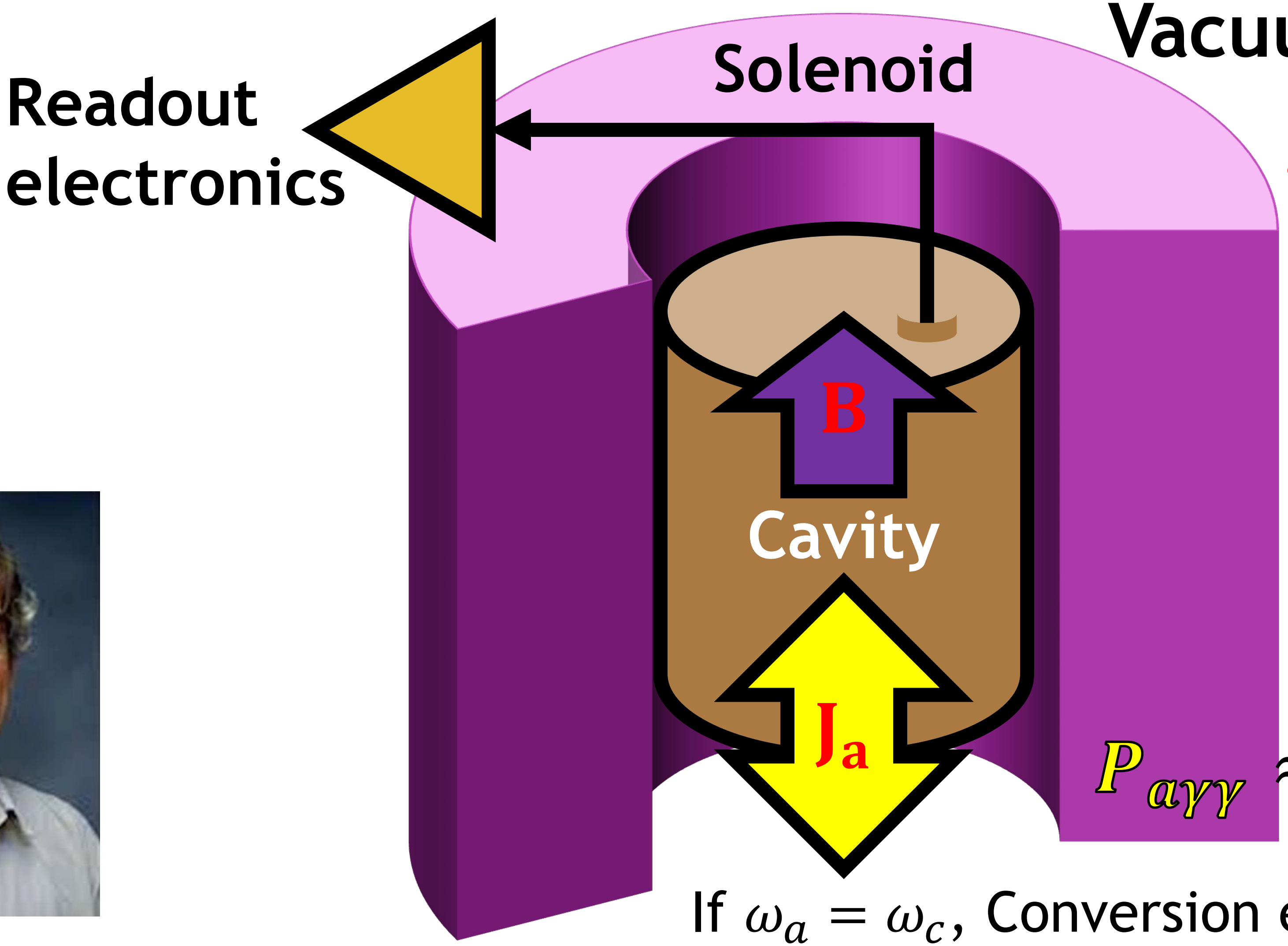

Vacuum current density

$$g_{a\gamma\gamma}(\nabla a \times \mathbf{E} + \partial_t a \mathbf{B})$$

Conversion

$$P_{a\gamma\gamma} \approx \frac{g_{a\gamma\gamma}^2 \rho_a}{m_a} \langle B^2 \rangle V_c Q_c C$$

If $\omega_a = \omega_c$, Conversion enhanced

[P. Sikivie]

Cavity Haloscope

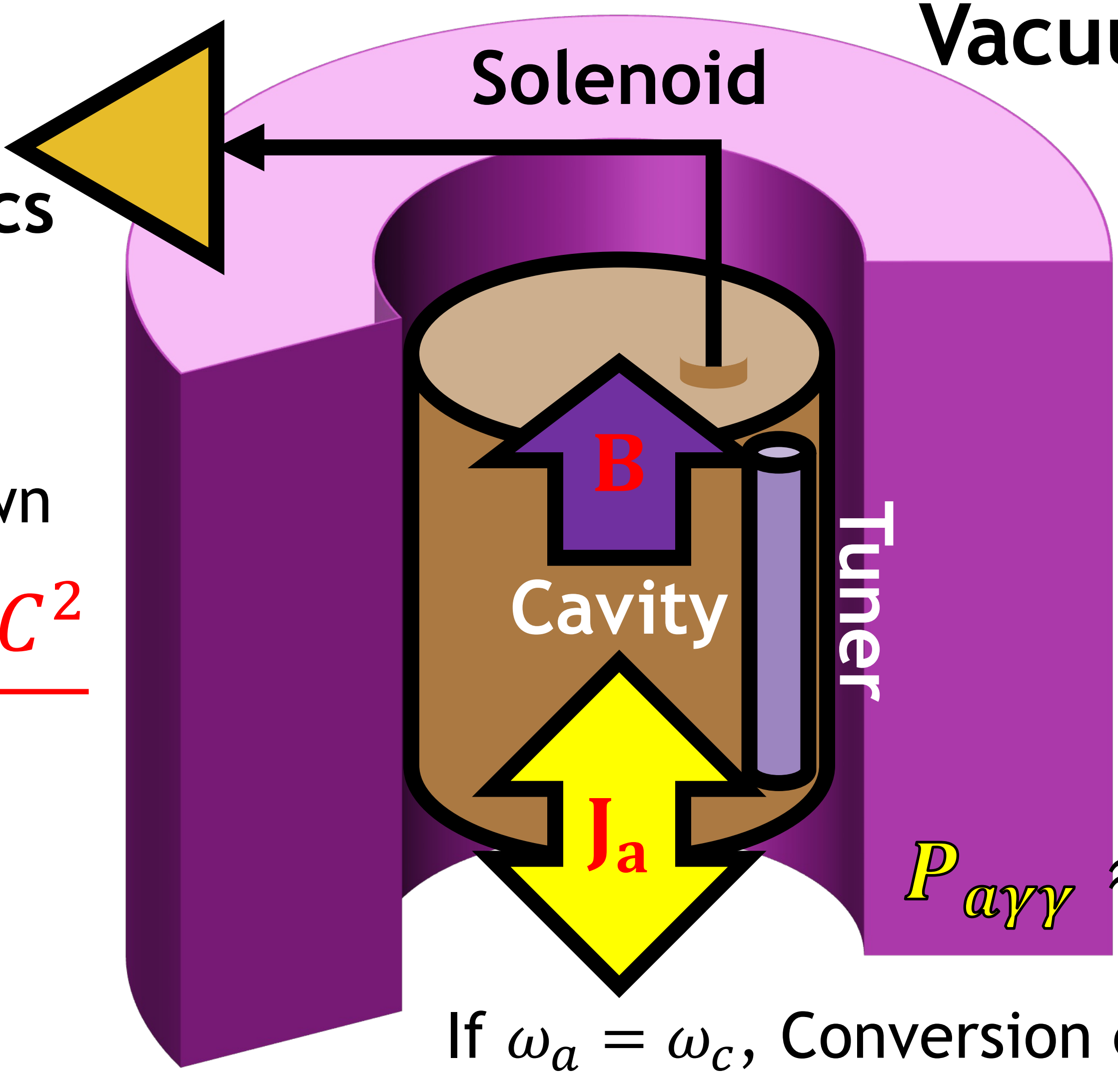

Vacuum current density

$$g_{a\gamma\gamma}(\nabla a \times \mathbf{E} + \partial_t a \mathbf{B})$$

Scanning rate

m_a is *a priori* unknown

$$\frac{df}{dt} \propto \frac{\langle B^2 \rangle^2 V_c^2 Q_c C^2}{T_{sys}^2}$$

Conversion

$$P_{a\gamma\gamma} \approx \frac{g_{a\gamma\gamma}^2 \rho_a}{m_a} \langle B^2 \rangle V_c Q_c C$$

If $\omega_a = \omega_c$, Conversion enhanced

Cavity Haloscope

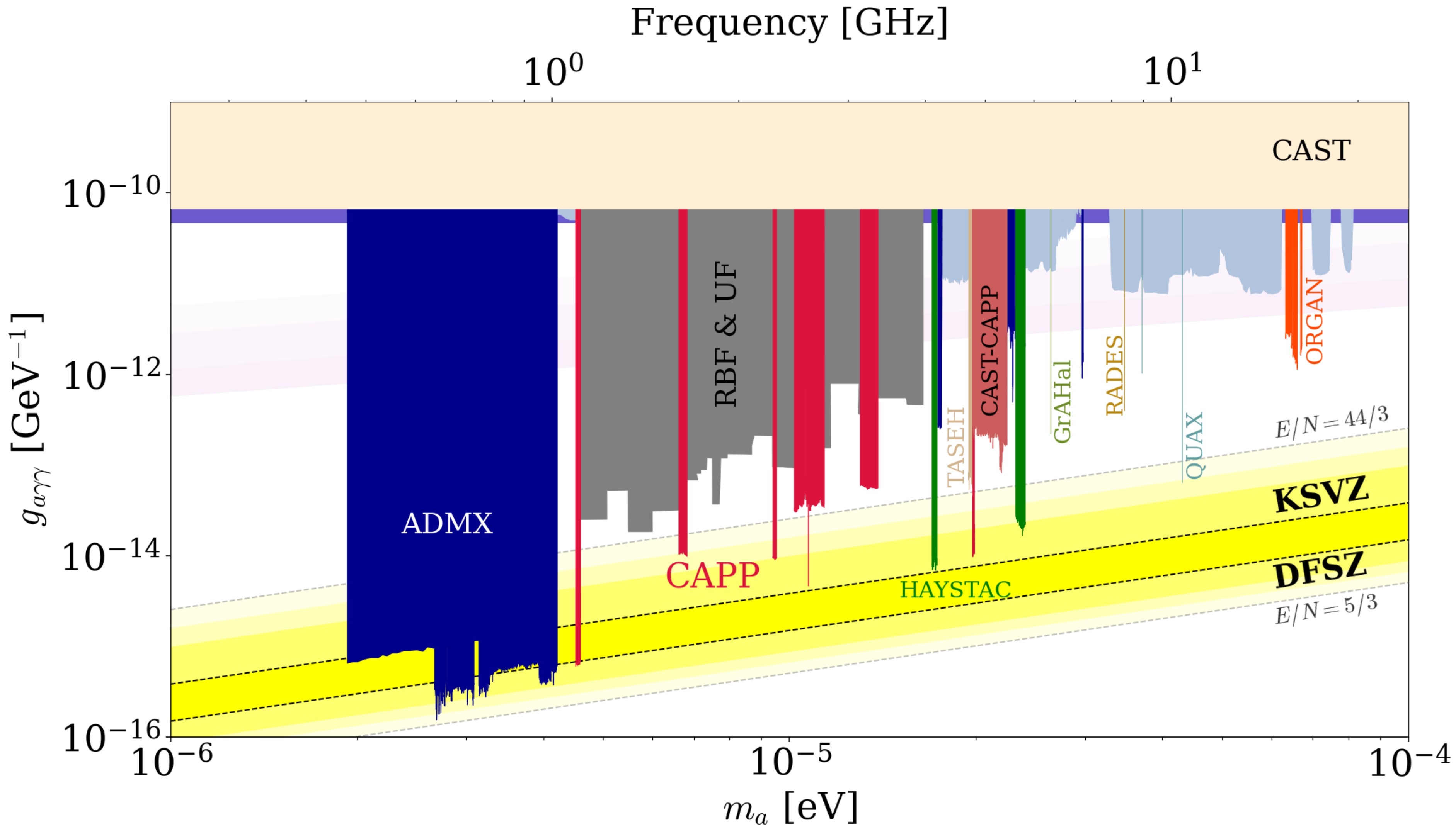

IBS-CAPP at KAIST

Institute for Basic Science
ibs
기초과학연구원
CAPP
Center for
Axion and Precision
Physics Research

Center for Axion and Precision Physics Research

CAPP of Institute for Baisc Science (IBS) at KAIST in Korea since October 2013

Project: Axion dark matter, Storage ring proton EDM, Axion mediated long range force

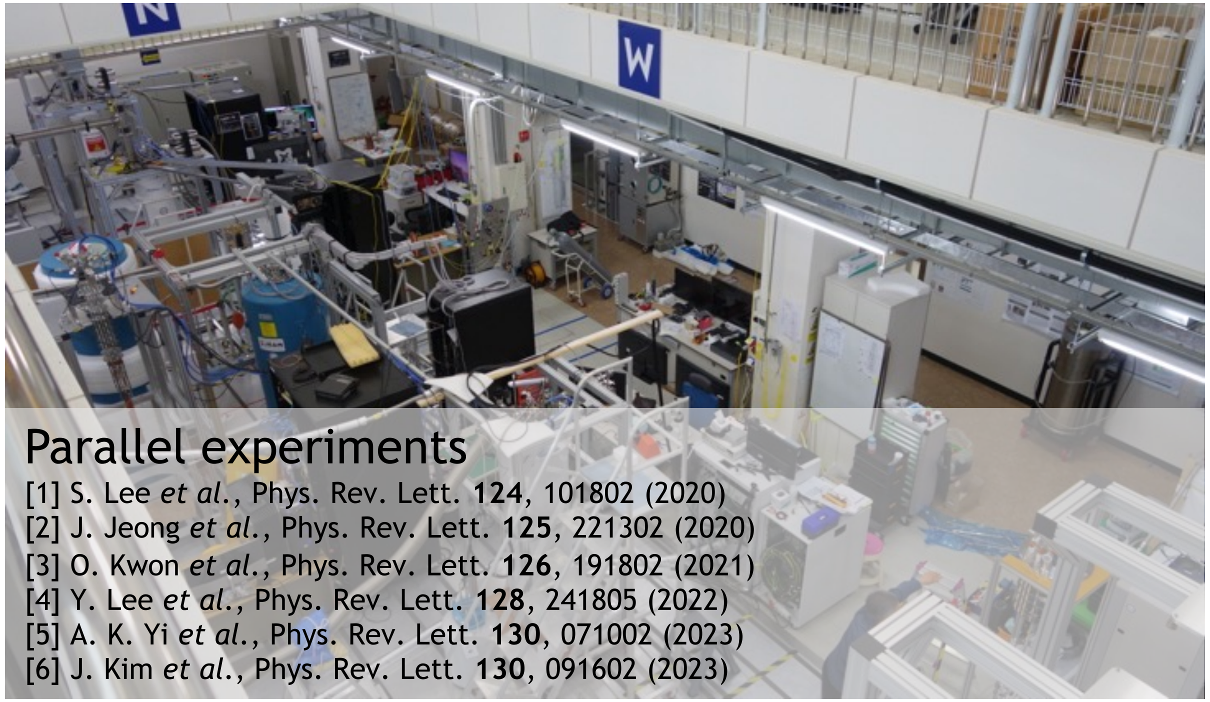

[1] S. Lee *et al.*, Phys. Rev. Lett. **124**, 101802 (2020)
[2] J. Jeong *et al.*, Phys. Rev. Lett. **125**, 221302 (2020)
[3] O. Kwon *et al.*, Phys. Rev. Lett. **126**, 191802 (2021)
[4] Y. Lee *et al.*, Phys. Rev. Lett. **128**, 241805 (2022)
[5] A. K. Yi *et al.*, Phys. Rev. Lett. **130**, 071002 (2023)
[6] J. Kim *et al.*, Phys. Rev. Lett. **130**, 091602 (2023)

CAPP-12TB, our Flagship experiment

$$\frac{df}{dt} \propto \frac{\langle B^2\rangle^2 V_c^2 Q_c C^2}{T_{sys}^2}$$

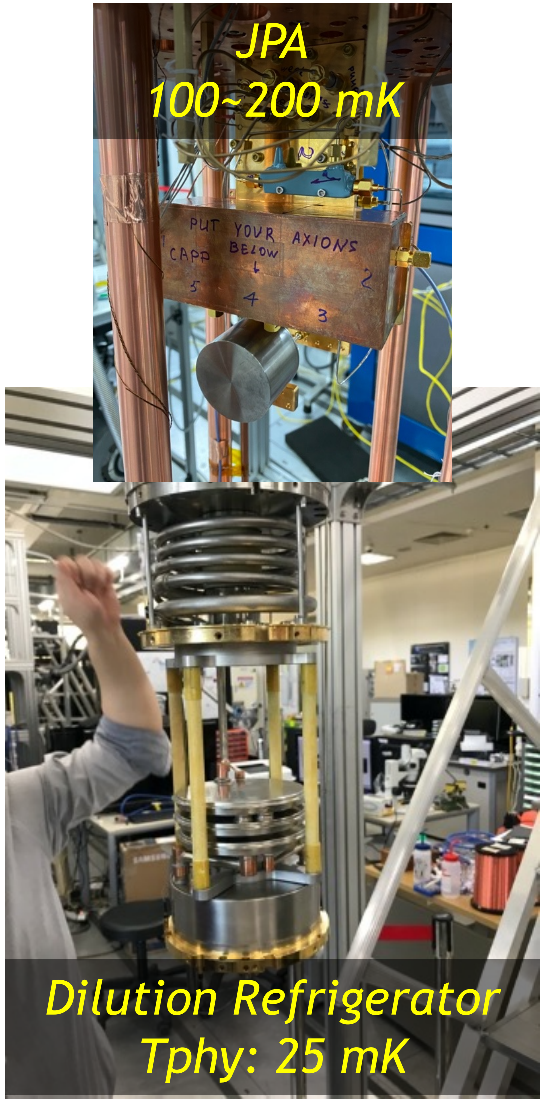

CAPP-12TB, our Flagship experiment

Axion to Photon conversion at 1.15 GHz

- KSVZ: 6.2×10^{-22} W or 10^3 photons/s
- DFSZ: 0.9×10^{-22} W or 10^2 photons/s

With T_{sys} of 200 mK ($Q_c = 10^5$, eff.=0.8)

- KSVZ: 50 GHz/year
- DFSZ: 1 GHz/year

$$\frac{df}{dt} \propto \frac{\langle B^2\rangle^2 V_c^2 Q_c C^2}{T_{sys}^2}$$

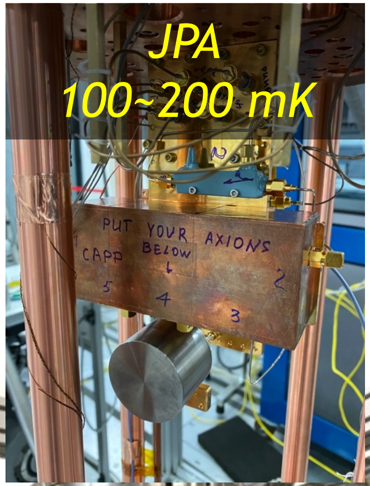

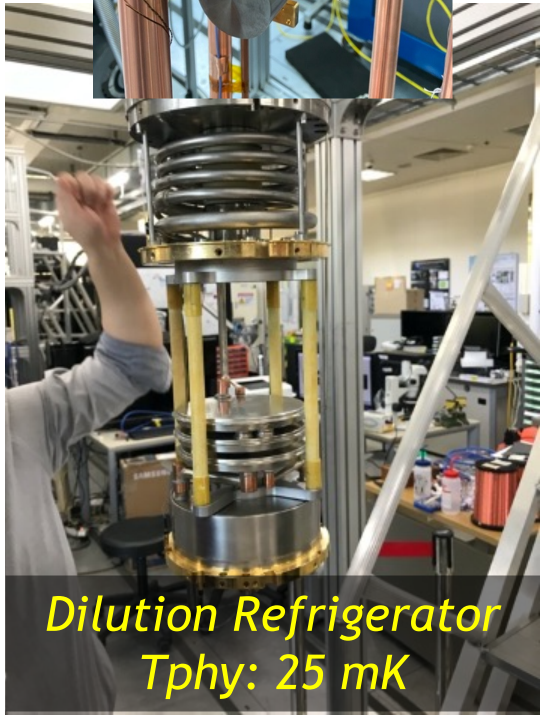

CAPP-12TB, our Flagship experiment

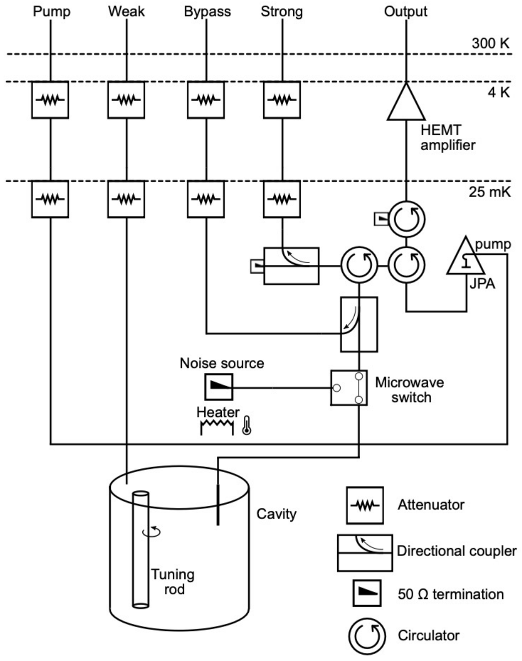

FIG. 2: CAPP-12TB receiver diagram.

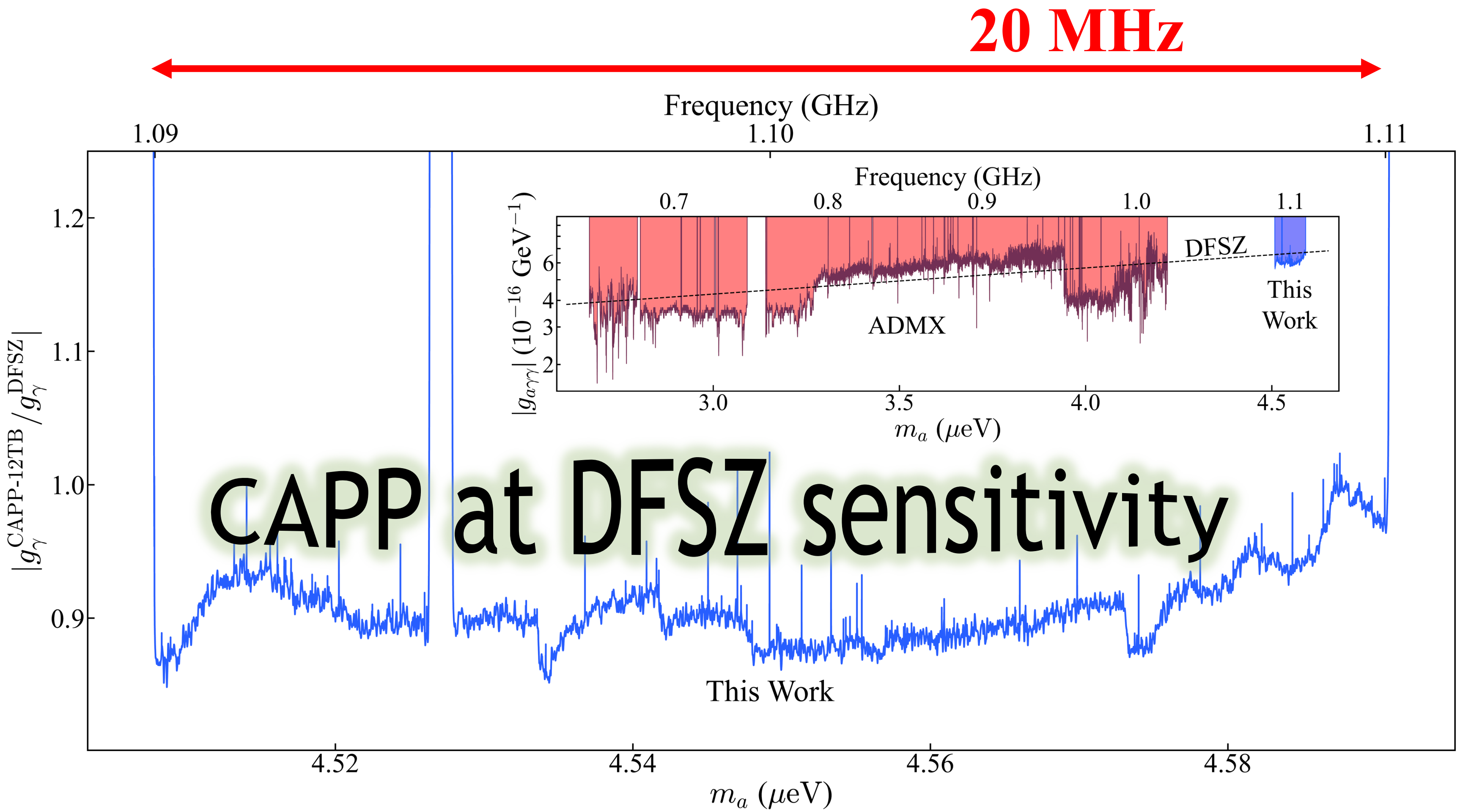

[*A. K. Yi et al.*, Phys. Rev. Lett. **130**, 071002 (2023)]

CAPP-12TB, our Flagship experiment

CAPP-12TB, our Flagship experiment

Preliminary results extending search frequencies, (3 MHz/day)

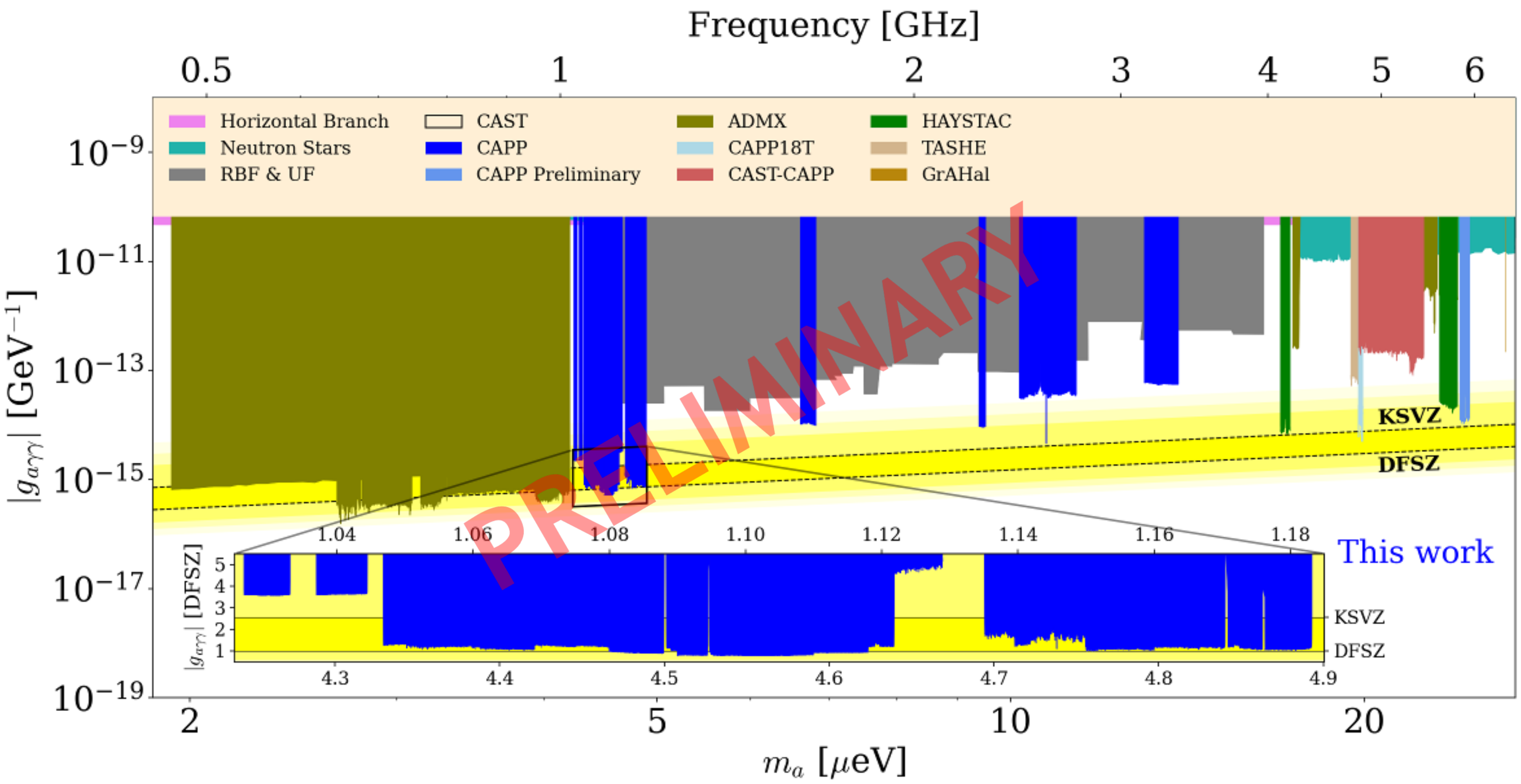

Exclusion Limits

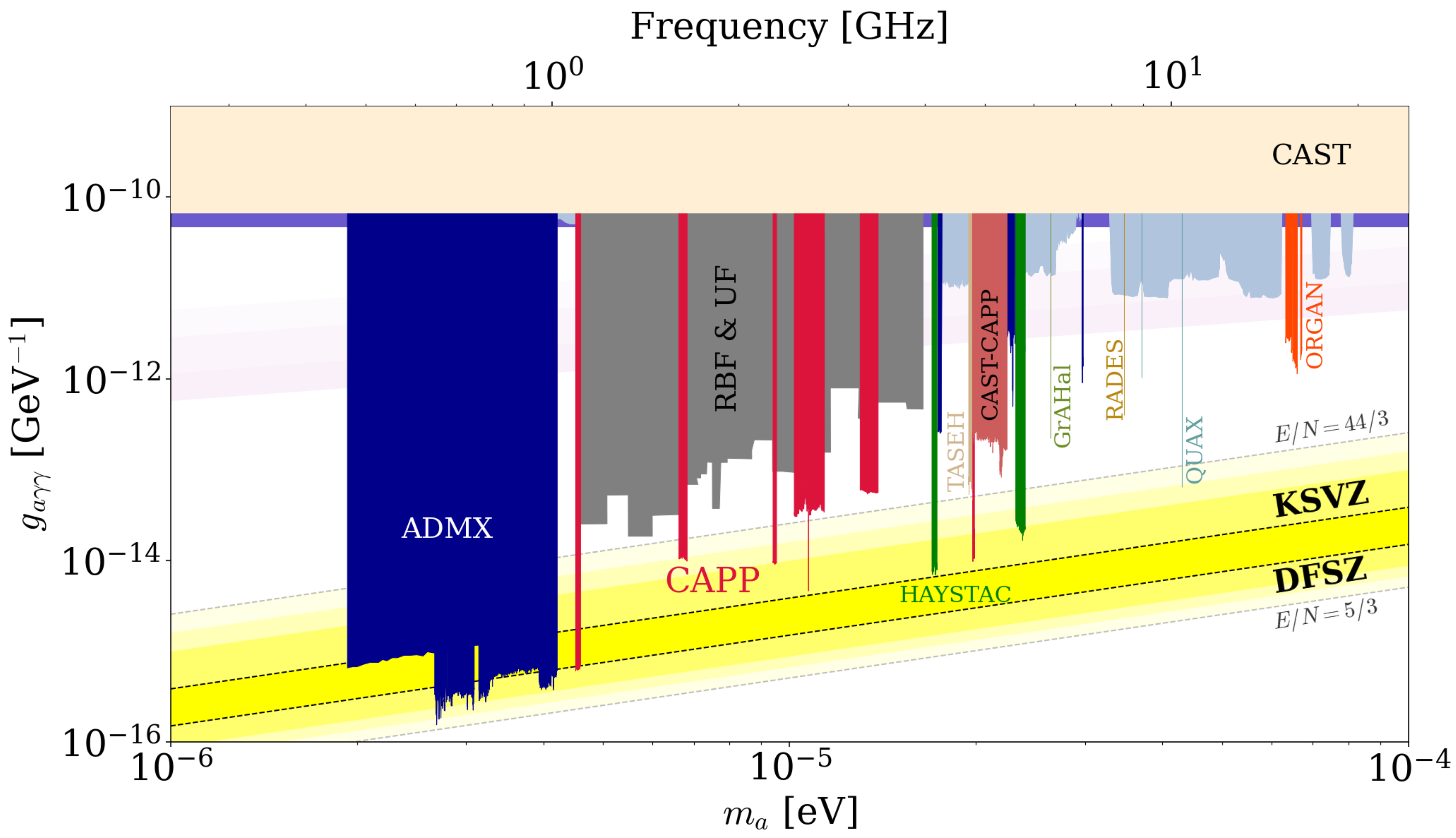

Preliminary

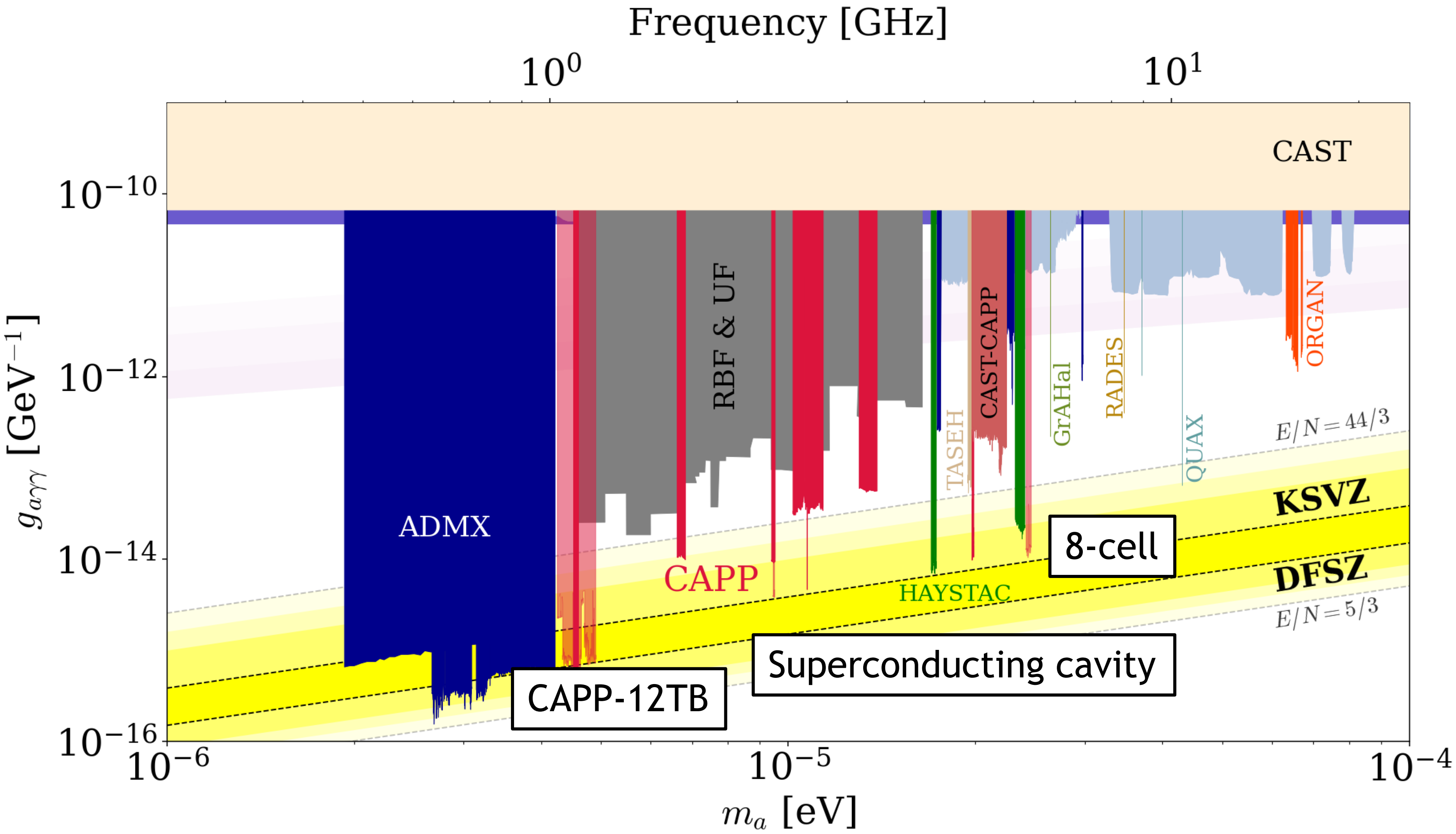

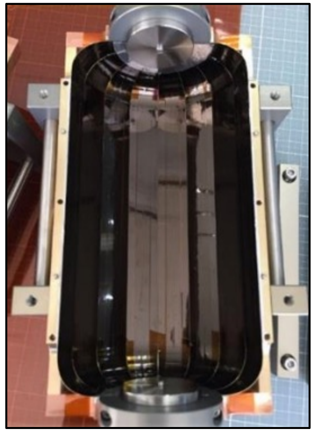

Future Plan

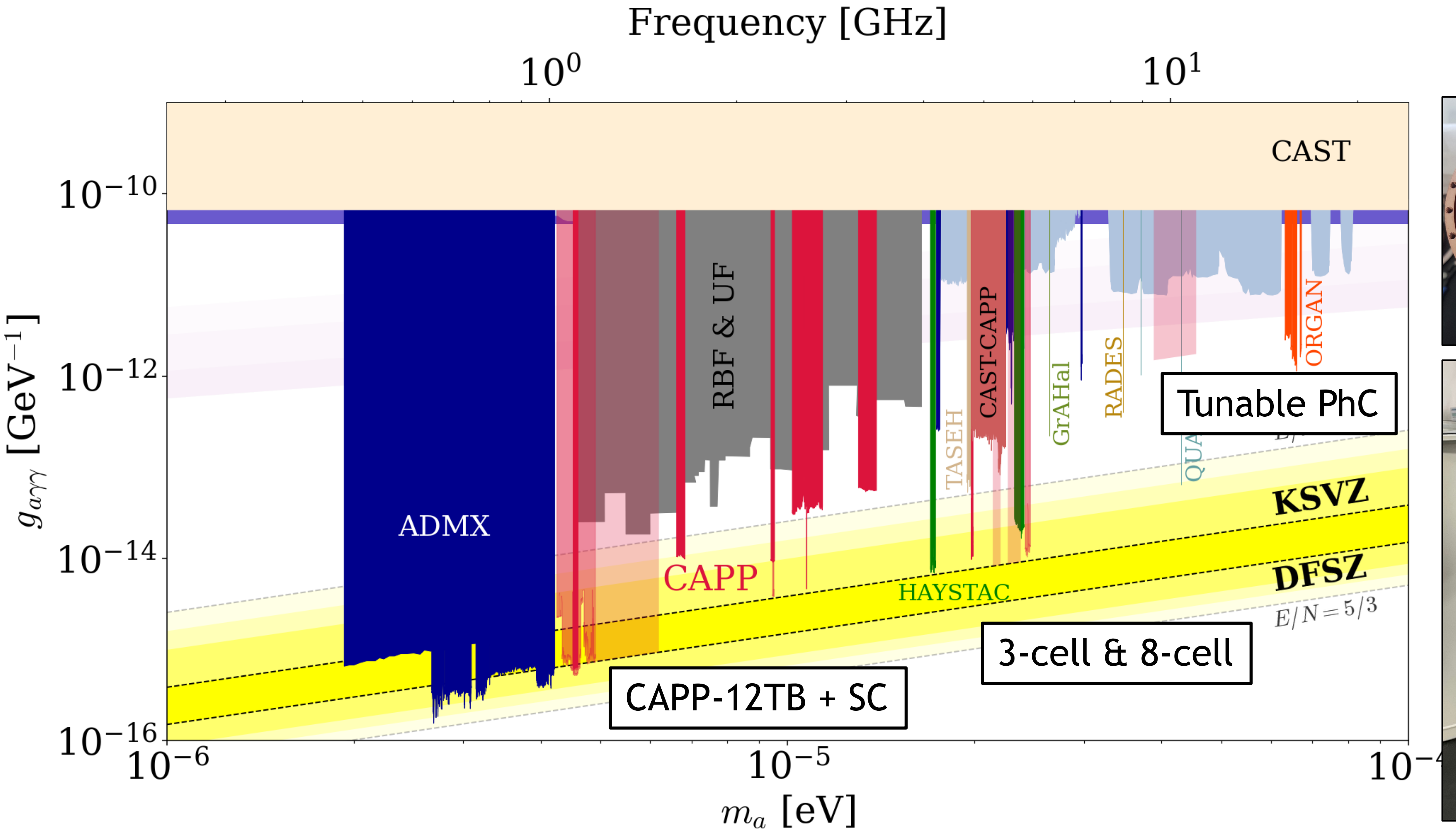

Frequency [GHz]
10^0
10^1
CAST
10^{-10}
10^{-12}
10^{-14}
10^{-16}
$g_{a\gamma\gamma}$ [GeV^{-1}]
ADMX
RBF & UF
CAPP
TASEH
CAST-CAPP
GrAHal
RADES
ORGAN
HAYSTAC
Tunable PhC
KSVZ
DFSZ
$E/N = 5/3$
3-cell & 8-cell
CAPP-12TB + SC
10^{-6}
10^{-5}
m_a [eV]

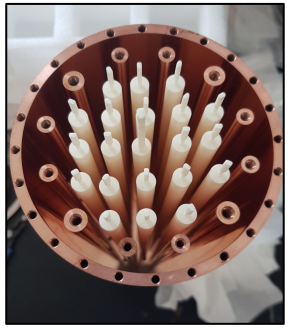

Dielectric Haloscope

$$\nabla \cdot \mathbf{E} = \rho_e - g_{a\gamma\gamma} \nabla a \cdot \mathbf{B}$$
$$\nabla \cdot \mathbf{B} = 0$$
$$\nabla \times \mathbf{E} = -\partial_t \mathbf{B}$$
$$\nabla \times \mathbf{B} = \partial_t \mathbf{E} + \mathbf{J}_e + g_{a\gamma\gamma}(\nabla a \times \mathbf{E} + \partial_t a \mathbf{B})$$

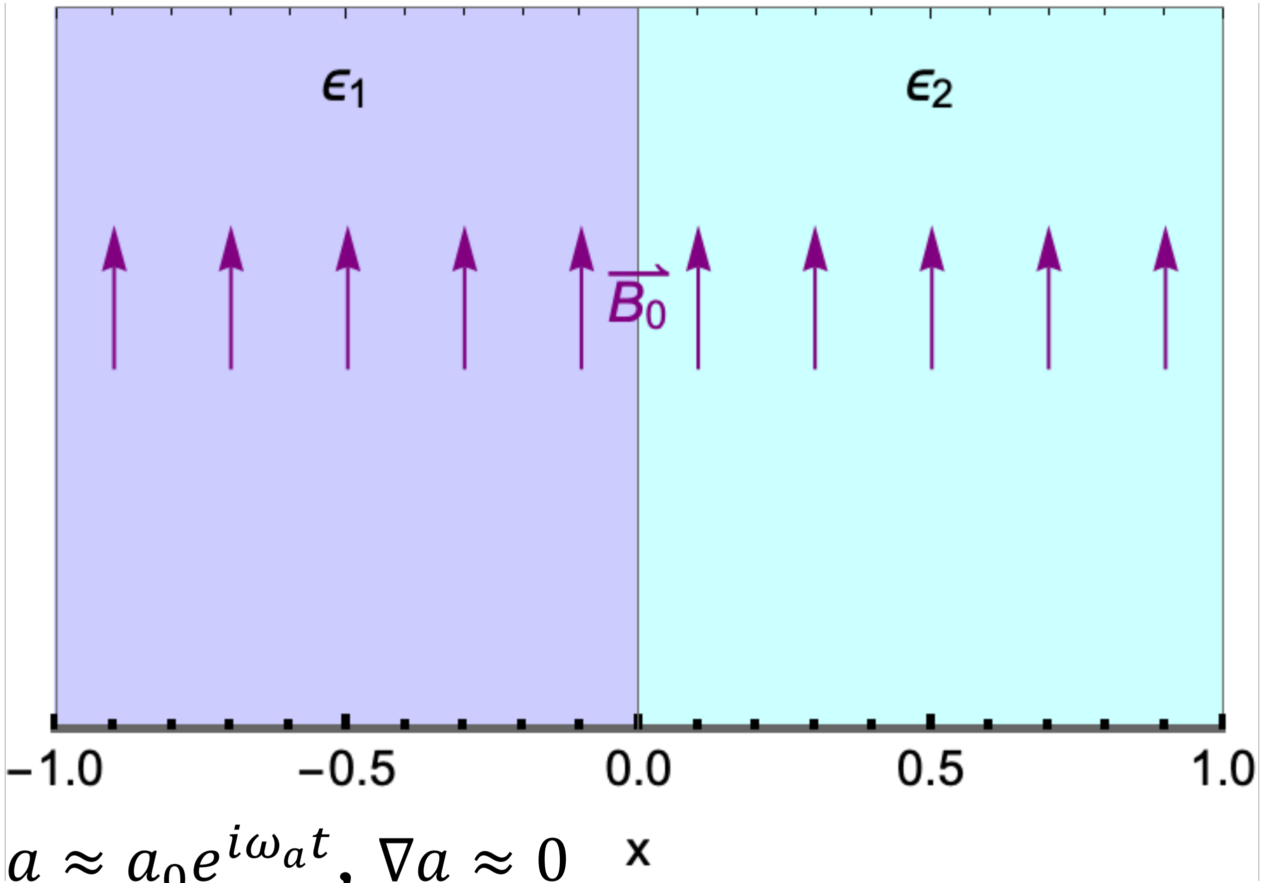

$a \approx a_0 e^{i\omega_a t}$, $\nabla a \approx 0$

Dielectric Haloscope

$$\nabla \cdot \mathbf{E} = \rho_e - g_{a\gamma\gamma} \nabla a \cdot \mathbf{B}$$
$$\nabla \cdot \mathbf{B} = 0$$
$$\nabla \times \mathbf{E} = -\partial_t \mathbf{B}$$
$$\nabla \times \mathbf{B} = \partial_t \mathbf{E} + \mathbf{J}_e + g_{a\gamma\gamma}(\nabla a \times \mathbf{E} + \partial_t a \mathbf{B})$$

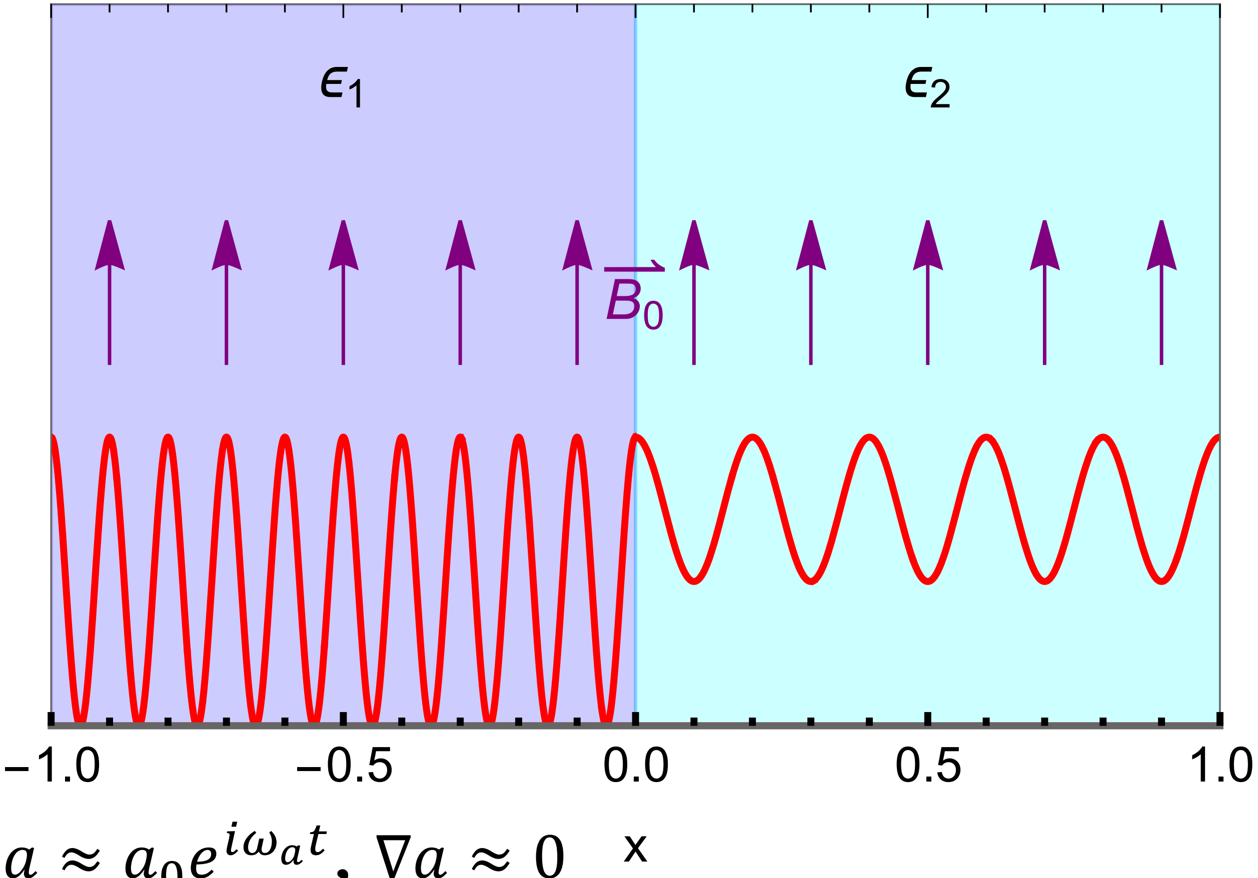

$a \approx a_0 e^{i\omega_a t}$, $\nabla a \approx 0$

$$\frac{P_{a\gamma\gamma}}{A} \approx \left[\frac{g_{a\gamma\gamma}^2 \rho_a \hbar^3}{m_a^2}\right] \frac{1}{\mu} f(\epsilon_1, \epsilon_2) B_0^2$$

Dielectric Haloscope

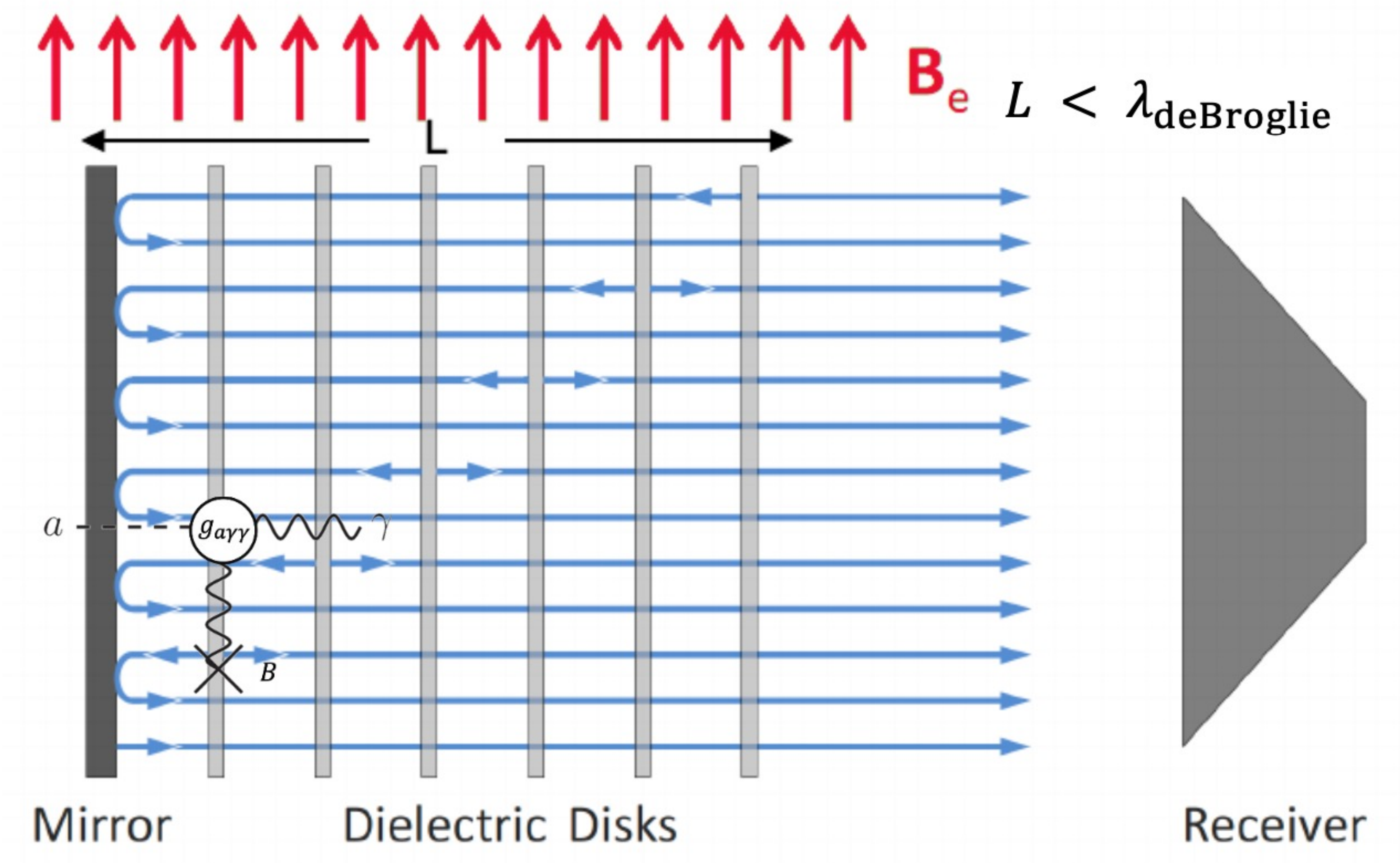

[Erika Garutti, PATRAS 2023]

$$\frac{P_{a\gamma\gamma}}{A} = \left[\frac{g_{a\gamma\gamma}^2 \rho_a}{m_a^2 c/\hbar^3}\right]\frac{c}{\mu}|\mathbf{B}_0 \times \hat{n}|^2 \beta^2$$

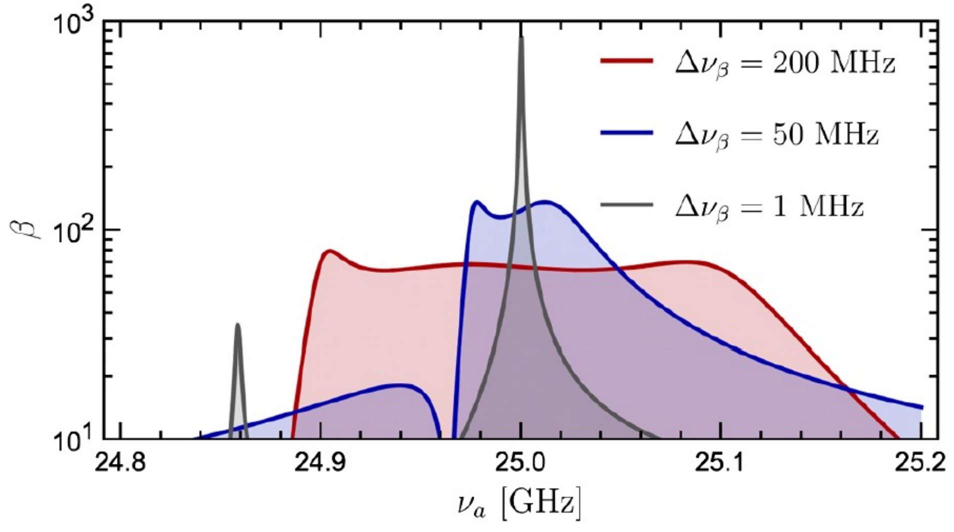

- Spacing determines frequency
- Huge magnet volume available

MADMAX

MAgnetized **D**isk and **M**irror **A**xion e**X**periment

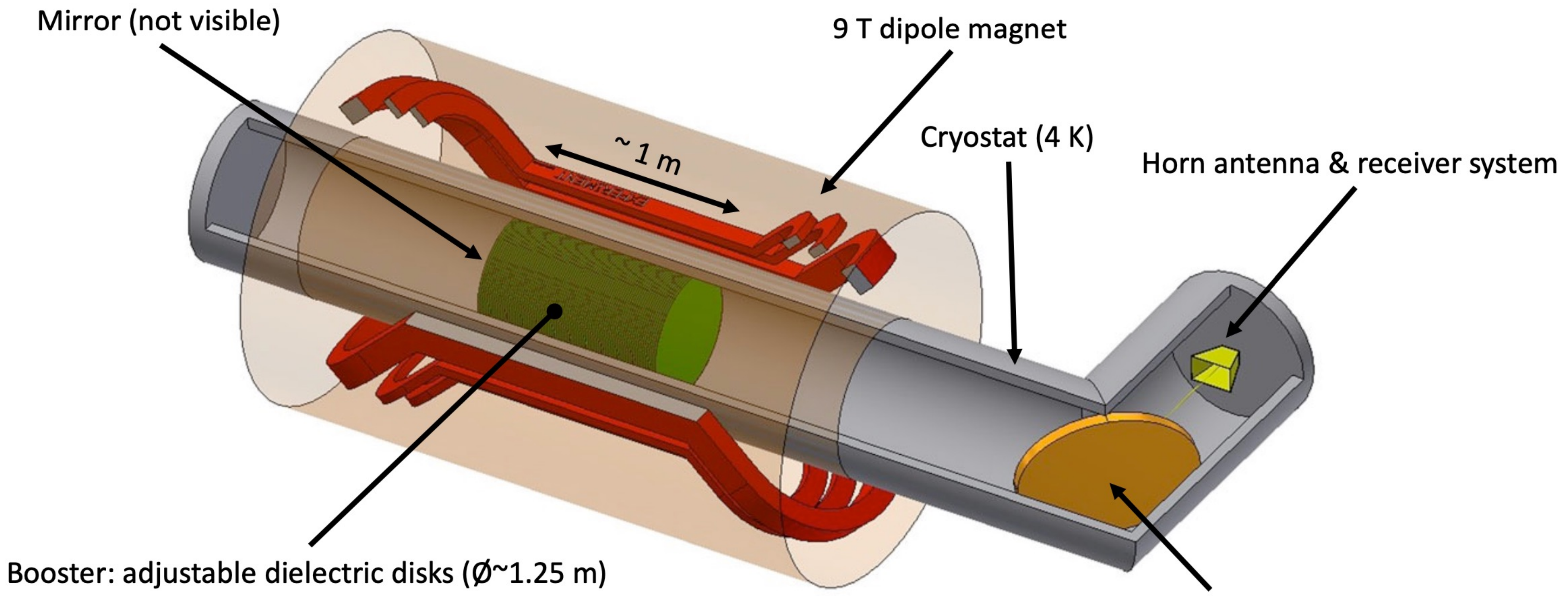

[Eur. Phys. J. C **79** (2019) 186]

MADMAX

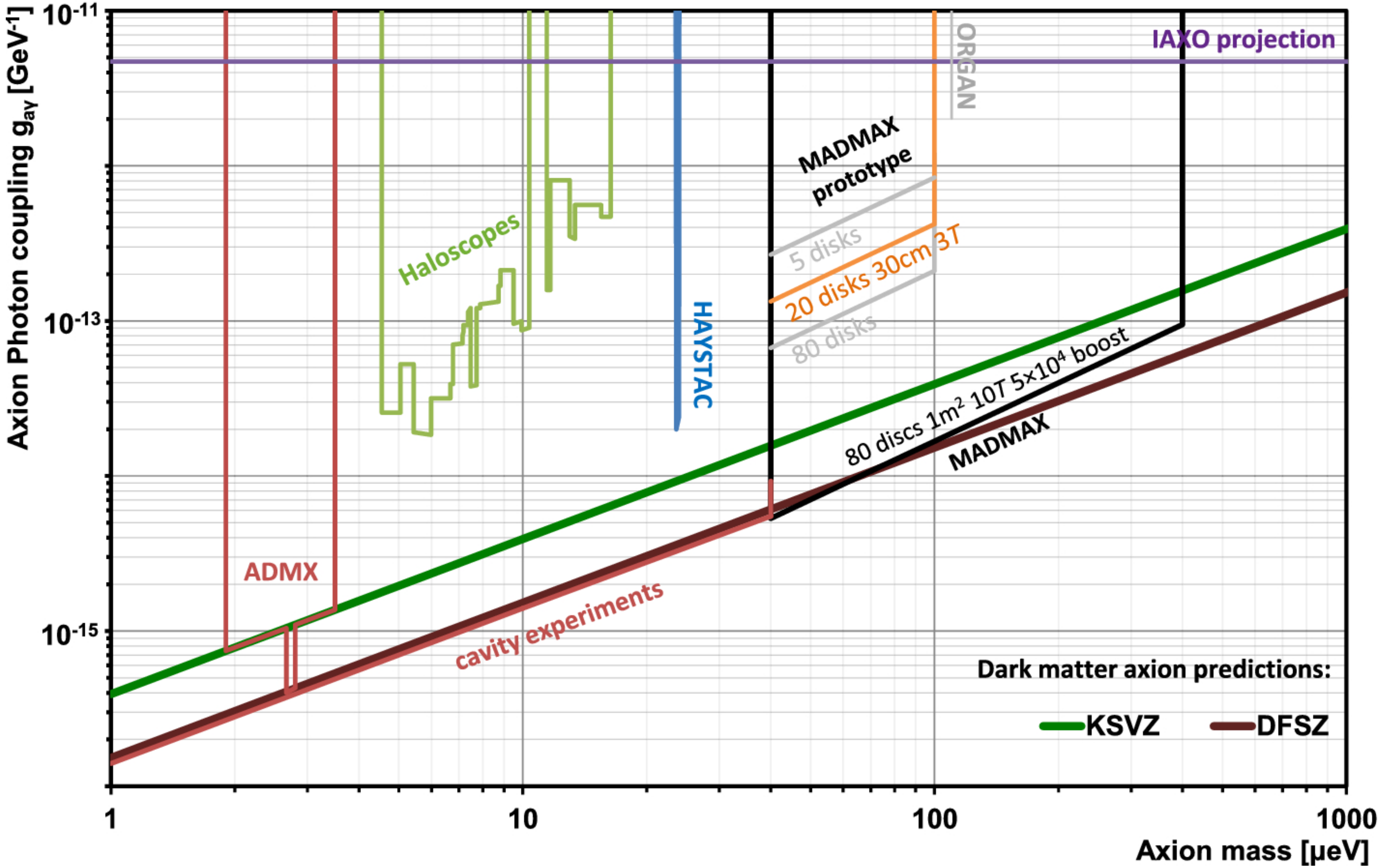

[Eur. Phys. J. C **79** (2019) 186]

Dish Antenna Haloscope

$$\nabla\cdot\mathbf{E} = \rho_e - g_{a\gamma\gamma}\nabla a\cdot\mathbf{B}$$

$$\nabla\cdot\mathbf{B} = 0$$

$$\nabla\times\mathbf{E} = -\partial_t\mathbf{B}$$

$$\nabla\times\mathbf{B} = \partial_t\mathbf{E} + \mathbf{J}_e + g_{a\gamma\gamma}(\nabla a\times\mathbf{E} + \partial_t a\mathbf{B})$$

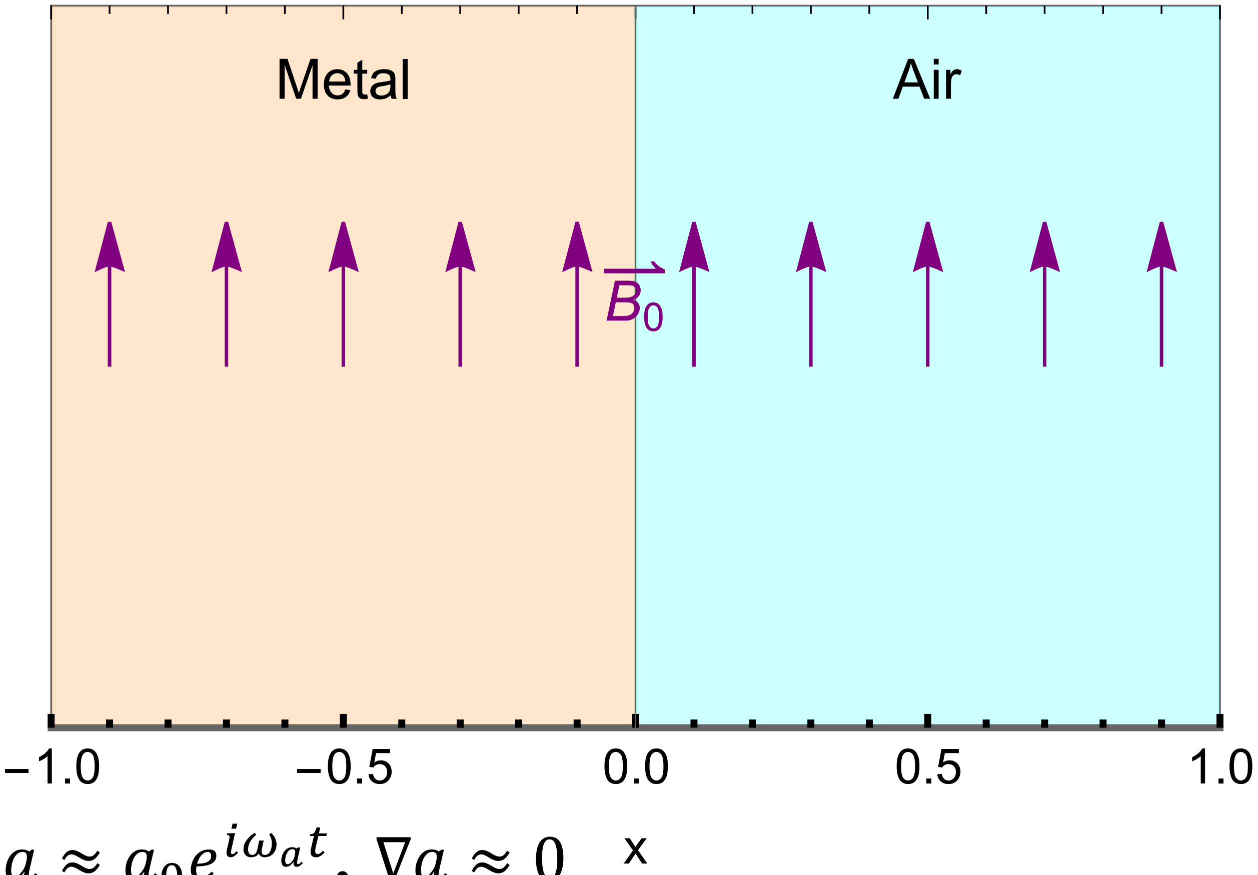

$a \approx a_0 e^{i\omega_a t}$, $\nabla a \approx 0$

Dish Antenna Haloscope

$$\nabla \cdot \mathbf{E} = \rho_e - g_{a\gamma\gamma} \nabla a \cdot \mathbf{B}$$
$$\nabla \cdot \mathbf{B} = 0$$
$$\nabla \times \mathbf{E} = -\partial_t \mathbf{B}$$
$$\nabla \times \mathbf{B} = \partial_t \mathbf{E} + \mathbf{J}_e + g_{a\gamma\gamma}(\nabla a \times \mathbf{E} + \partial_t a \mathbf{B})$$

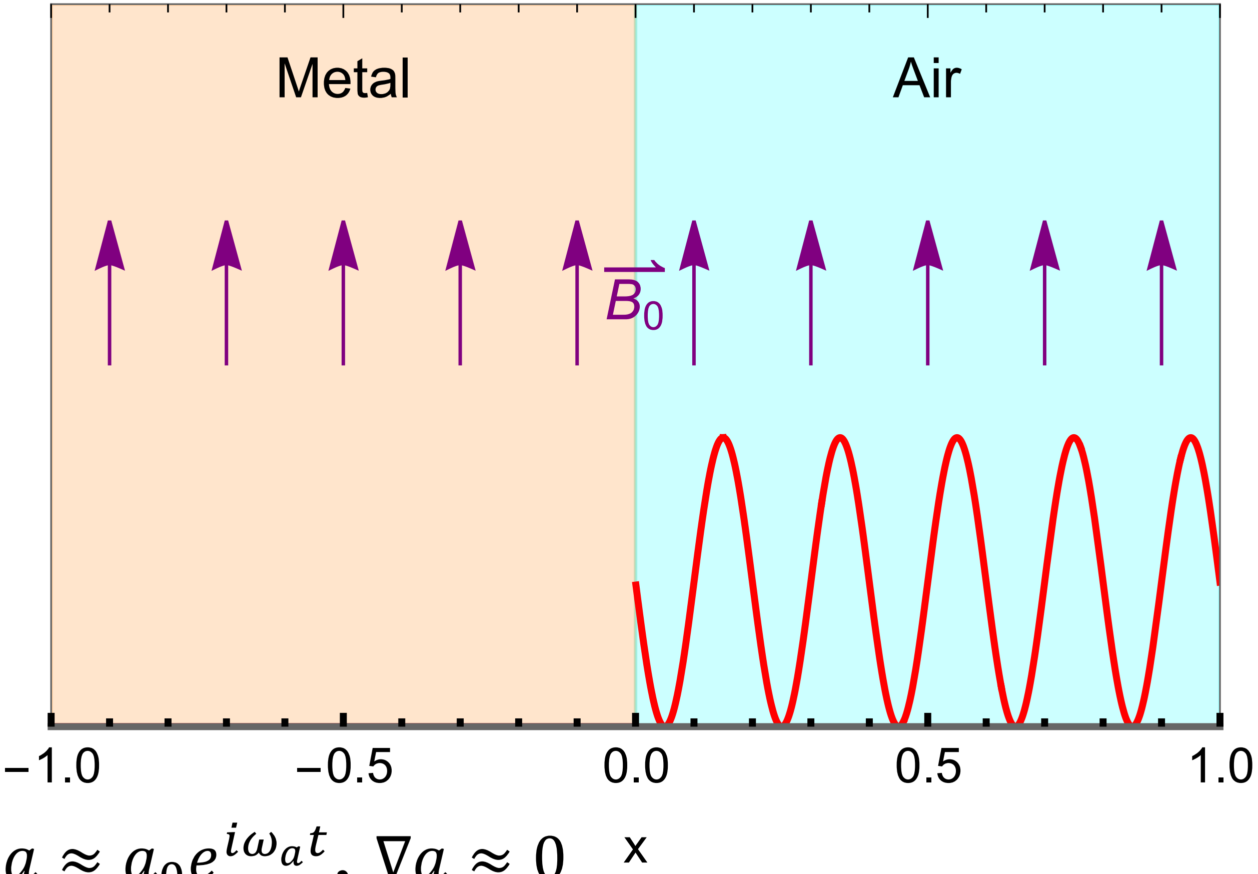

$a \approx a_0 e^{i\omega_a t}$, $\nabla a \approx 0$

$$\frac{P_{a\gamma\gamma}}{A} \approx \left[\frac{g_{a\gamma\gamma}^2 \rho_a \hbar^3}{m_a^2}\right] \frac{1}{\mu} B_0^2$$

Dish Antenna Haloscope

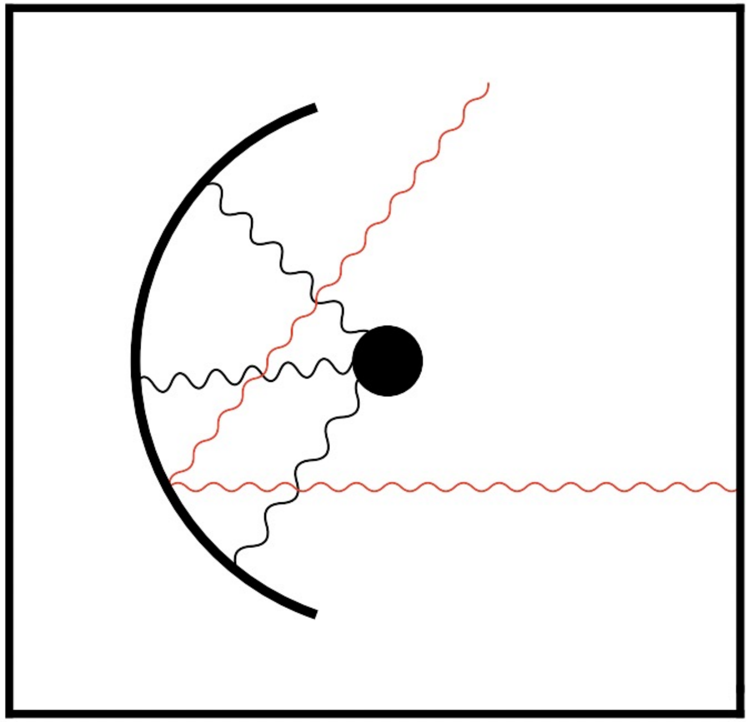

Circular antenna
[JCAP04(2013)016]

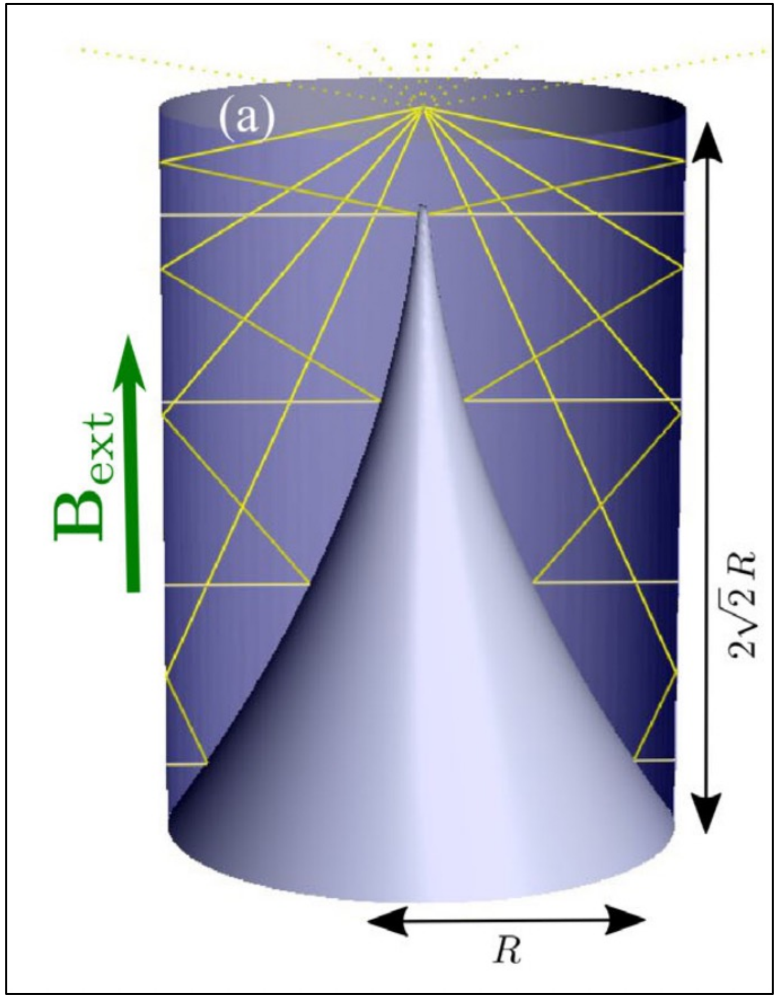

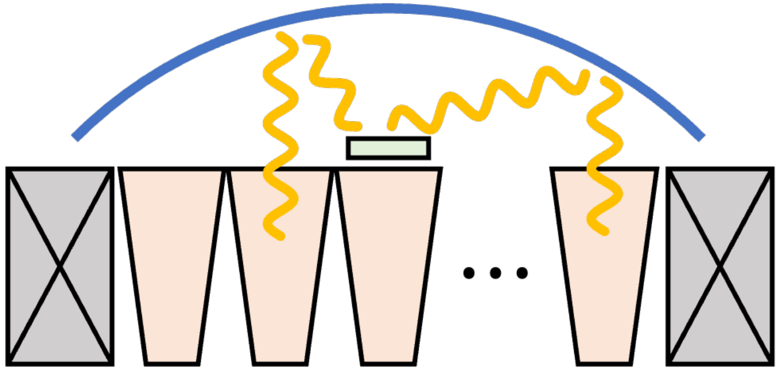

Array of horn antenna
[arXiv:2306.11317]

- Broadband search
- Much higher frequencies

Solenoidal antenna with a parabolid [PRL **128** 131801]

BREAD (Broadband Reflector Experiment for Axion Detection)

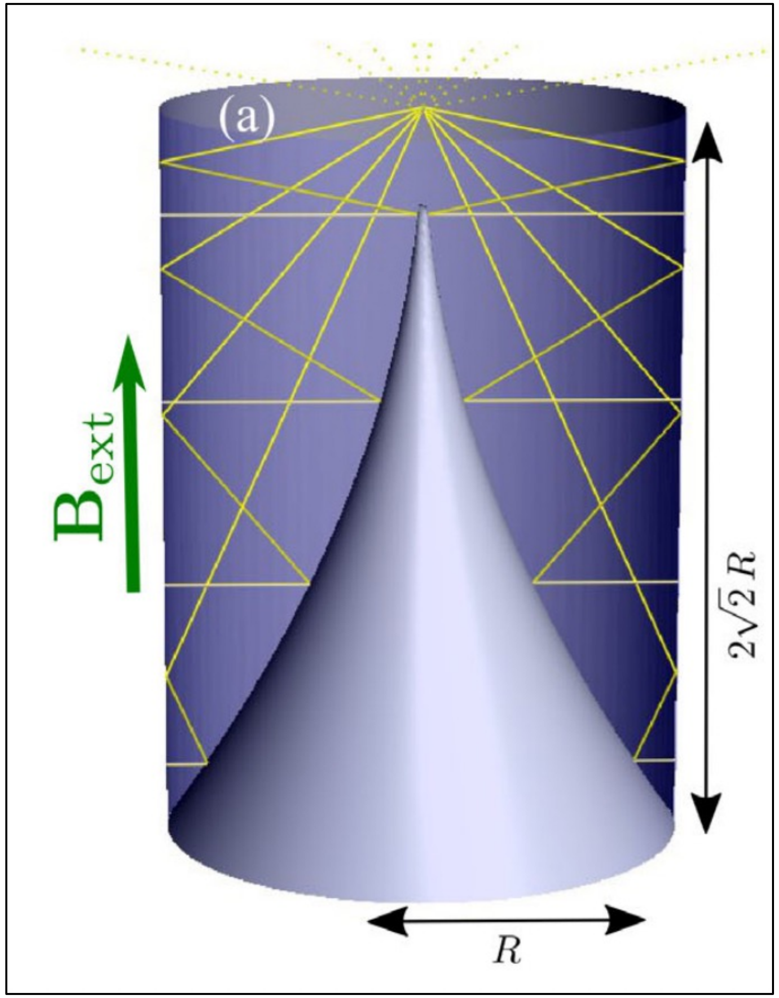

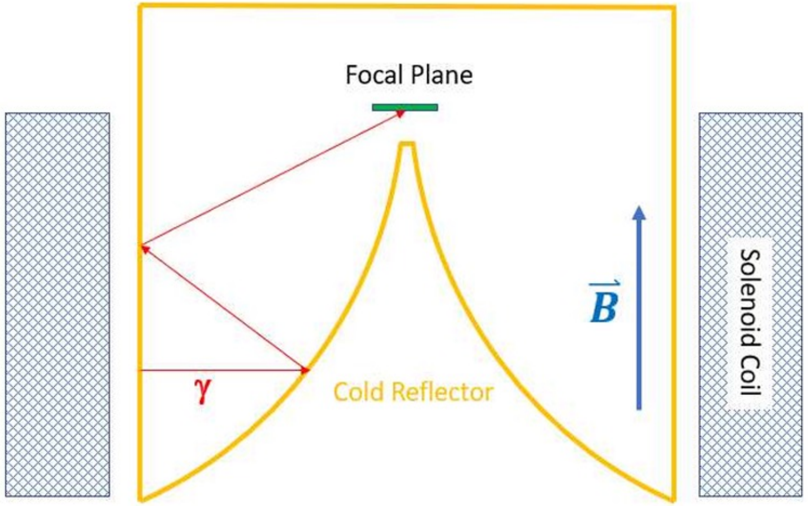

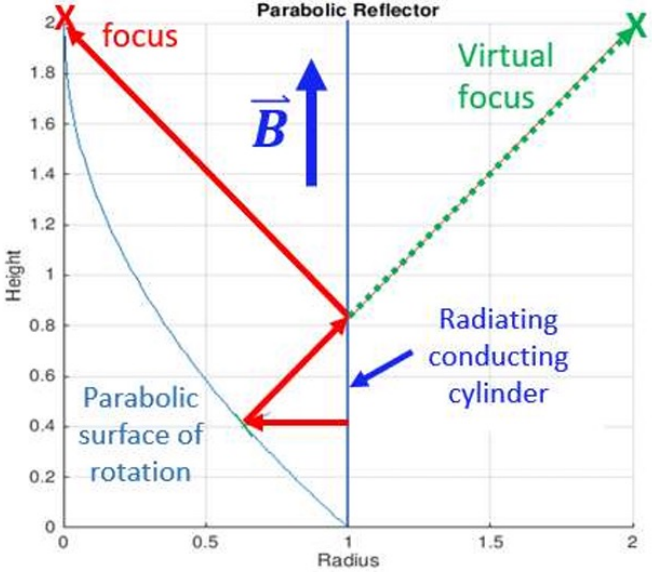

$$P_{\mathrm{BREAD}} \approx 1.3\times10^{-25}\mathrm{W}\left(\frac{B_0}{10\ \mathrm{T}}\right)^2\left(\frac{g_\gamma}{0.97}\right)^2\left(\frac{R}{0.75\ \mathrm{m}}\right)\left(\frac{h}{2.1\ \mathrm{m}}\right)$$

[Andrew Sonnenschein, CPAD Workshop 2021]

BREAD (Broadband Reflector Experiment for Axion Detection)

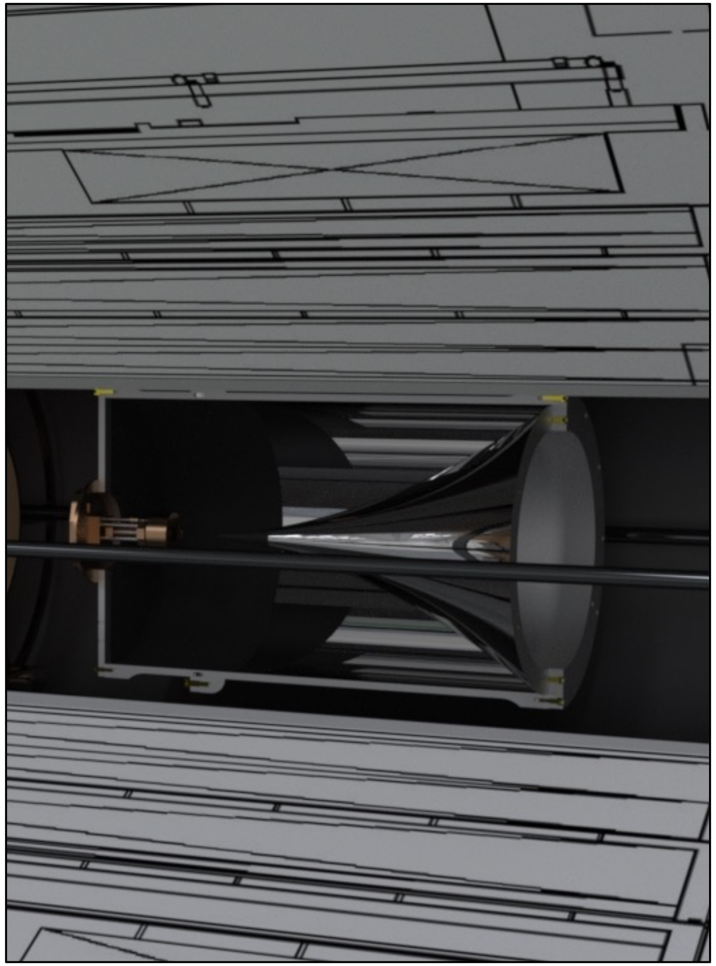

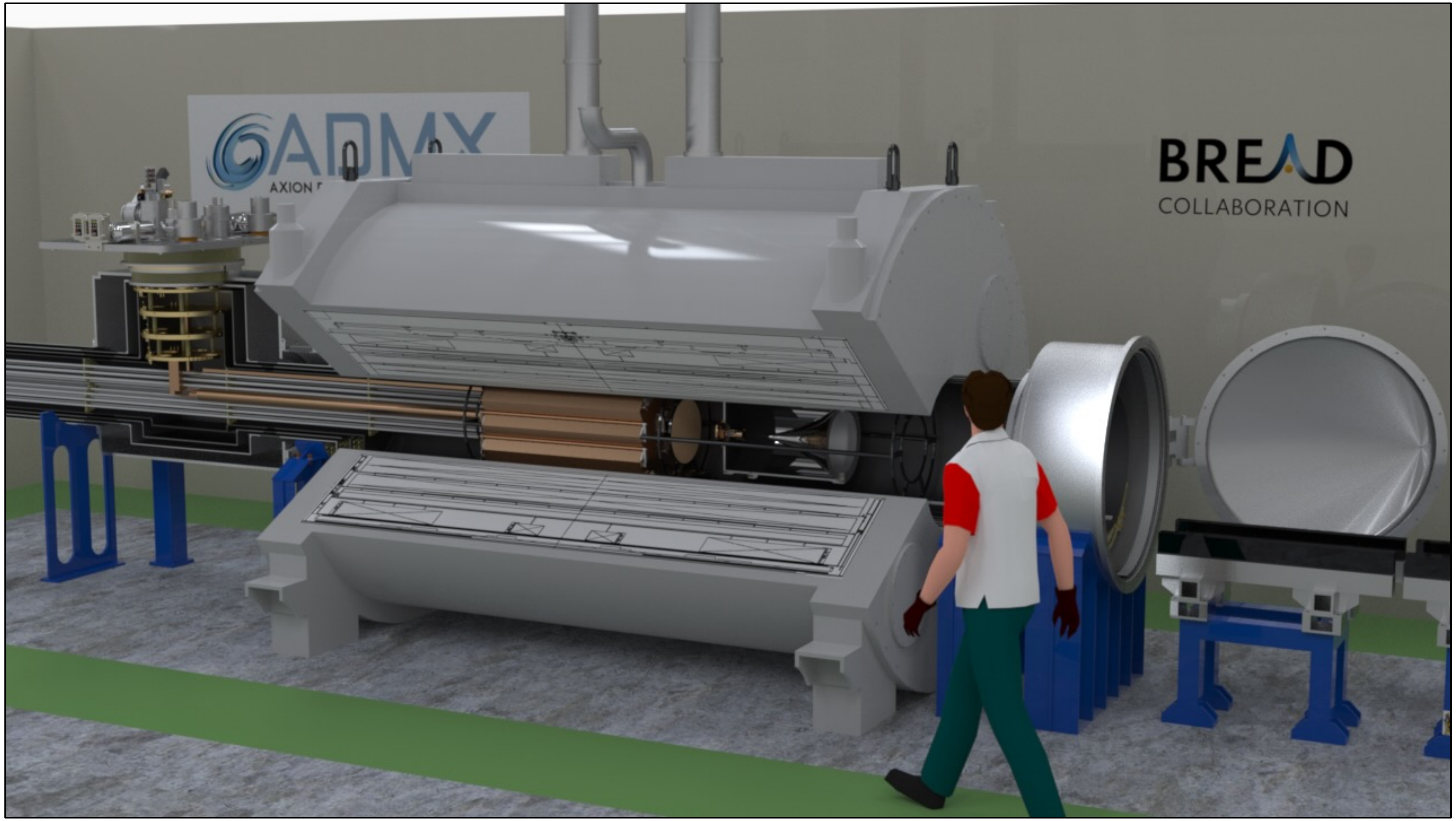

9.4 T MRI Magnet at Fermilab

BREAD (Broadband Reflector Experiment for Axion Detection)

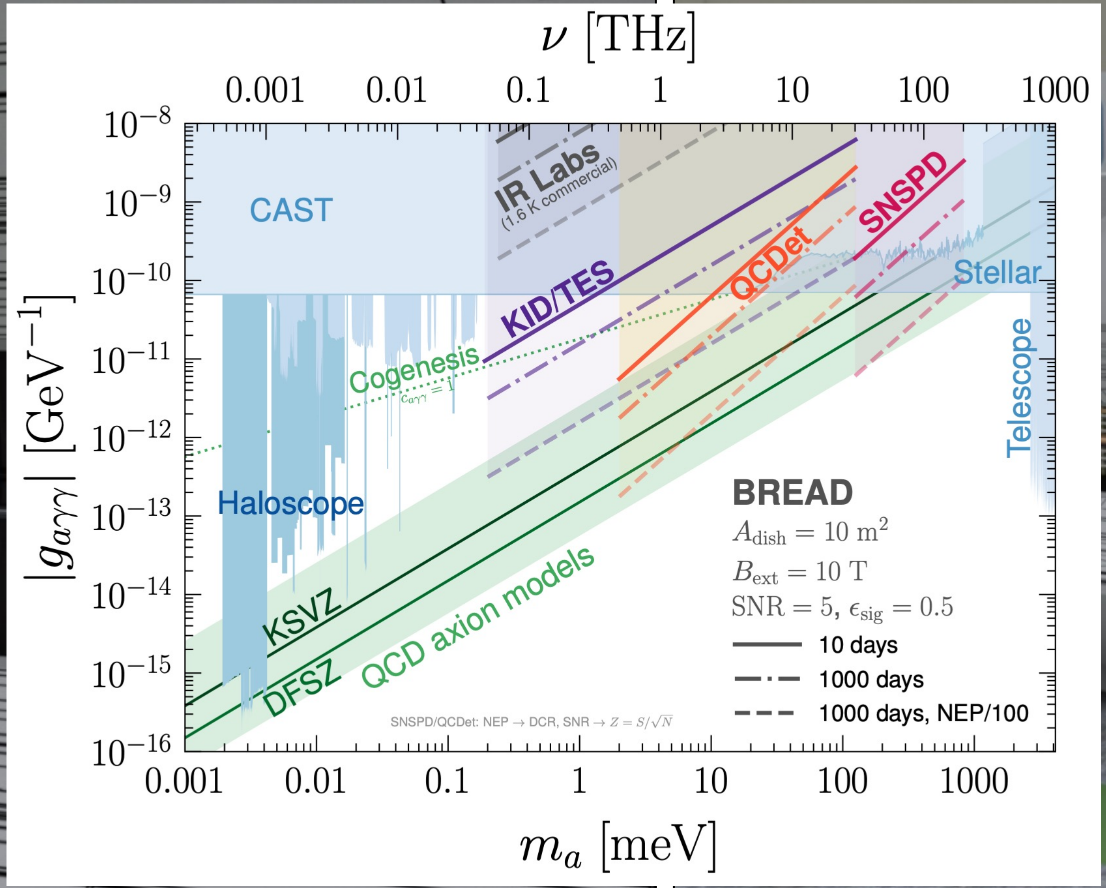

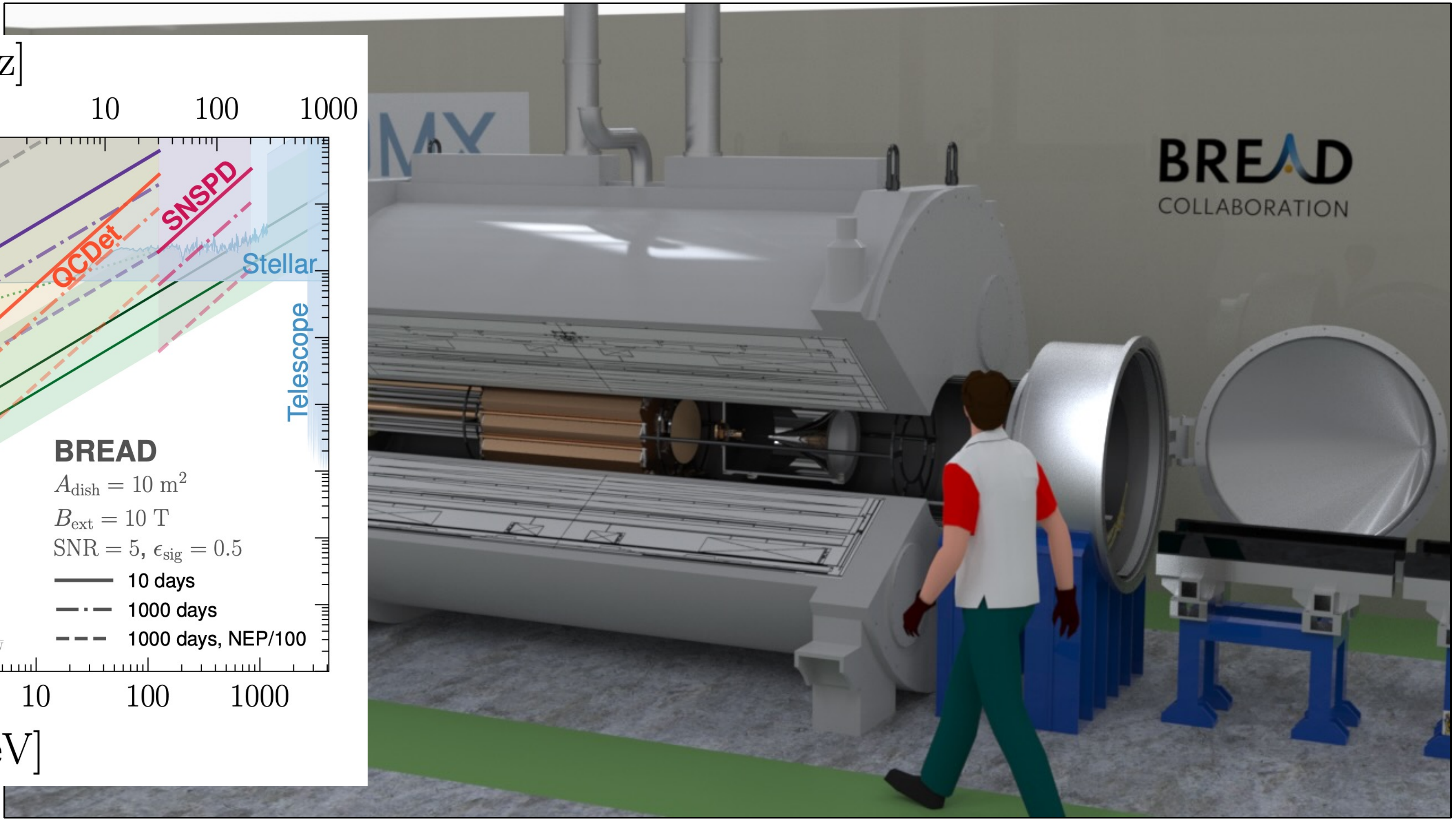

9.4 T MRI Magnet at Fermilab

Array of Horn Antenna

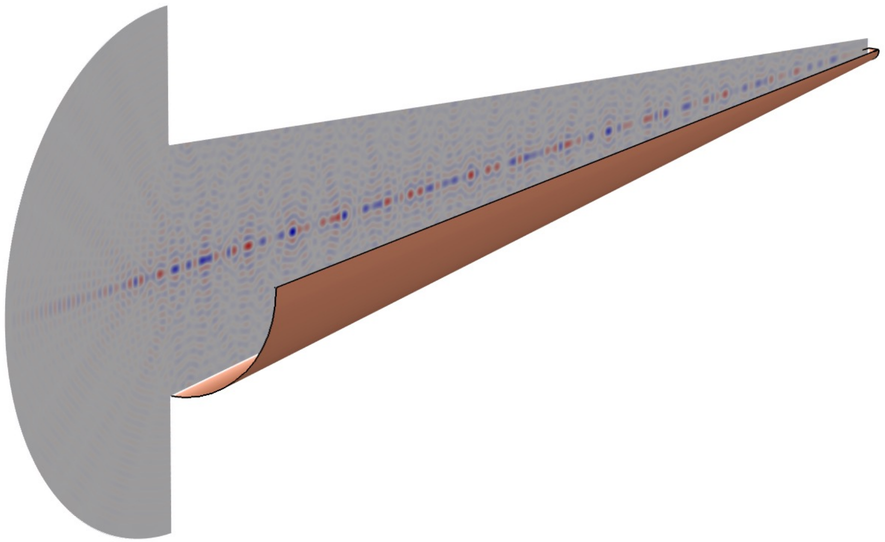

$$P_{\text{single}} \approx 4.5\times10^{-29}\text{W}\left(\frac{B_0}{10\text{ T}}\right)^2\left(\frac{g_\gamma}{0.97}\right)^2\left(\frac{A_{\text{horn}}}{3470\text{ mm}^3}\right)$$

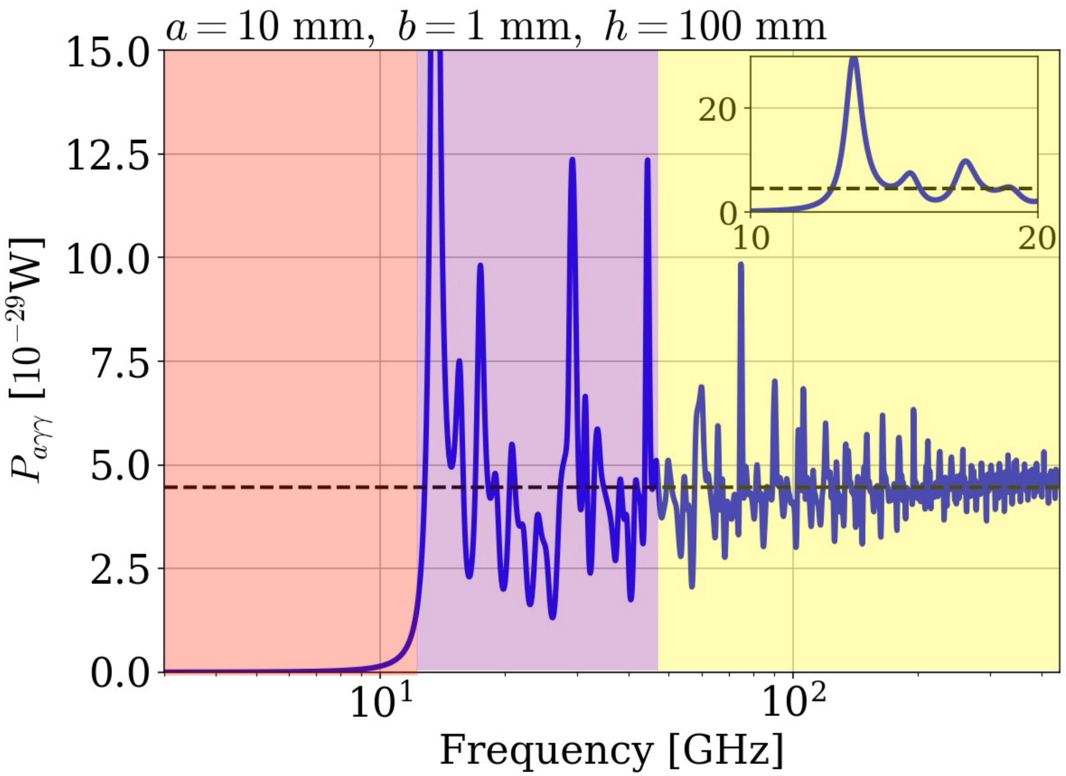

Low frequency: no converion

Intermediate frequency: resonance peaks

High frequency: dish antenna haloscope

Array of Horn Antenna

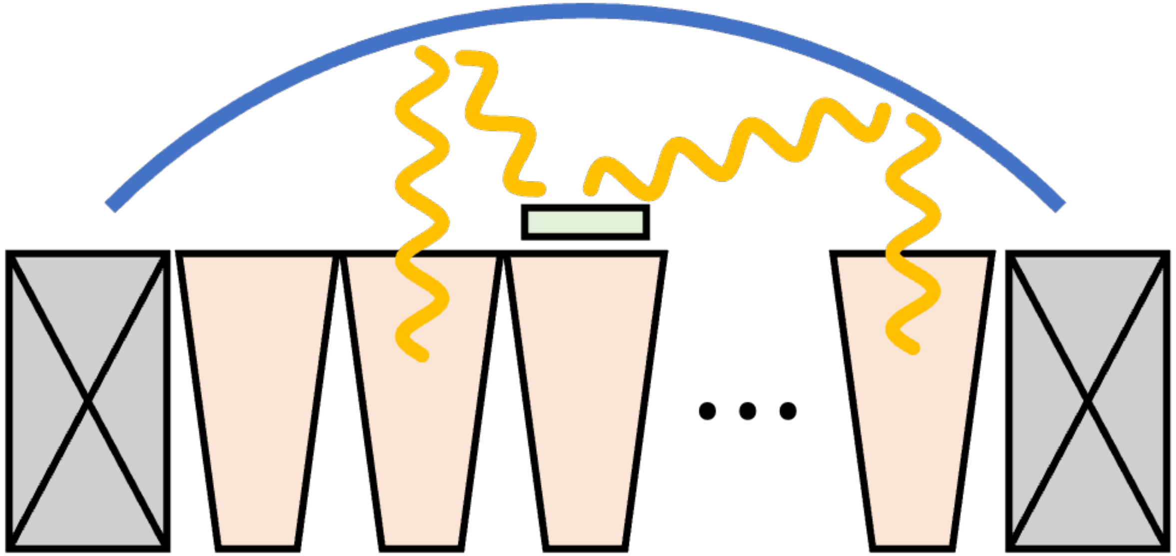

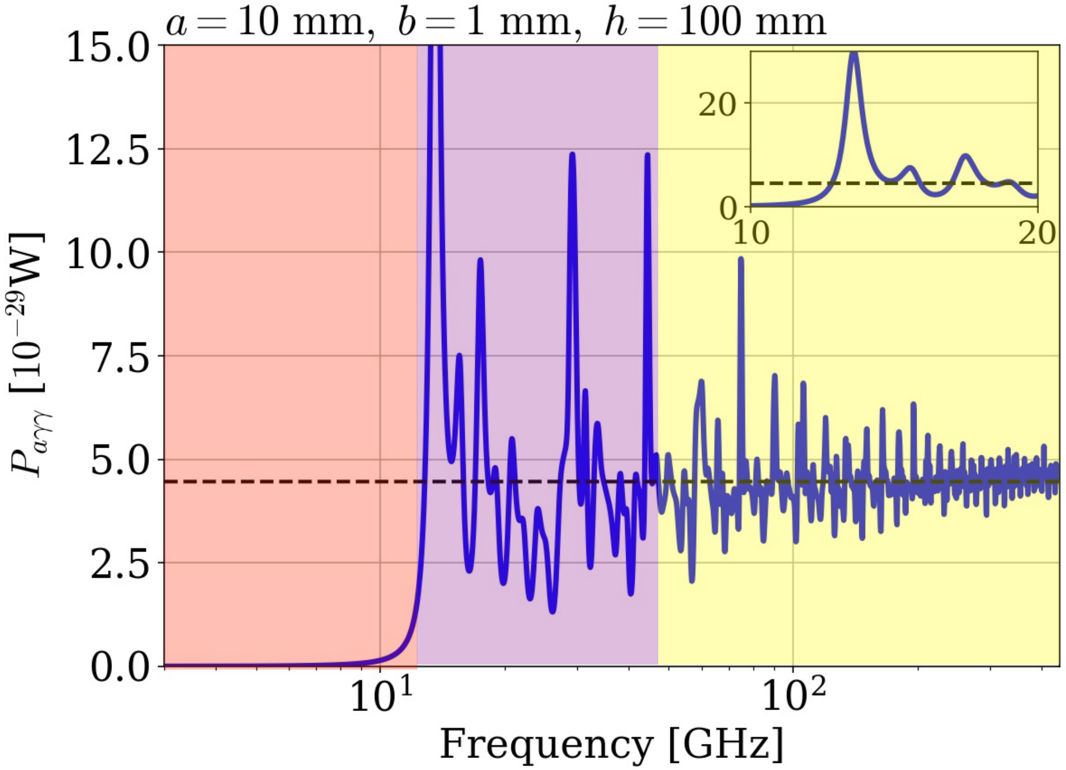

$$P_{\text{single}} \approx 4.5\times10^{-29}\text{W}\left(\frac{B_0}{10\ \text{T}}\right)^2\left(\frac{g_\gamma}{0.97}\right)^2\left(\frac{A_{\text{horn}}}{3470\ \text{mm}^3}\right)$$

$$P_{\text{array}}^{\text{long}} \approx 3.9\times10^{-24}\text{W}\left(\frac{B_0}{10\ \text{T}}\right)^2\left(\frac{g_\gamma}{0.97}\right)^2\left(\frac{\Gamma}{0.75}\right)\left(\frac{R}{0.75\ \text{m}}\right)^2\left(\frac{h}{2.1\ \text{m}}\right)$$

$$P_{\text{BREAD}} \approx 1.3\times10^{-25}\text{W}\left(\frac{B_0}{10\ \text{T}}\right)^2\left(\frac{g_\gamma}{0.97}\right)^2\left(\frac{R}{0.75\ \text{m}}\right)\left(\frac{h}{2.1\ \text{m}}\right)$$

Array of Horn Antenna

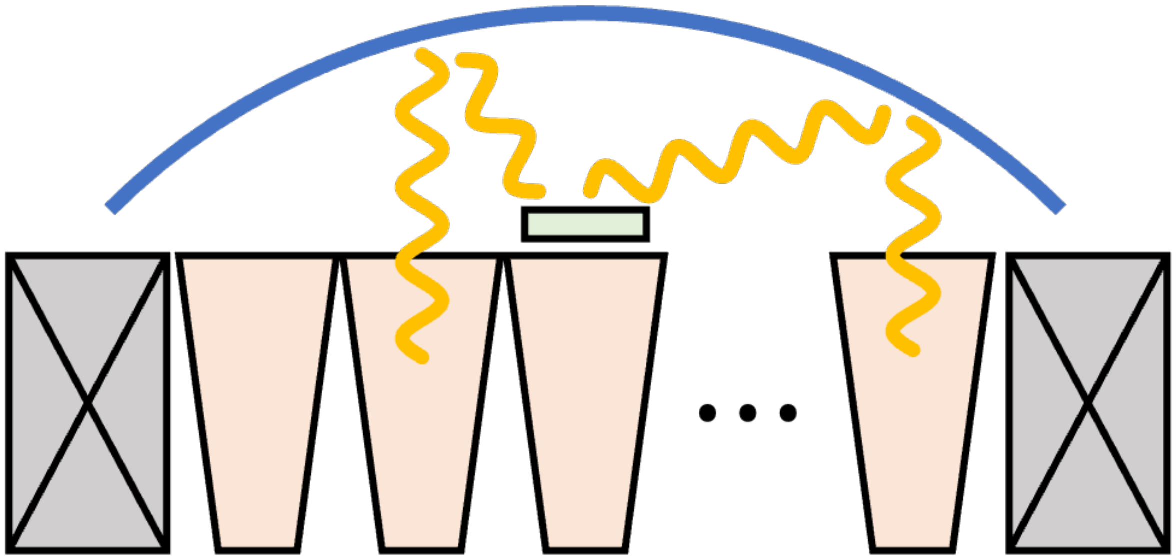

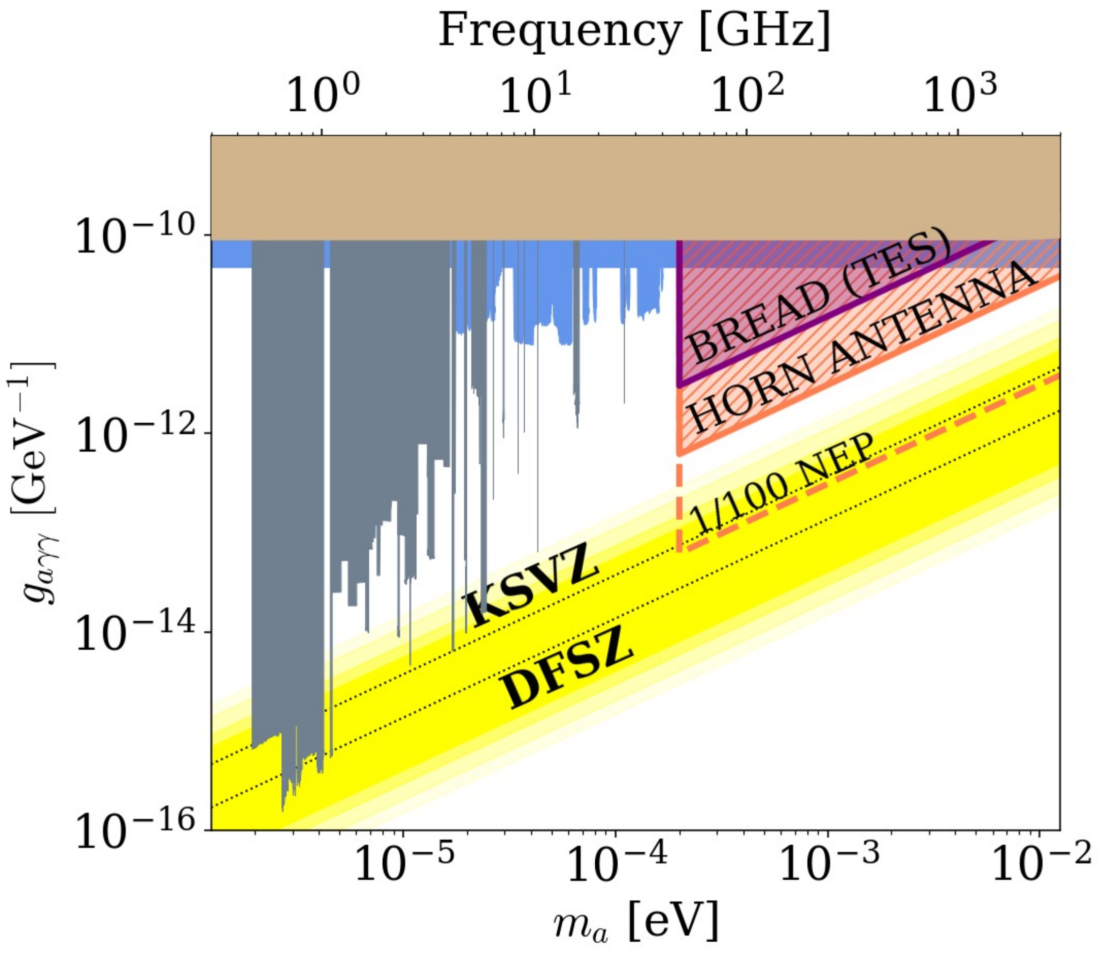

$$P_{\text{single}} \approx 4.5\times10^{-29}\text{W}\left(\frac{B_0}{10\ \text{T}}\right)^2\left(\frac{g_\gamma}{0.97}\right)^2\left(\frac{A_{\text{horn}}}{3470\ \text{mm}^3}\right)$$

$$P_{\text{array}}^{\text{long}} \approx 3.9\times10^{-24}\text{W}\left(\frac{B_0}{10\ \text{T}}\right)^2\left(\frac{g_\gamma}{0.97}\right)^2\left(\frac{\Gamma}{0.75}\right)\left(\frac{R}{0.75\ \text{m}}\right)^2\left(\frac{h}{2.1\ \text{m}}\right)$$

Lumped Element Haloscope

If $c/\omega_a \gg L_{\text{lab}}$, $\partial_t \mathbf{E} \ll \nabla\times\mathbf{B}$

Quasistatic approximation

$$\nabla\cdot\mathbf{E} = \rho_e - g_{a\gamma\gamma}\nabla a\cdot\mathbf{B}$$
$$\nabla\cdot\mathbf{B} = 0$$
$$\nabla\times\mathbf{E} = -\partial_t\mathbf{B}$$
$$\nabla\times\mathbf{B} = \partial_t\mathbf{E} + \mathbf{J}_e + g_{a\gamma\gamma}(\nabla a\times\mathbf{E} + \partial_t a\mathbf{B})$$

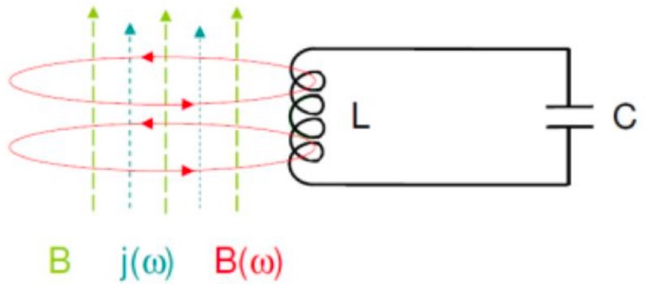

$$\mathbf{J}_{\text{ax}} \sim g_{a\gamma\gamma}\sqrt{2\rho_{\text{DM}}}\cos(m_a t)\mathbf{B}$$

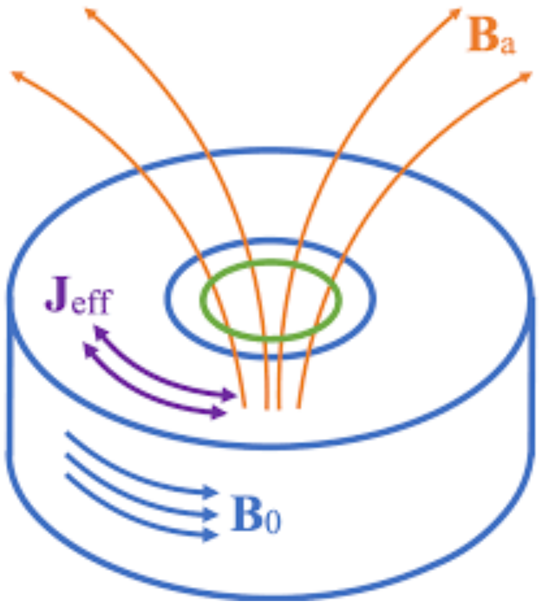

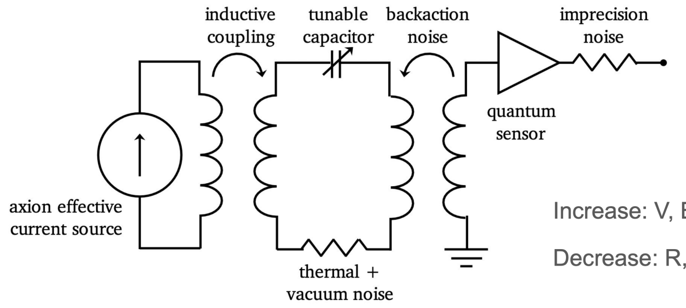

Increase: V, B, Q

Decrease: R, T, Imp, BA

[DMRadio Collaboration]

DMRadio

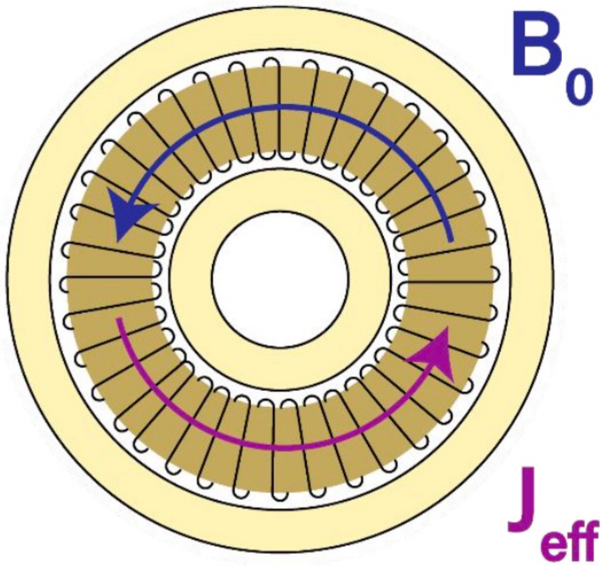

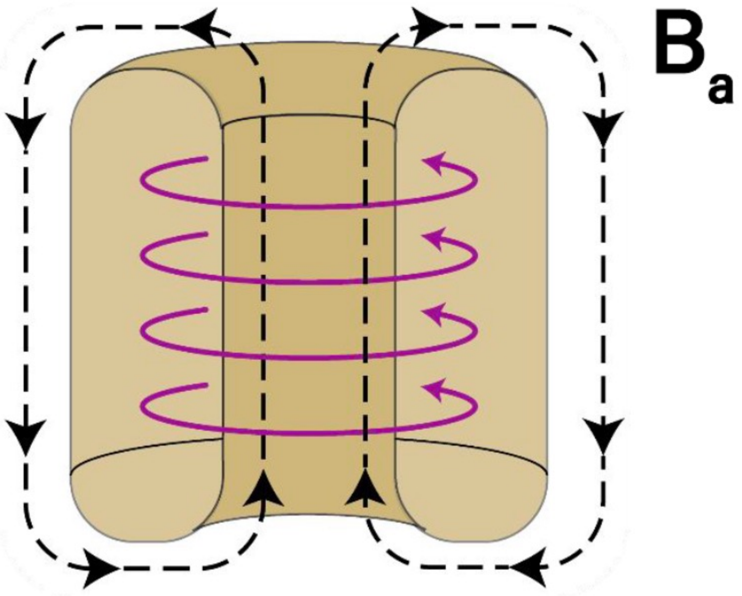

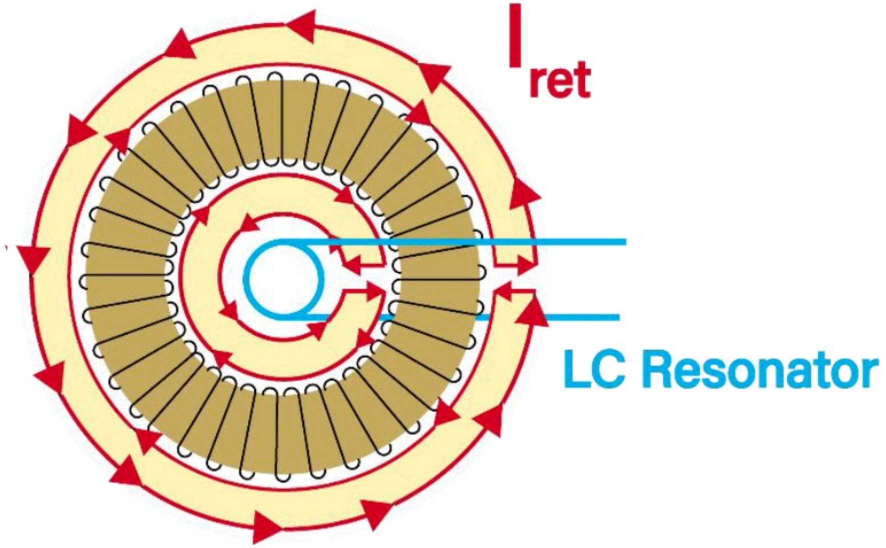

Toroidal magnet with field B_0 creates current J_{eff}

J_{eff} creates magnetic field B_a

B_a induces I_{ret} which is enhanced by an LC resonator and picked up by a sensor

[Maria Simanovskaia, PATRAS 2023][1]

DMRadio-50L

Dilution refrigerator in the lab.

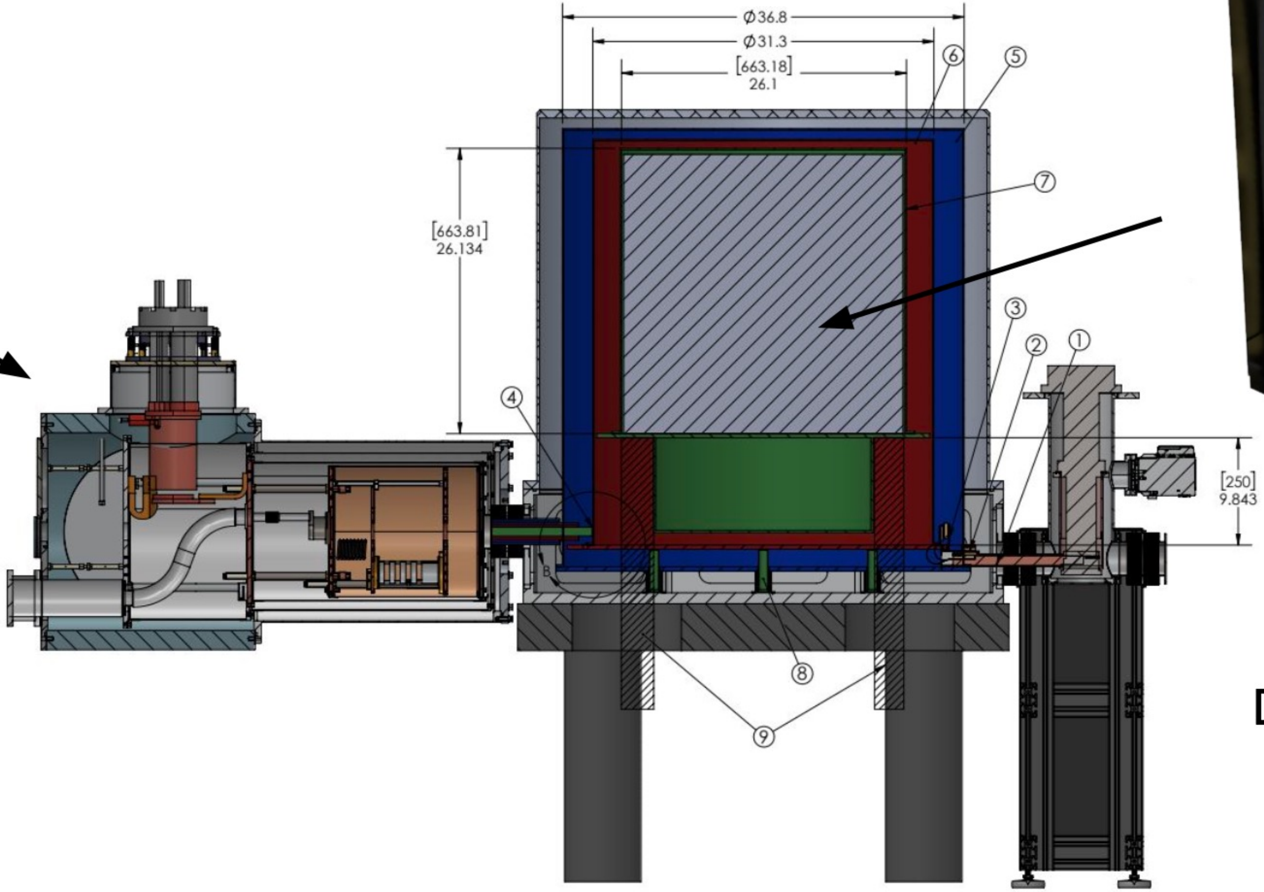

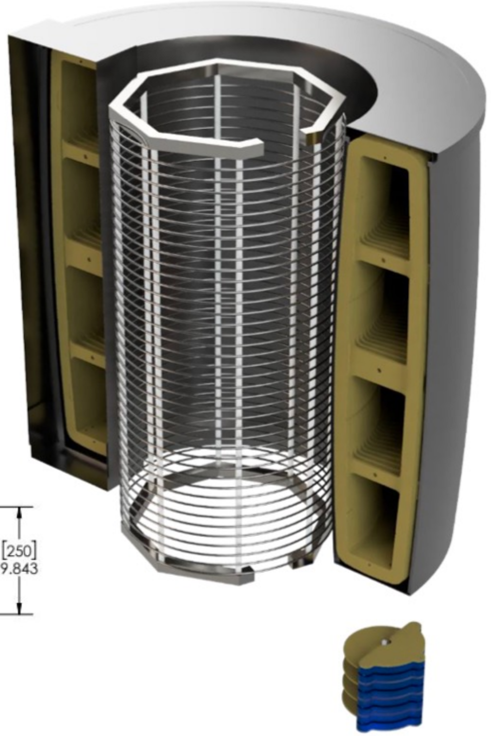

Detector and receiver CAD models.

DMRadio-50L cryosystem CAD model.

1?

[Maria Simanovskaia, PATRAS 2023]

DMRadio

DMRadio-50L

- 5 kHz - 5 MHz
- Quantum sensor testbed

DMRadio-m^3 (PRD **106** (2022): 103008, arXiv:2302.14084)

- Primary goal: DFSZ 30 MHz - 200 MHz
- Secondary goal: KSVZ down to 10 MHz
- Extended goal: QCD axion band to 5 MHz
- DOE DMNI

DMRadio-GUT (PRD **106** (2022): 112003.)

- DFSZ 100 kHz - 30 MHz
- Next-generation detector

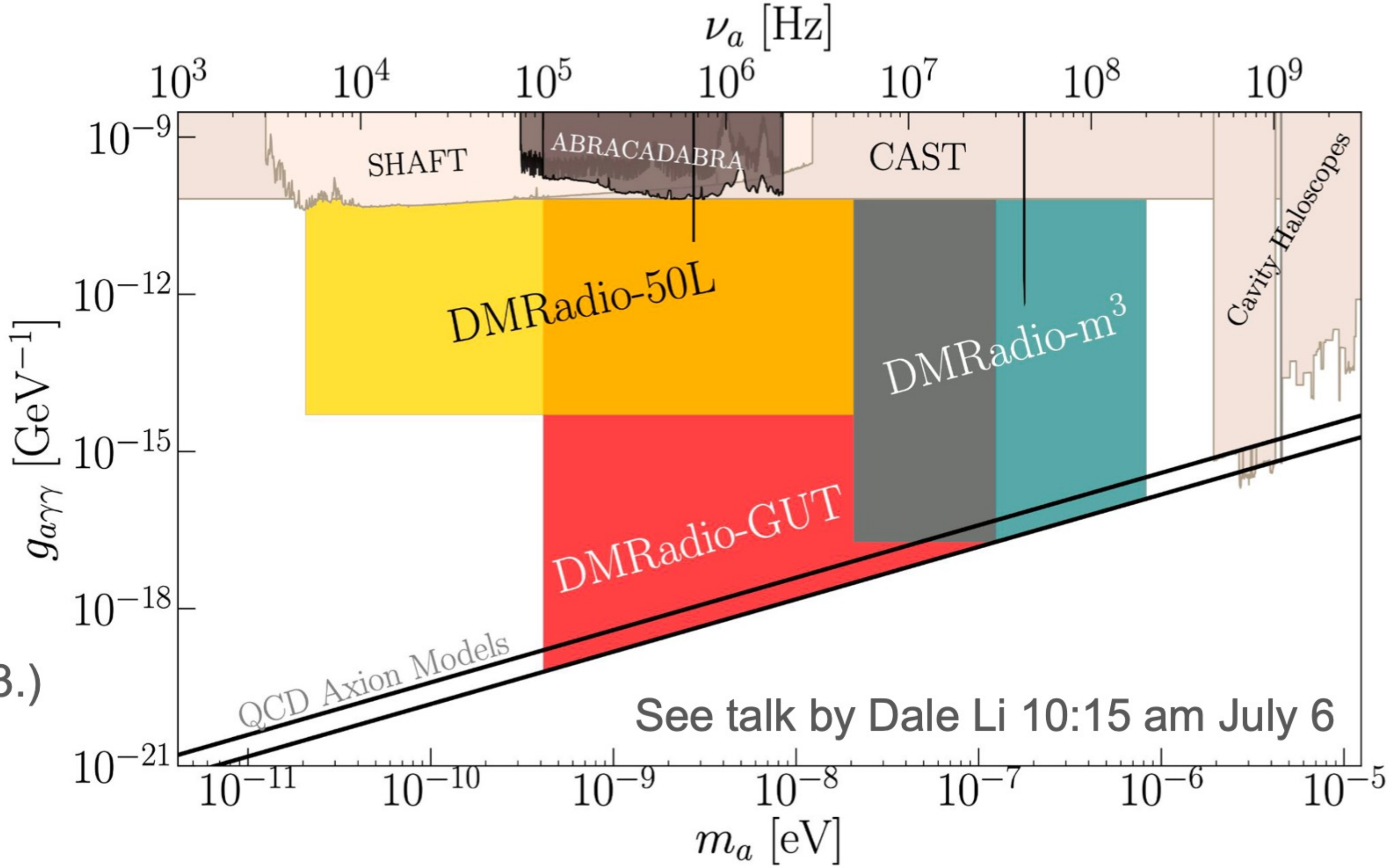

[Maria Simanovskaia, PATRAS 2023]

Axion-Fermion Coupling

Axion-Photon Coupling

Axion-Fermion Coupling

Axion Source

Dark Matter Axion

Solar Axion

Lab-Produced Axion

Others

Axion Detector

Axion-Fermion Coupling

Axion-Fermion coupling

$$\mathcal{L}_{a\bar{f}f} = -\frac{g_f}{2f_a}(\partial_\mu a)\bar{f}\gamma^\mu\gamma^5 f$$

Axion-Fermion Coupling

Axion-Fermion coupling

$$\mathcal{L}_{a\bar{f}f} = -\frac{g_f}{2f_a}(\partial_\mu a)\bar{f}\gamma^\mu\gamma^5 f$$

non-relativistic limit

Axion-Spin coupling

$$\mathcal{H}_{a\bar{f}f} = \frac{1}{f_a}\left[\frac{g_f}{2}\left(\vec{\sigma}\cdot\vec{\nabla}a + \frac{\vec{p}\cdot\vec{\sigma}}{m_f}\partial_t a\right)\right]$$

Axion-Fermion Coupling

Axion-Fermion coupling

$$\mathcal{L}_{a\bar{f}f} = -\frac{g_f}{2f_a}(\partial_\mu a)\bar{f}\gamma^\mu\gamma^5 f$$

non-relativistic limit

Axion-Spin coupling

$$\mathcal{H}_{a\bar{f}f} = \frac{1}{f_a}\left[\frac{g_f}{2}\left(\vec{\sigma}\cdot\vec{\nabla}a + \frac{\vec{p}\cdot\vec{\sigma}}{m_f}\partial_t a\right)\right]$$

Chiral Magnetic Effect

Axion-Fermion Coupling

Axion-Fermion coupling

$$\mathcal{L}_{a\bar{f}f} = -\frac{g_f}{2f_a}(\partial_\mu a)\bar{f}\gamma^\mu\gamma^5 f$$

non-relativistic limit

Axion-Spin coupling

$$\mathcal{H}_{a\bar{f}f} = \frac{1}{f_a}\left[\frac{g_f}{2}\left(\vec{\sigma}\cdot\vec{\nabla}a + \frac{\vec{p}\cdot\vec{\sigma}}{m_f}\partial_t a\right)\right]$$

Axion Wind-Spin coupling

Axion-Fermion Coupling

Axion-Fermion coupling

$$\mathcal{L}_{a\bar{f}f} = -\frac{g_f}{2f_a}(\partial_\mu a)\bar{f}\gamma^\mu\gamma^5 f$$

non-relativistic limit

Axion-Spin coupling

$$\mathcal{H}_{a\bar{f}f} = \frac{1}{f_a}\left[\frac{g_f}{2}\left(\vec{\sigma}\cdot\vec{\nabla}a + \frac{\vec{p}\cdot\vec{\sigma}}{m_f}\partial_t a\right)\right]$$

$$\mathcal{H}_{\mathrm{spin}} = -\frac{\gamma}{2}\vec{B}_0\cdot\vec{\sigma}$$

Axion Wind-Spin coupling

$$\vec{B}_{\mathrm{eff}} = -\frac{g_f}{\gamma f_a}\vec{\nabla}a$$

Magnetic Resonance

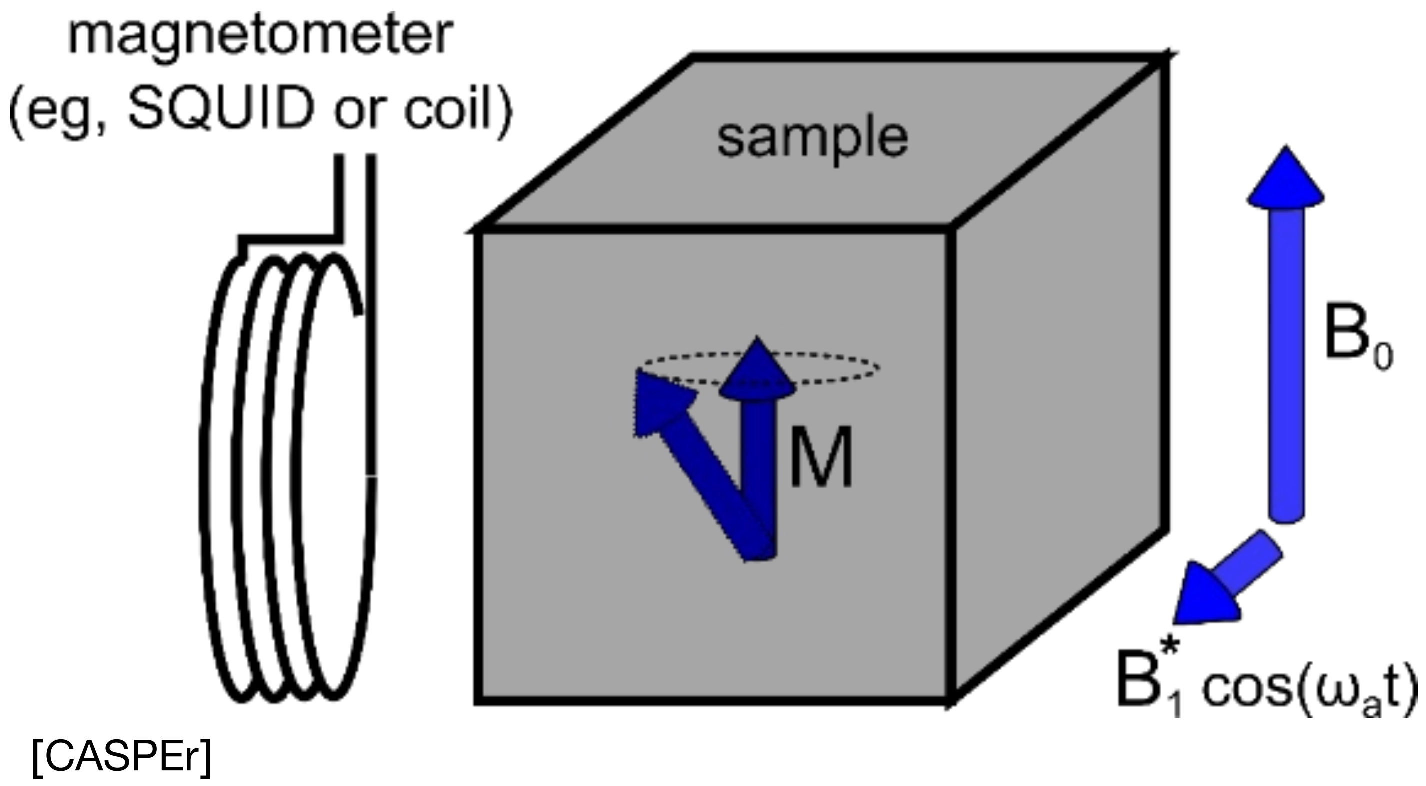

$$\vec{B}_{\text{eff}} = -\frac{g_f}{\gamma f_a}\vec{\nabla} a$$

- When $\omega_a = \gamma B_0$, Flip spins and make a precession
- Magnetometer detects the precessing field
- Similar to NMR

CASPEr-Wind

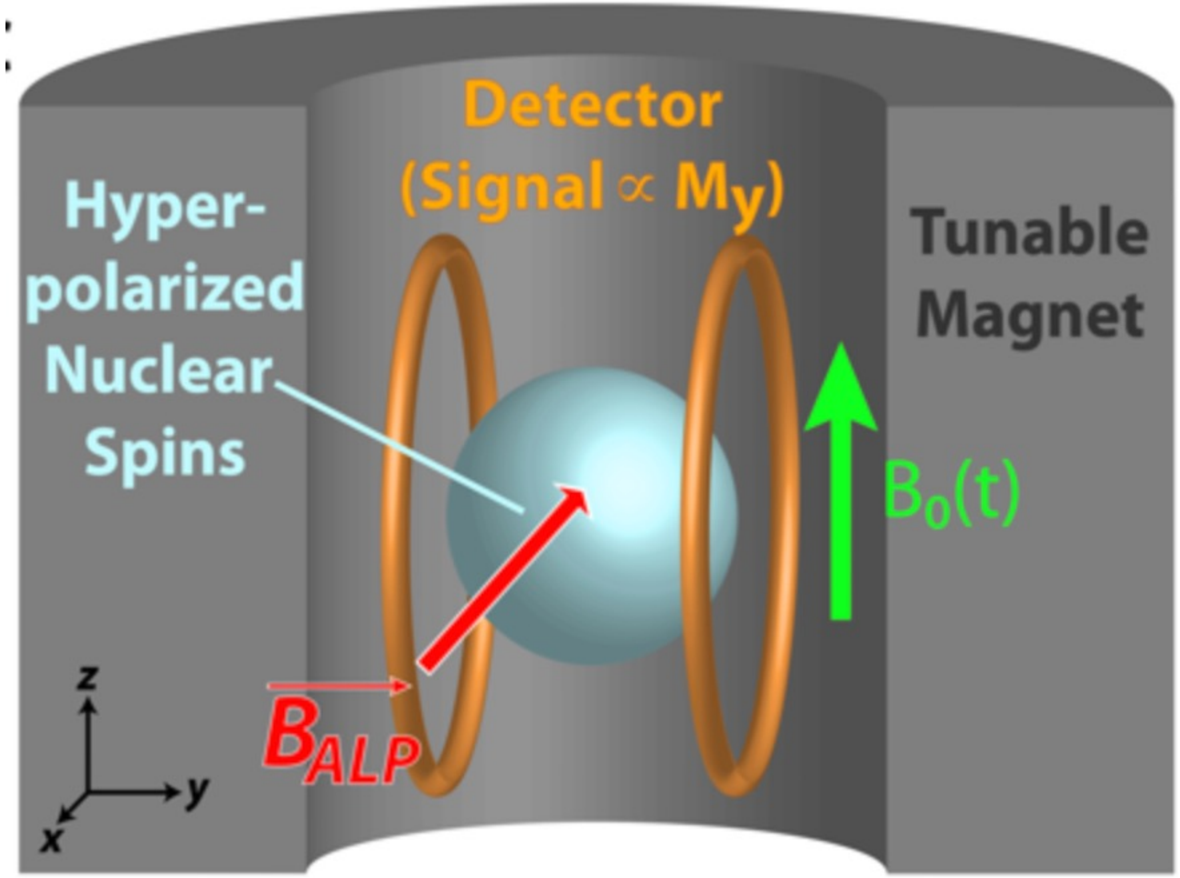

[Budker Group]

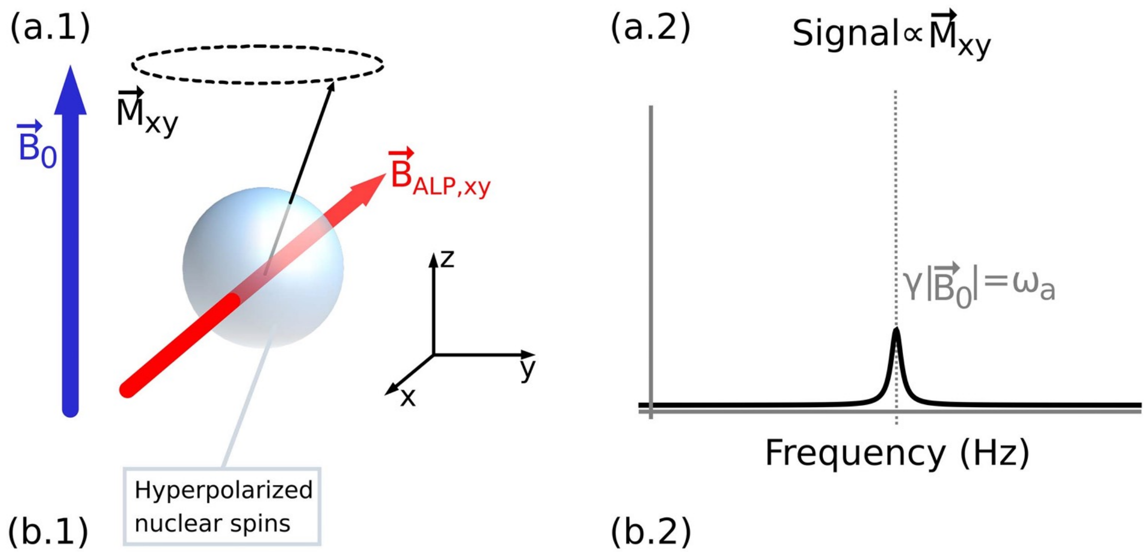

[Quantum Sci. Technol. **3** (2018) 014008]

CASPEr-Wind

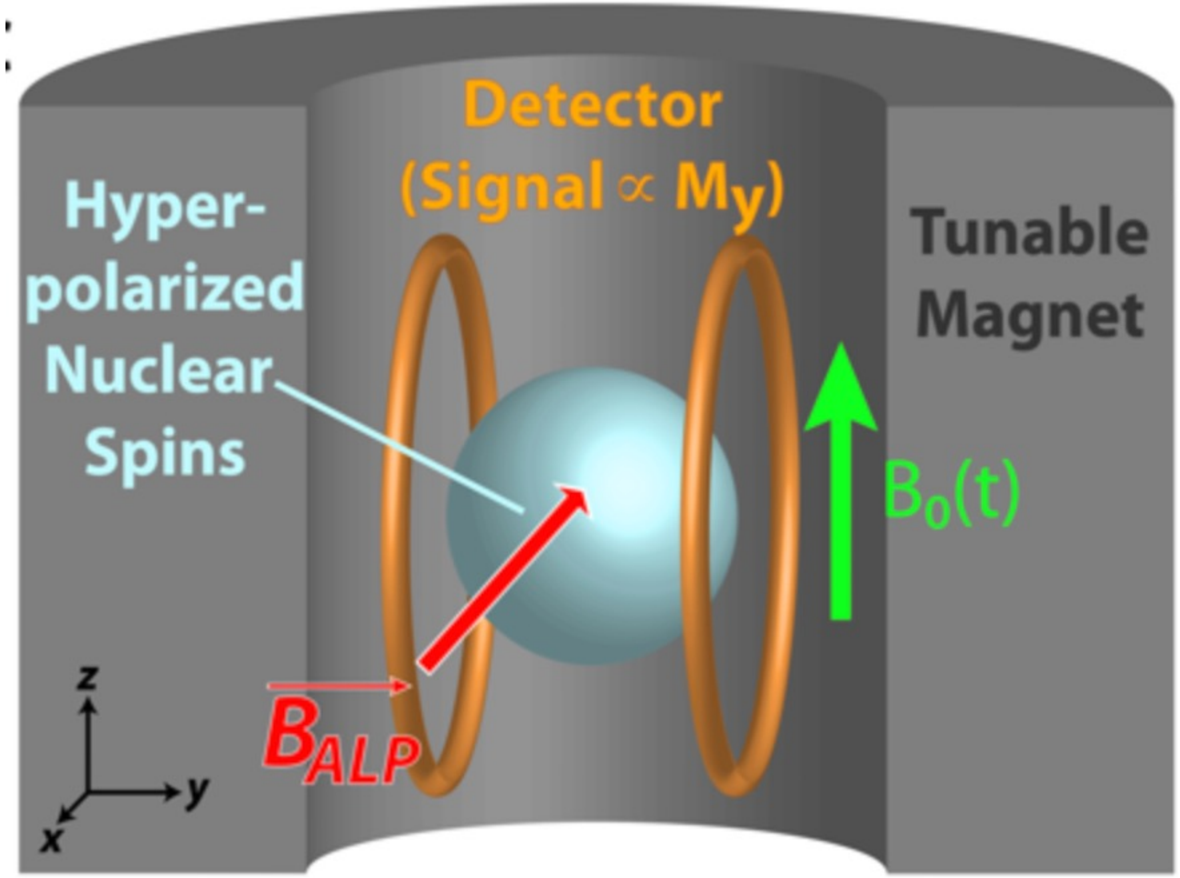

[Budker Group]

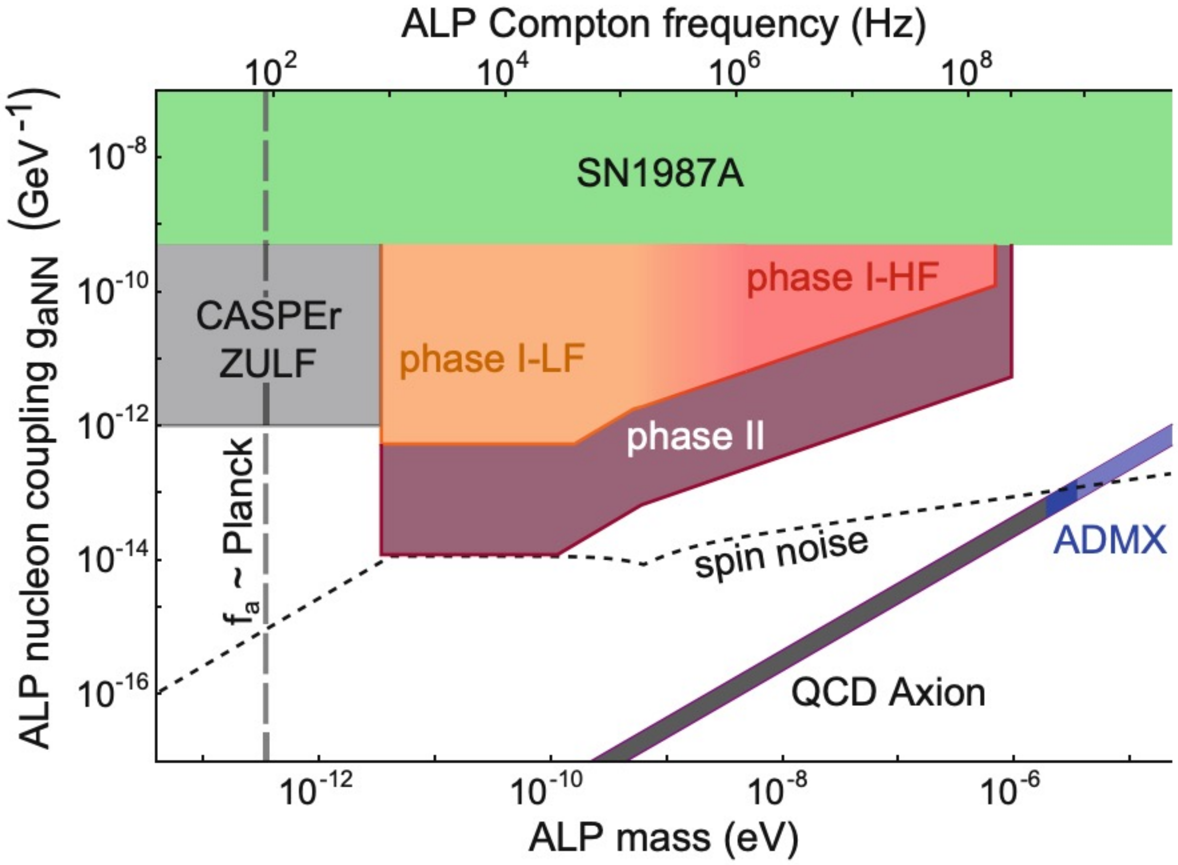

[D. F. Kimball, 3rd Cavity Workshop (2020)]

Axion Helioscope

Axion Source

- Dark Matter Axion
- Solar Axion
- Lab-Produced Axion
- Others

Axion Detector

- Axion-Photon Coupling
- Axion-Fermion Coupling

Axion Helioscope

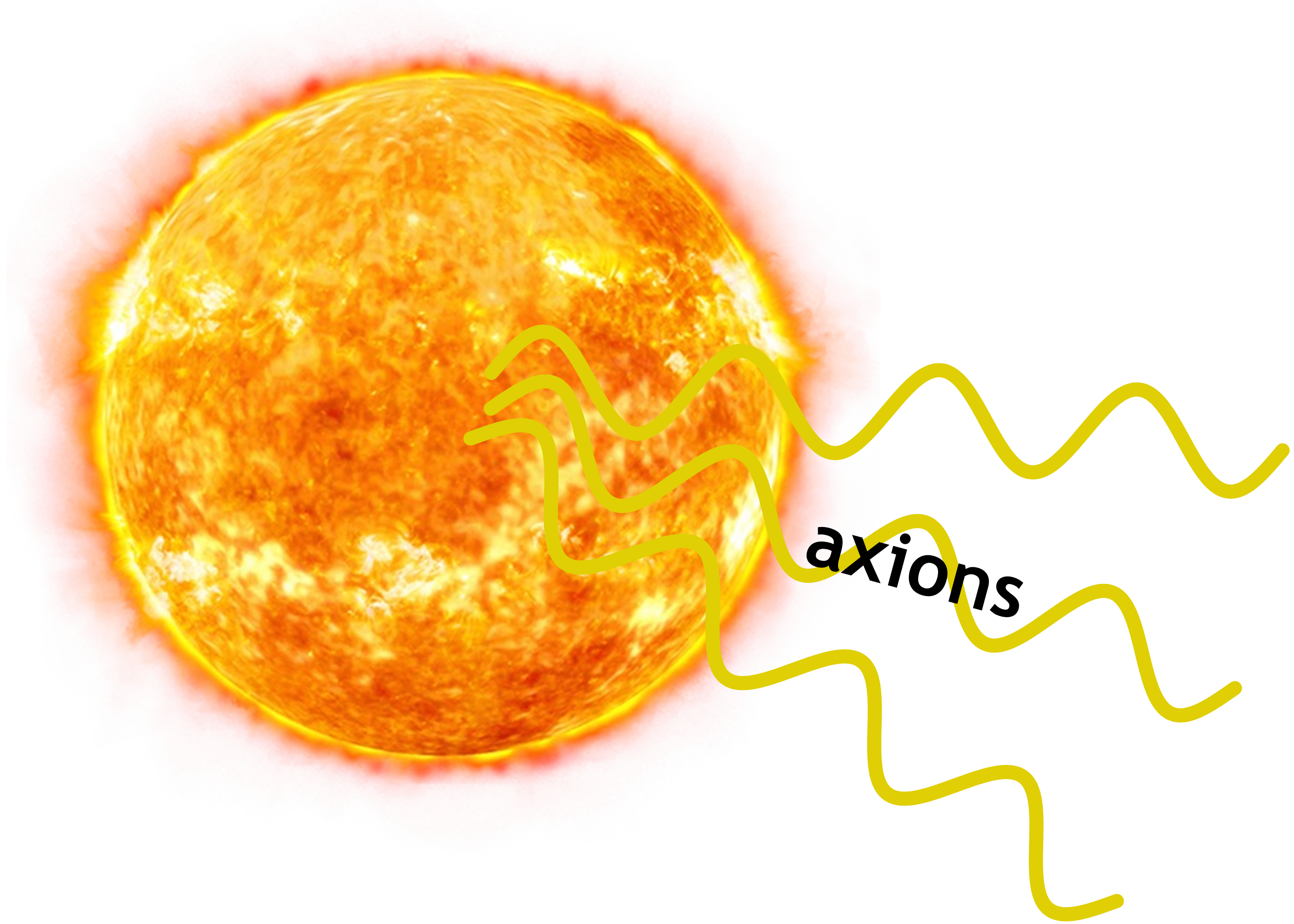

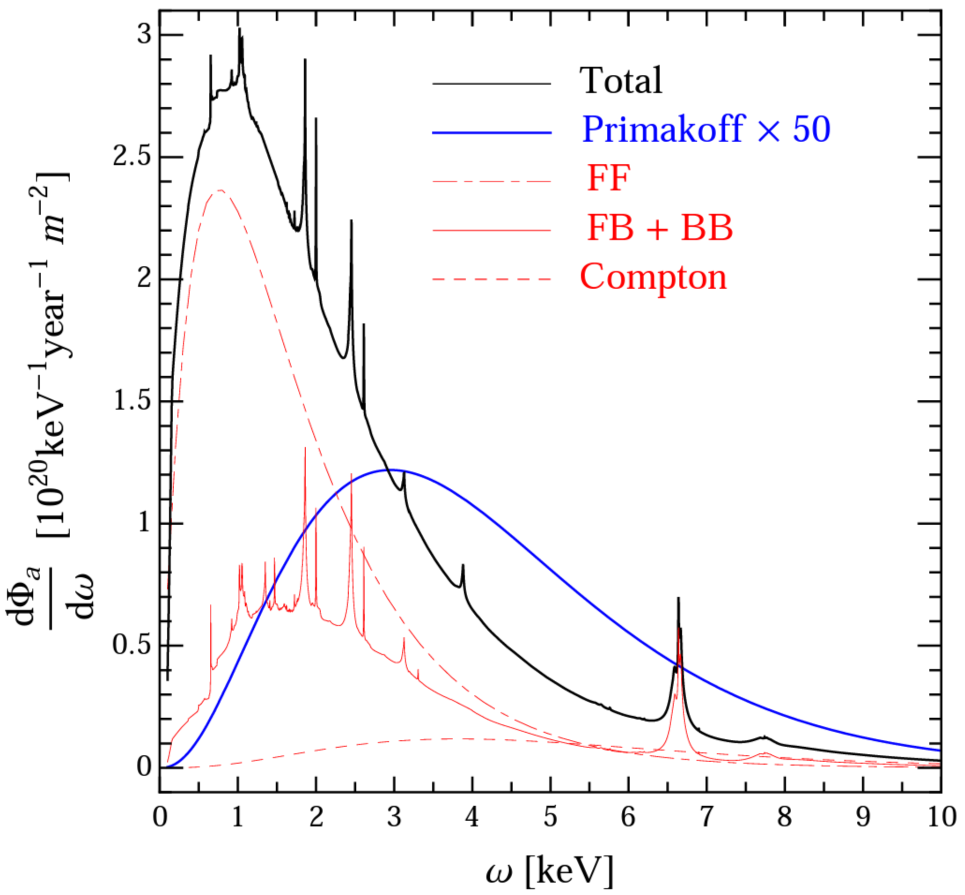

[J. Redondo, JCAP12(2013)008]

Axion Helioscope

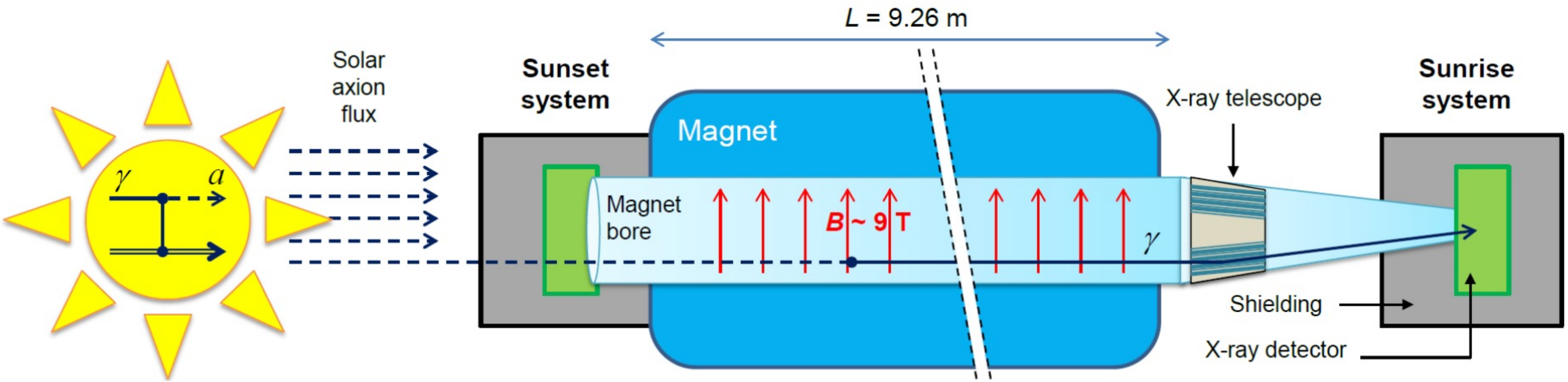

[Nature Physics **13**, 584 (2017)]

$$P_{a\to\gamma} = \left(\frac{g_{a\gamma\gamma}B_0}{q}\sin\left(\frac{qL}{2}\right)\right)^2, \qquad q \equiv \frac{m_a^2}{2E_a}$$

- Sun is the strongest and the closest axion generator
- The keV energy scale corresponds to the X-ray range
- Solar axions (hot) are converted into photons under the magnetic field

IAXO (International Axion Observatory)

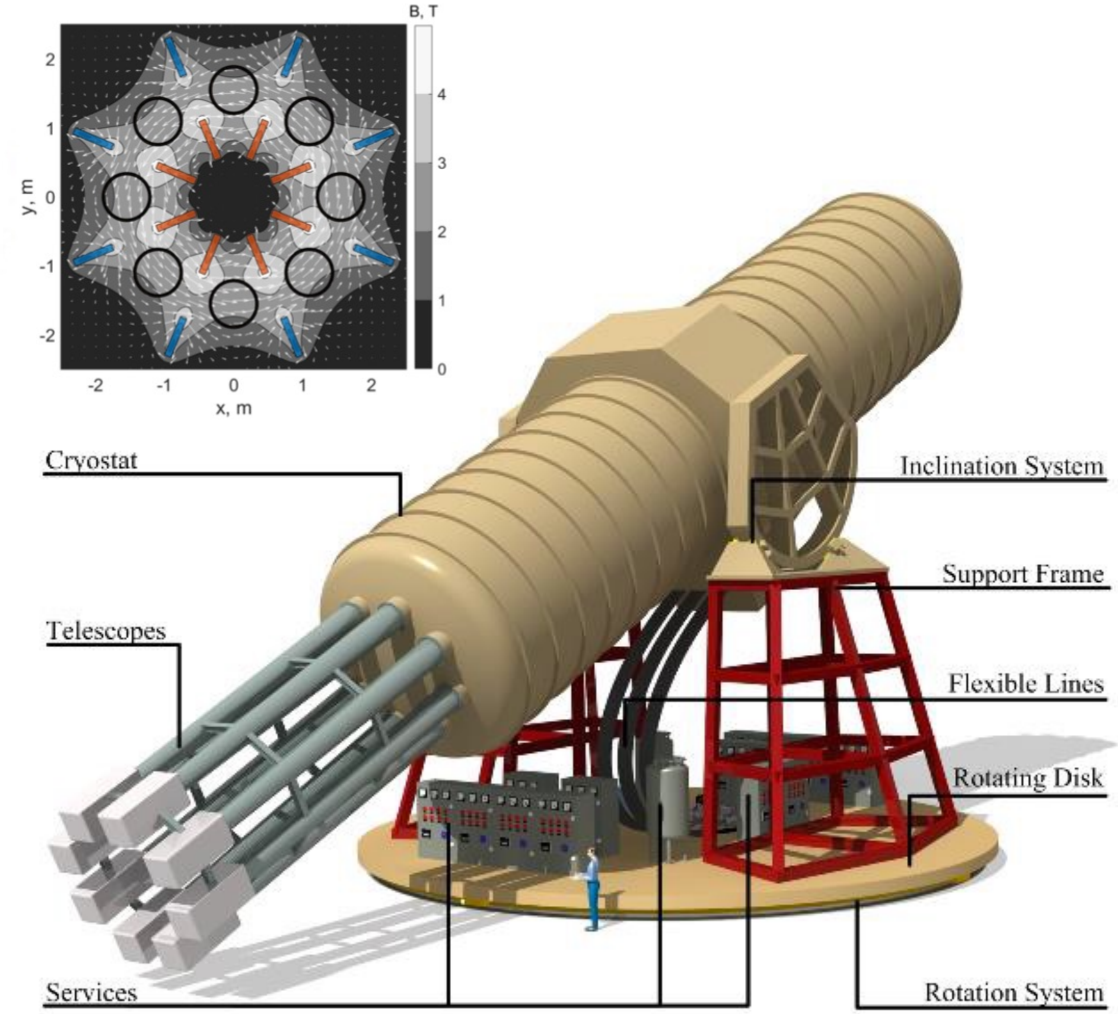

[Uwe Schneekloth, PATRAS 2023]

- Next generation after CAST (CERN helioscope)
- Large toroidal geometry
  - 8 magnets w/ L = 20 m
  - 5.4 T / 600 mm bore
- Advanced X-ray detector
- ~50% Sun-tracking time / 50% bg data

IAXO (International Axion Observatory)

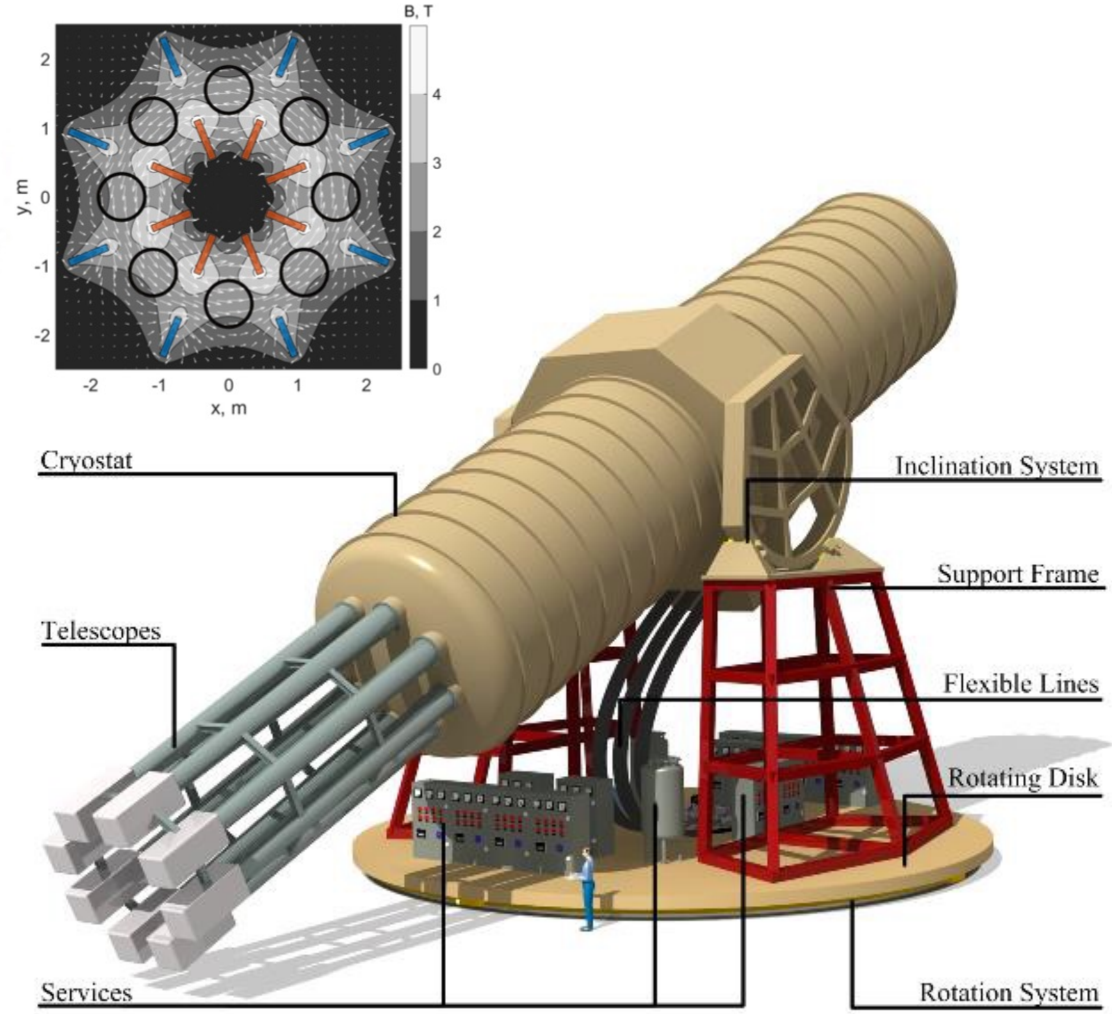

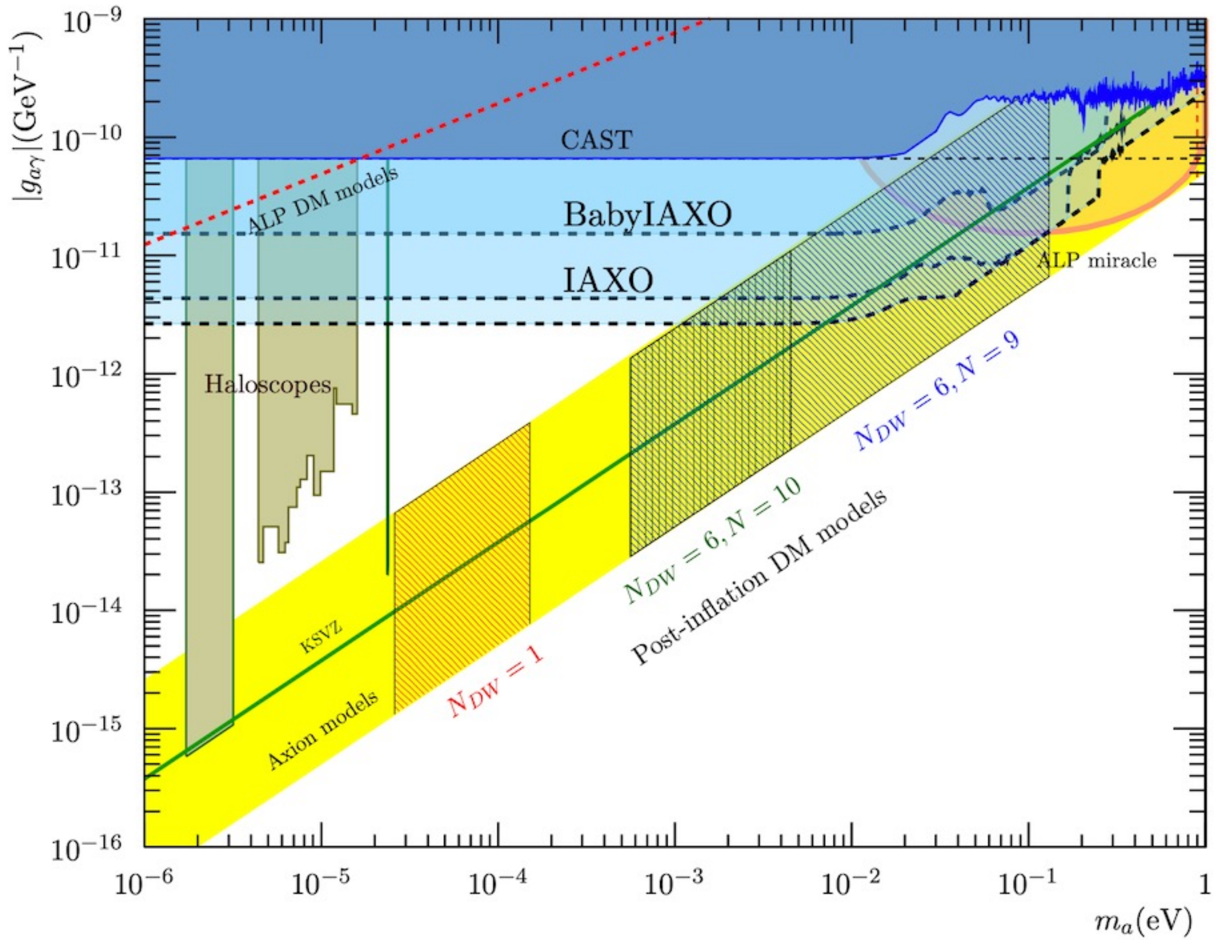

[Uwe Schneekloth, PATRAS 2023]

Lab-Produced Axion Searches

Axion Source

- Dark Matter Axion
- Solar Axion
- Lab-Produced Axion
- Others

Axion Detector

- Axion-Photon Coupling
- Axion-Fermion Coupling

Axion Photon Regeneration

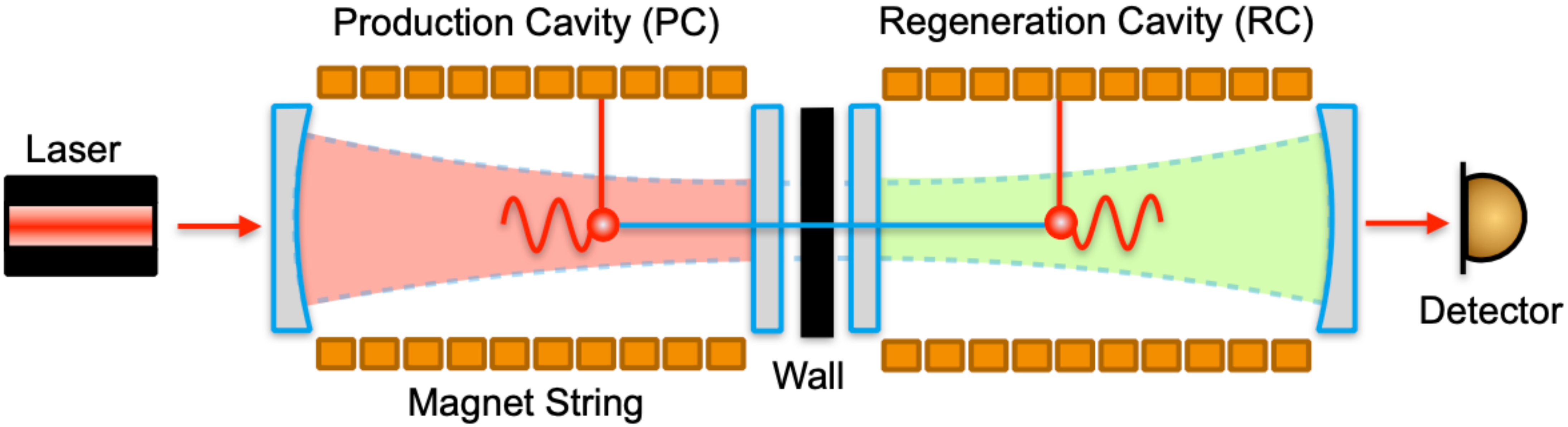

- Long & strong magnet
- High power laser system
- Two optical cavities
- Heterodyne detection system

ALPS II

- Two 122 m long optical cavity
- 100 m of magnetic fields (5.3 T)
- 70 W at 1064 nm LASER
  - Goal: 150 kW

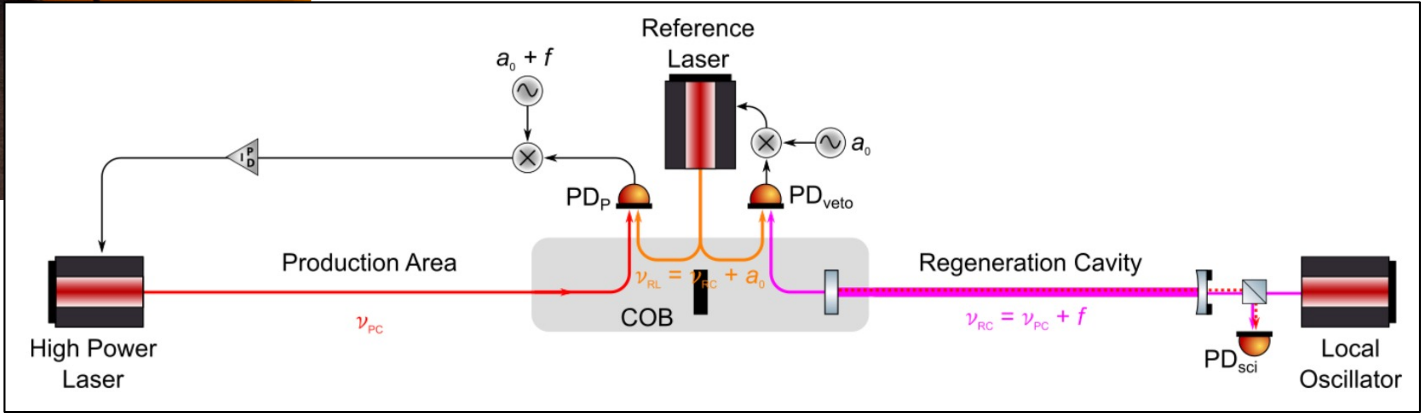

[ALPS II], [Aaron D. Spector, PATRAS 2023]

ALPS II

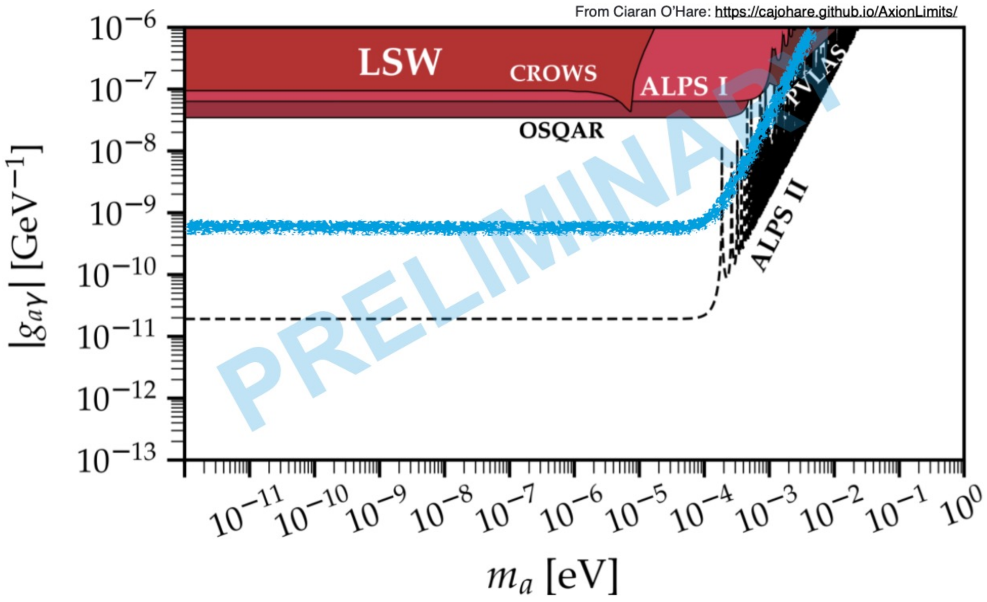

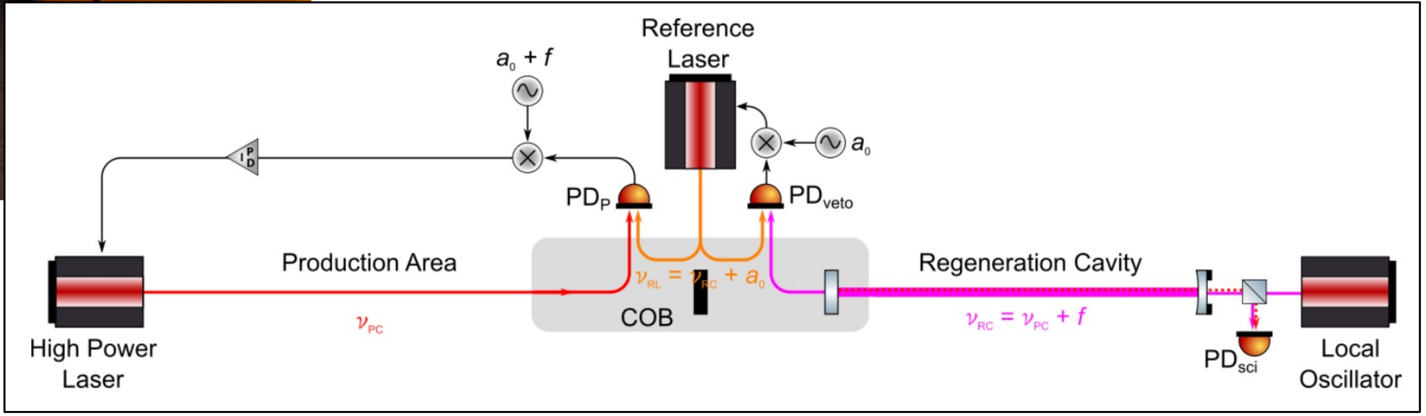

[ALPS II], [Aaron D. Spector, PATRAS 2023]

Vacuum Dichroism and Birefreingence

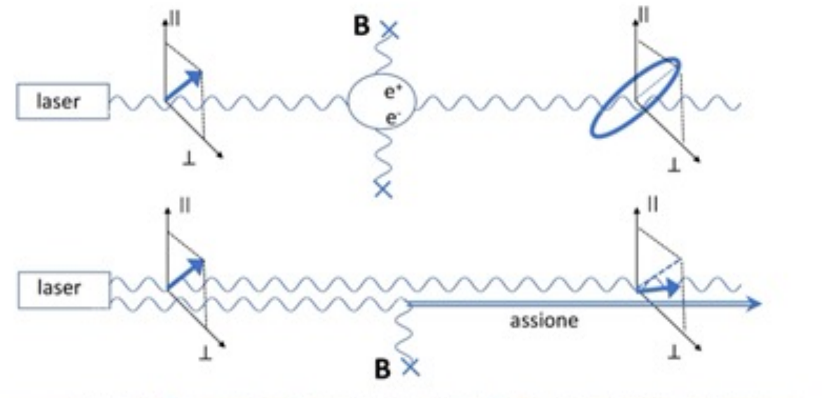

[PVLAS, INFN]

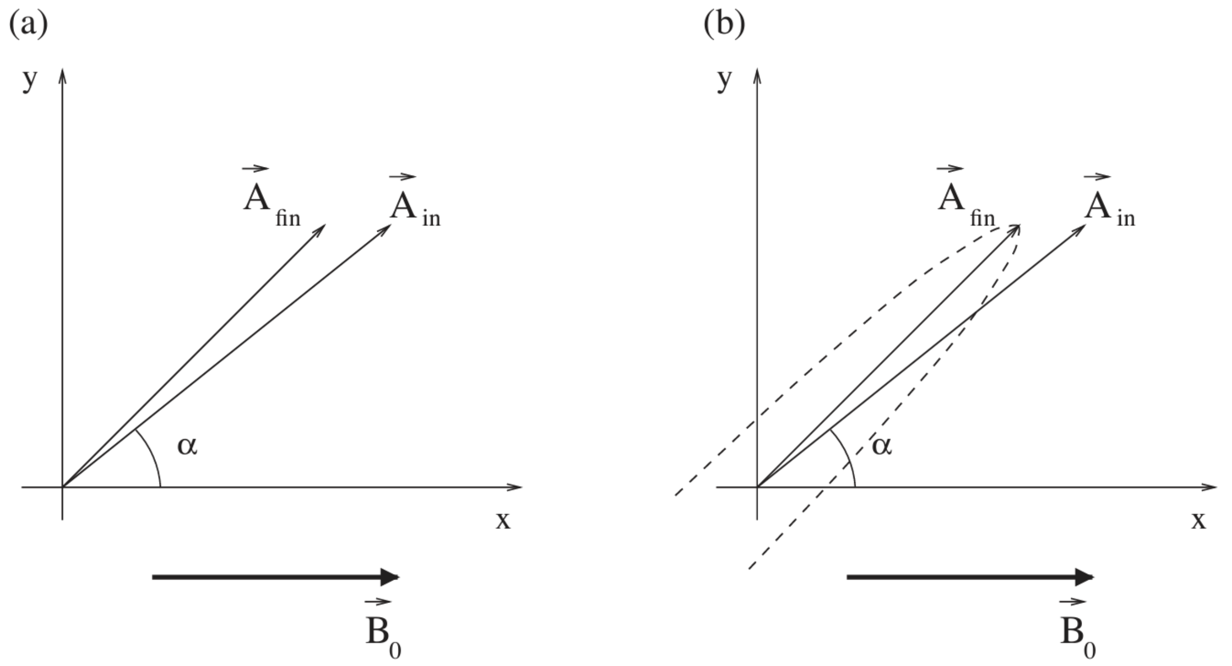

[P. Sikivie, Rev. Mod. Phys. **93** 015004]

When linearly polarized light is propagating under magnetic fields

- Dichroism: Photons polarized along the B field partially convert into axions
- Birefreigence: Phase difference is induced between two polarizations

Summary (1)

- Axion is a theoretically well-estabilished hypothetical pseudoscalar particle, and a strong candidate for dark matter.
- The field of axion is receiving significant attention and is a highly promising area with great growth potential.

- Various methods for exploring axions have been introduced.

Summary (2)

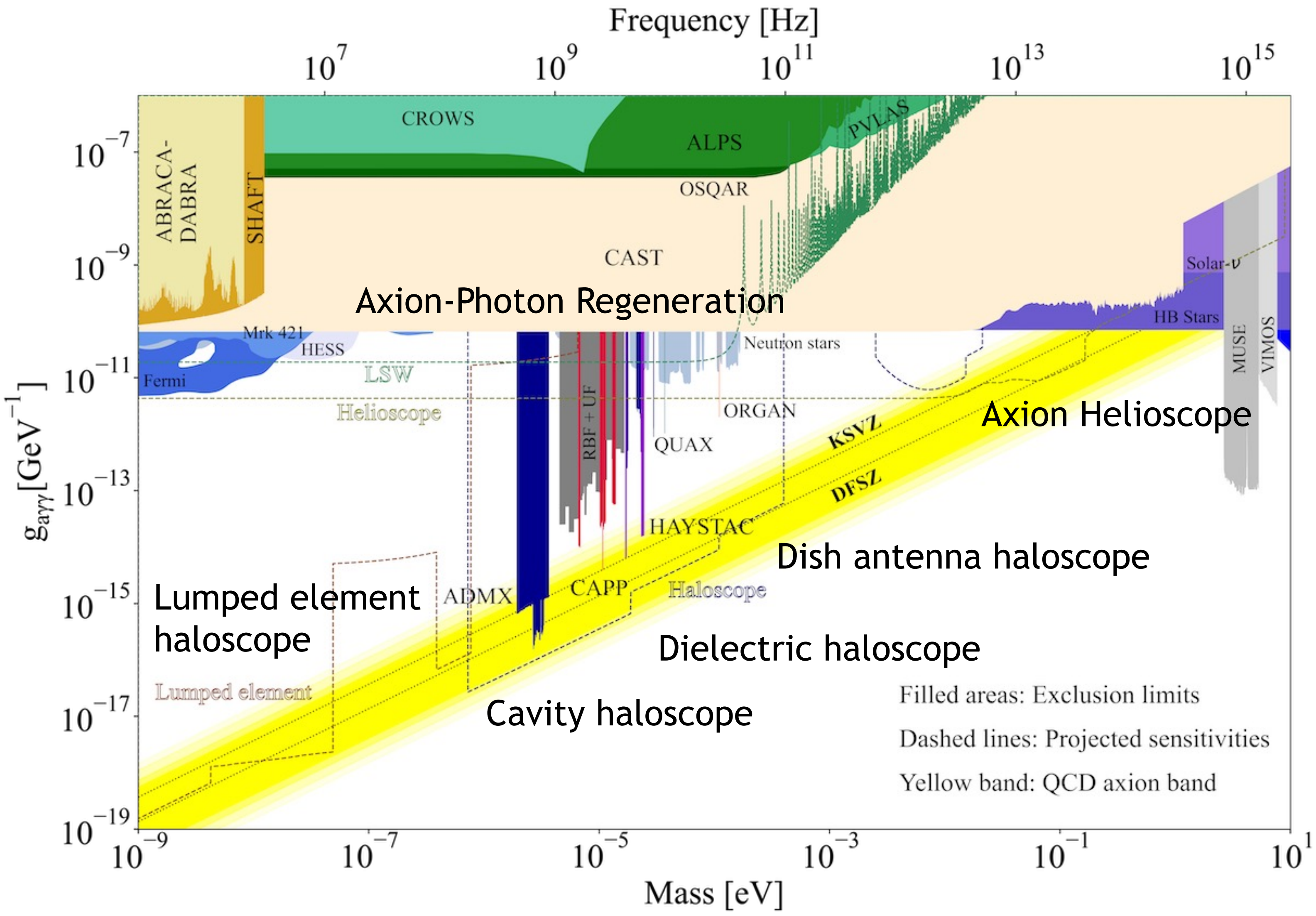

Frequency [Hz]
CROWS
ALPS
PVLAS
OSQAR
CAST
ABRACA-DABRA
SHAFT
Axion-Photon Regeneration
Mrk 421
HESS
Fermi
LSW
Helioscope
Neutron stars
Solar-ν
HB Stars
MUSE
VIMOS
RBF + UF
QUAX
ORGAN
KSVZ
DFSZ
Axion Helioscope
HAYSTAC
Dish antenna haloscope
Lumped element haloscope
ADMX
CAPP
Haloscope
Dielectric haloscope
Lumped element
Cavity haloscope
Filled areas: Exclusion limits
Dashed lines: Projected sensitivities
Yellow band: QCD axion band
$g_{a\gamma\gamma}$[GeV^{-1}]
Mass [eV]

TOORAD (TOpOlogical Resonant Axion Detection)

$$\epsilon\ddot{\mathbf{E}} - \nabla^2\mathbf{E} + \frac{\alpha}{\pi}[\mathbf{B}_0\ddot{\theta}_Q - \nabla(\nabla\theta_Q\cdot\mathbf{B}_0)] = \mathbf{A}\cos\omega_a t\,,$$
$$\ddot{\theta}_Q - v_Q^2\nabla^2\theta_Q + m_Q^2\theta_Q - \frac{\alpha}{4\pi^2 f_Q^2}\mathbf{B}_0\cdot\mathbf{E} = 0\,, \qquad (6)$$

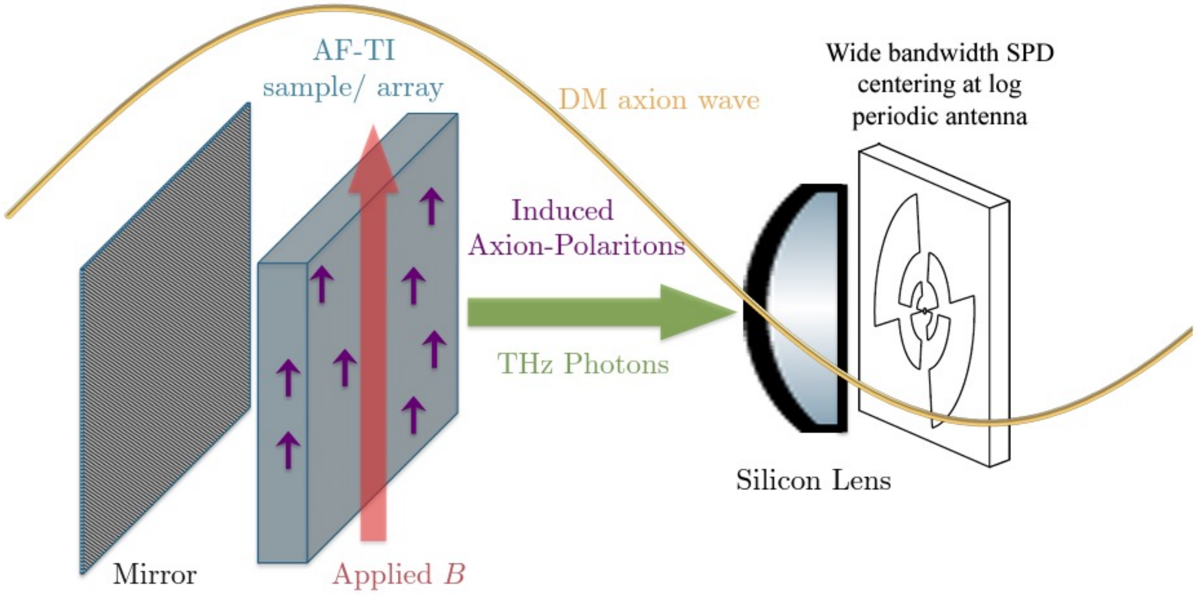

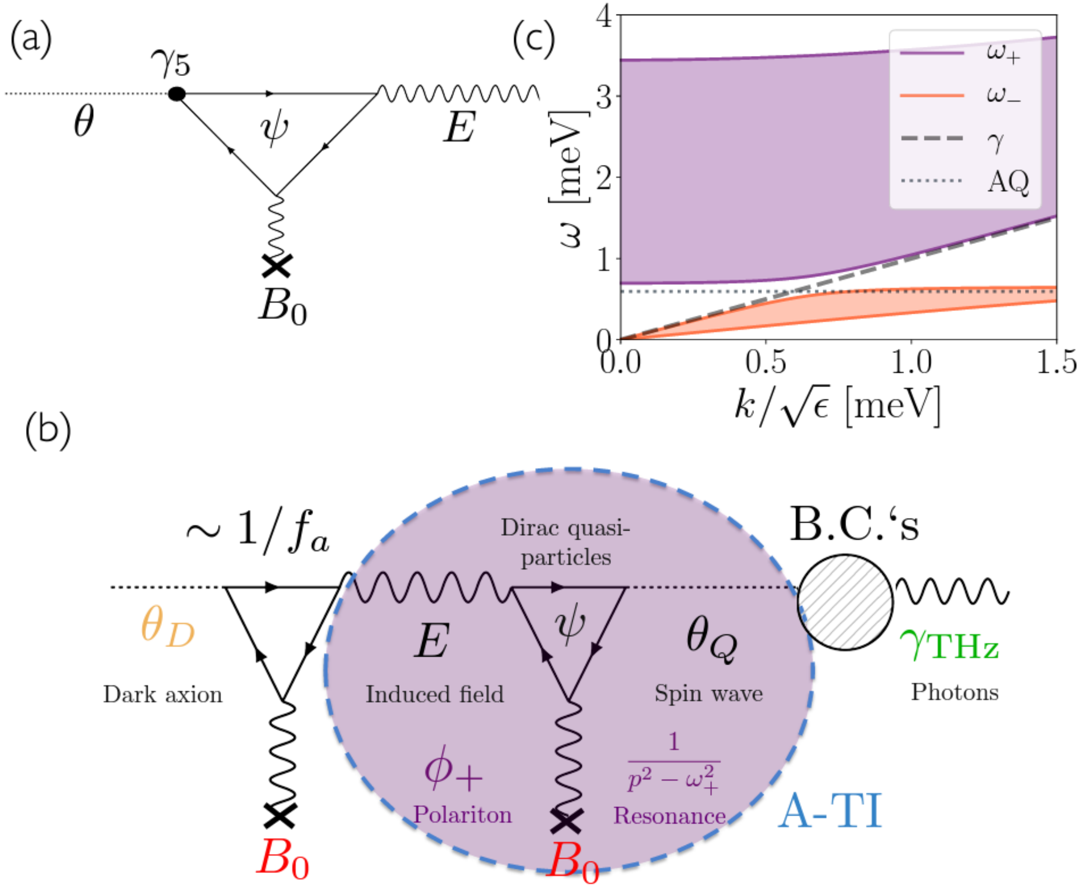

[D. Marsh, Phys. Rev. Lett. **123**, 121601]

ARIADNE (Axion Resonant InterAction DetectioN Experiment)

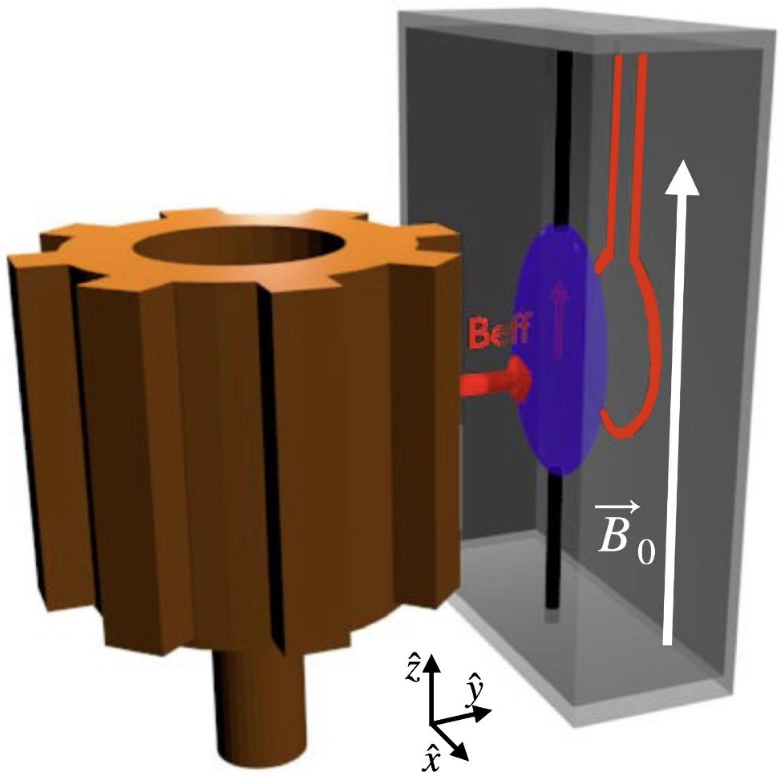

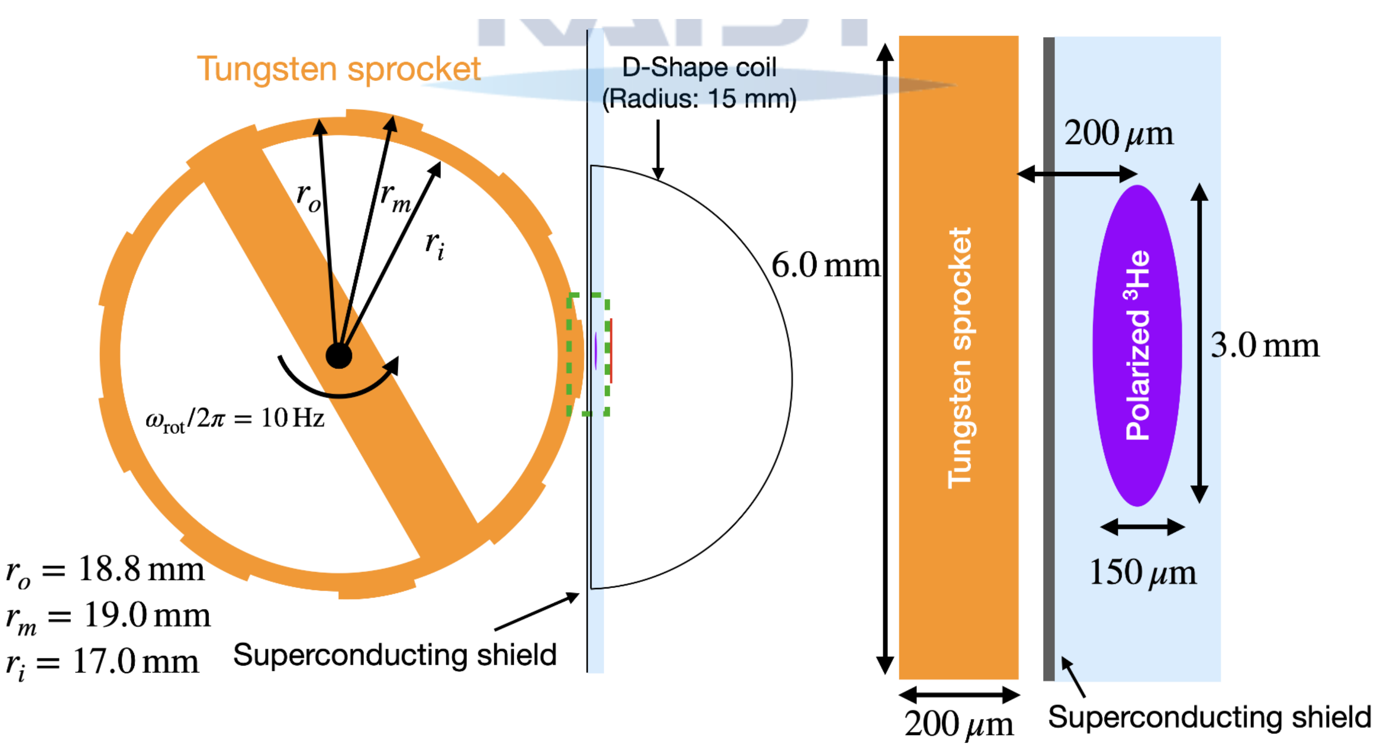

[Y. Kim, KAIST Thesis]

[ARIADNE Collaboration]

$$V_{sp}(r) = -\frac{g_1^p g_2^s}{8\pi m_1}(\sigma_1 \cdot \hat{r})\left(\frac{M_\phi}{r} + \frac{1}{r^2}\right)e^{-M_\phi r}$$

ARIADNE (Axion Resonant InterAction DetectioN Experiment)

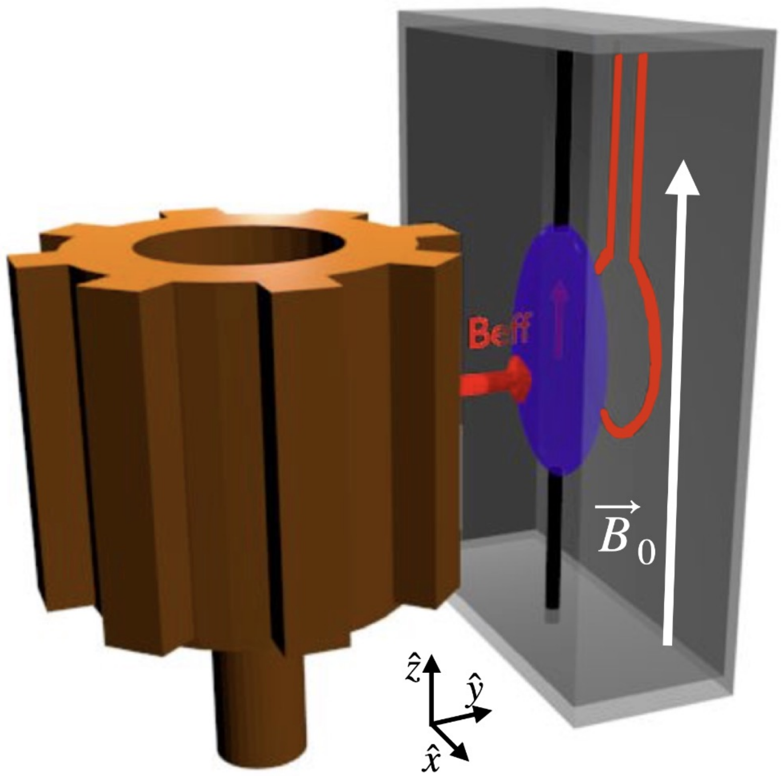

[ARIADNE Collaboration]

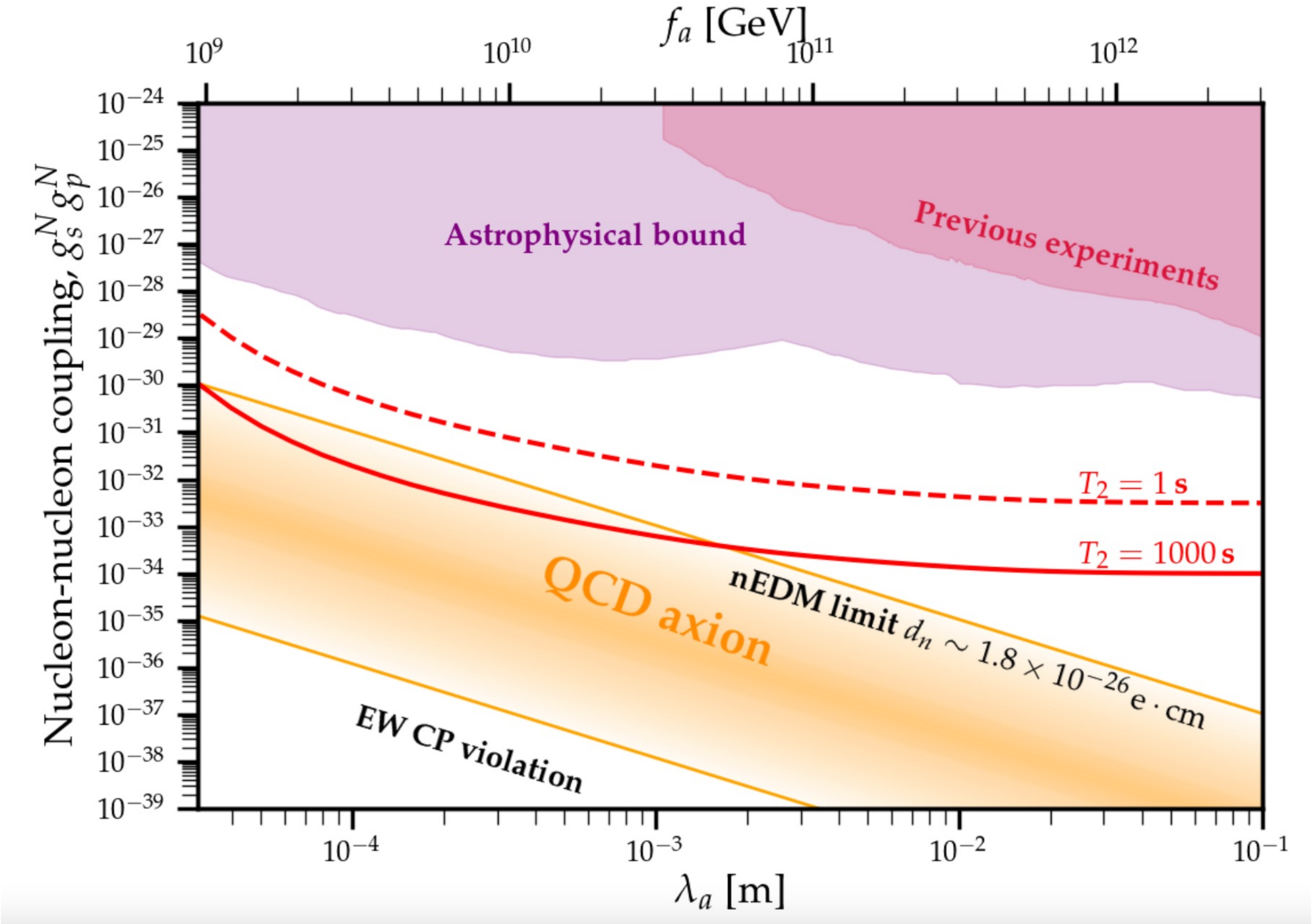

[Y. Kim, KAIST Thesis]